Tacticity Directed Peptide Systems for Targeted Drug Delivery

A thesis submitted in partial fulfillment of the requirements for the degree of

DOCTOR OF PHILOSOPHY

by

GAURAV JERATH

Department of Biosciences and Bioengineering
Indian Institute of Technology Guwahati
Guwahati-781039, India

February 2019

Tacticity Directed Peptide Systems for Targeted Drug Delivery

A thesis submitted in partial fulfillment of the requirements for the degree of

DOCTOR OF PHILOSOPHY

by

GAURAV JERATH

Department of Biosciences and Bioengineering
Indian Institute of Technology Guwahati
Guwahati-781039, India

February 2019

Dedicated to Cancer Patients worldwide.

Gaurav Jerath

INDIAN INSTITUTE OF TECHNOLOGY GUWAHATI

DEPARTMENT OF BIOSCIENCES AND BIOENGINEERING

DECLARATION

I do hereby declare that the research findings of this thesis is the result of research work carried out by me in the Department of Biosciences and Bioengineering, Indian Institute of Technology Guwahati, Guwahati, India, under the supervision of Dr. Vibin Ramakrishnan and Prof. Vishal Trivedi.

As per the general norms of reporting research findings, I take full responsibility for the data represented. Acknowledgements have been made, wherever the research findings of other researchers have been cited in this thesis.

Date: **Gaurav Jerath**

INDIAN INSTITUTE OF TECHNOLOGY GUWAHATI

DEPARTMENT OF BIOSCIENCES AND BIOENGINEERING

CERTIFICATE

It is certified that the work described in this thesis entitled **"Tacticity Directed Peptide Systems for Targeted Drug Delivery"** by Mr. Gaurav Jerath for the award of degree of Doctor of Philosophy is an authentic record of the results obtained from the research work carried out under our supervision in the Department of Biosciences and Bioengineering, Indian Institute of Technology Guwahati, India, and this work has not been submitted elsewhere for the award of any other degree.

Dr. Vibin Ramakrishnan (Supervisor)

Prof. Vishal Trivedi (Co-Supervisor)

Acknowledgements

I would like to extend thanks to the many people, who so generously contributed to the work presented in this thesis.

Special mention goes to my enthusiastic supervisor, Dr. Vibin Ramakrishnan. My PhD has been an amazing experience and I thank him wholeheartedly, not only for his tremendous academic support, but also for giving me so many wonderful opportunities to focus my energy towards something for a greater good. Each meeting or discussion with him would motivate me to think broader and work harder.

Similar, profound gratitude goes to my co-supervisor Prof. Vishal Trivedi, who has been a truly dedicated mentor. I am particularly indebted to him for his constructive criticism and inputs throughout this study.

I am also hugely appreciative to Dr. T.R. Santhoshkumar, especially for his support when so generously hosting me at Rajiv Gandhi Centre for Biotechnology, Thiruvananthapuram. I have very fond memories of my time there.

I am also thankful to the members of Molecular Informatics Design Lab, Protein Biophysics Lab and Malaria Research Group with special mentions to Prakash, Sajitha, Gaurav, Ruchika, Jahnu, Vivek, Anjali, Vinay, Debika, Anshuman, Banesh, Anil and Suman for encouraging me during my not so good times.

Finally, but by no means least, I thank my parents, siblings and my wife for almost unbelievable support. They are the most important people in my world and I partly dedicate this thesis to them.

Table of Contents

List of Figures

List of Tables

Abstract

Ever since Paul Ehrlich proposed the concept of “magic bullet”, the pharmaceutical sector has been on the lookout for that special molecule. However, with the reducing chemical universe and strict Food and Drug Administrator regulations, the drug discovery pipeline for new small molecular entities as potential drug candidates is drying. Further, it has also led to the increase in the research and development costs involved in the development of a novel drug candidate. Therefore, pharmaceutical industry is more absorbed towards the development of peptide-based drug therapies in recent times. At such a critical juncture, the pharmaceutical industry is also open to discovering new avenues for drug repurposing and designing therapies using existing drug molecules. Peptides offer a wide source of novel therapeutic molecules and therapies owing to the distinct probabilities of chemical sequence combinations. Moreover, peptides also provide ample chemistry for the attachment of multiple molecules through simple chemical reactions. Given the biological origin against traditional chemical nature of existing drugs, it also offers avenues for better biocompatibility and a reduced post action toxicity.

Cell penetrating peptides (CPPs) are short peptides which have the ability to pass through the cell membrane while maintaining low levels of toxicity. The uptake of CPPs may be an energy dependent or independent process and does not involve chiral recognition by specific cellular receptors. Since the discovery of the transducing capabilities of the Tat peptide in 1988, many peptides capable of cell penetration have been discovered and designed. They have been utilized for transporting various cargoes: small molecules, nanoparticles, nucleic acids liposomes and proteins inside the cells and thus, show promising application as drug delivery vehicles. CPPs exhibit vast range of physiochemical properties

along with a rich diversity of sequence variation. Such diversity has led to various attempts to classify them on different bases like origin, sequence characteristics, charge, hydrophobicity, pathway of internalization, etc. The CPP database, "CPPsite" has more than 1800 entries for peptides with cell penetrating activity. Majority of these peptides have been derived from various proteins, while the others are either chimeric (formed by fusion of two sequences) or synthetic (rationally designed) sequences.

In the present thesis, the evolution of three distinct peptide series/families with cell penetrative capabilities will be discussed. About fifty peptides were designed and synthesized, after multiple rounds of sequence optimization. After primary screening, three series of peptides were selected on the basis of their design philosophy, efficacy and physico-chemical characteristics. The peptides were biocompatible in human plasma and bovine serum. I also tested the cargo delivering potency of the designed peptides. The characterization of the three series of peptides provides sufficient data for the emergence of a functional design platform for future design of peptides with tailored features and consequential functions. The design platform encompasses different variables of peptide backbone design, electrostatic potential distributions and amino acid sequence optimization. Further, a set of bioinformatics tools were developed during the course of this study to supplement the design platform. The thesis is divided into four working chapters detailing the design and characterization of three peptide series and the design platform developed.

1

Introduction

The call for the development of targeted drug delivery vectors has gained momentum in the past two decades. The use of peptides as targeted carriers is a lucrative option due to the various advantages of peptides over other polymer-based delivery vectors. The biological nature, high number of sequence combinations and the ease of chemical conjugation of cargoes provide peptides a distinction over other molecules. However, the use of peptides as delivery vectors has been hampered due to their susceptibility to proteolytic cleavage and resulting reduced plasma half-life. In the course of this study, we will attempt to address the key challenges in the use of peptides as targeted drug delivery vectors for clinical applications.

Peptides have a unique positioning in pharmaceutical space, and have been playing an important role in medical practice, since the advent of insulin therapy [1]. In terms of molecular size, they are poised between small molecules and proteins, but they maintain a distinct identity in their biochemical activity and therapeutic potential. With a reducing unexplored chemical universe and strict Food and Drug Administrator regulations, the drug discovery pipeline for new small molecular entities as potential drug candidates is drying [2]. This has led to the increase in the research and development costs involved in the development of a novel drug candidate. Therefore, attention of pharmaceutical industry is focused towards the development of peptide-based therapies more than ever before [3-6]. At such a critical juncture, the pharmaceutical industry is also open to discovering new avenues for drug repurposing and designing therapies using existing drug molecules. Peptides offer a wide source of novel therapeutic molecules and therapies owing to their distinct probabilities of chemical sequence combinations. Moreover, peptides also provide ample chemistry for the attachment of multiple molecules through simple chemical reactions [7]. Given the biological origin against traditional chemical nature of existing drugs, it also offers avenues for better biocompatibility and a reduced post action toxicity.

The development of peptide-based vectors for cargo delivery have gained momentum in the past couple of decades [8]. The discovery of protein transduction domains from HIV-TAT and Antennapedia homeodomain, a transcription factor of *Drosophilia* proteins has led to the development of peptides capable to penetrate live cells [9]. These cell-penetrating peptides (CPP) are short peptides with the ability to pass through live cell membranes while maintaining low levels of toxicity [7]. Many CPPs have been identified and developed from different sources of origin including plants, viruses, frogs, snakes, humans etc. [10]. They have been utilized for transporting various cargoes: small molecules, nanoparticles, nucleic acids liposomes and proteins inside the cells and thus, show promising application as drug delivery vehicles [11]. CPPs exhibit vast range of physiochemical properties along with a rich diversity of sequence variation. Such diversity has led to various attempts to classify them on different bases like origin, sequence characteristics, charge,

hydrophobicity, pathway of internalization, etc. The CPP database, "CPPsite" has more than 1800 entries for peptides with cell penetrating activity [10]. Majority of these peptides have been derived from various proteins, while the others are either chimeric (formed by fusion of two sequences) or synthetic (rationally designed) sequences [11].

Majority of CPPs reported to date have been identified or developed from naturally occurring protein sequences of different origins and are polymers of L-amino acids only [10]. The cellular uptake of CPPs occurs through endocytosis or membrane transduction [12]. The uptake of poly-L CPPs is mostly through the receptor-based mechanisms of endocytosis [13, 14]. This recognition of such CPPs by receptors helps in their uptake but also results in their entrapment in endosomes and degradation in lysosomes [15, 16]. In the absence of endosomal escape, these peptides are no longer able to deliver the active cargo to the cytosol. The uptake through membrane transduction does not involve receptors or chiral recognition [17]. Therefore, CPPs penetrating through this mechanism have an increased bioavailability in the cytosol upon uptake.

The uptake of CPPs can be dependent on cell-type in addition to other physico-chemical conditions [7, 11, 12, 14, 17, 18]. The cell-type specificity is both an advantage and disadvantage, as per the contrasting views of different research groups. It is a prospective property of CPPs for applications in targeted drug delivery. Conversely, it may lead to the accumulation of peptides at one site, which may reduce the systemic bioavailability of the drug delivered, resulting in drug inaction. However, this issue of utility of the cell-type specificity of CPPs is critically dependent on the cargo being delivered. For example, the delivery of an anticancer drug should pre-dominantly be cell-type specific in order to increase its bioavailability in the tumor macro-environment and reduce side effects. On the other hand, if the cargo is a plasmid or other gene therapy vector, the CPP used should not in principle be cell-type specific for the delivery of the cargo at the systemic level. Therefore, it is the therapeutic application of the cargo, which is detrimental for the use of cell-type specific or non-specific CPPs for drug

delivery applications. For the confines of the present thesis, the development of cell-type specific vectors for targeted delivery to cancer cells was considered.

Another roadblock for the development of peptide-based drug delivery vectors for clinical applications is their susceptibility to proteolytic cleavage [19-22]. The peptides are recognized by multiple proteases and lysozymes, which leads to their premature degradation. This leads to their reduced cellular uptake in presence of biological fluids like plasma, serum, etc. The incorporation of unnatural amino acids in peptide sequences results in increased stability in biological fluids. However, the use of poly-D analogues of TAT and Penetratin have been reported to lower cellular uptakes than their poly-L analogues [18]. A mechanistic study on the effect of incorporating single unnatural amino acid in a peptide sequence on its cellular uptake has not been reported thus far.

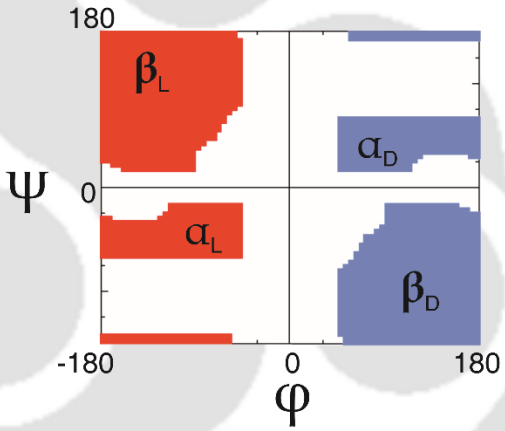

Figure 1.1. ***Ramachandran Map.*** *The allowed regions of Ramachandran Map for L- and D- amino acids.*

Tacticity refers to the stereochemical sequence of successive chiral centers in a polymer [23]. Proteins and peptides are polymers of amino acids with a constant main-chain and a variable side-chain. The orientation of the chiral center, i.e. the C-α carbon in amino acids is responsible for the amino acid associated stereochemistry in peptide sequences. Barring a few exceptions, most natural proteins comprise of L-amino acids, i.e., they are isotactic. The allowed regions in the Ramachandran map for L- amino acids is limited due to the steric hindrances of the different side-chains. This leads to a limited protein folding space

accessible on the Ramachandran map for designing peptide sequences capable of forming different stable structural scaffolds. The use of D-amino acids in peptide sequences assists in accessing the "forbidden" regions of the Ramachandran Map for the advent of new peptide sequences composed of a mixture of L- and D-amino acids (heterotactic) as illustrated in Figure 1.1.

The use of protein engineering tools to design novel cell penetrating peptide sequences has been limited due to the protein-folding problem. Most of the CPPs exist as an ensemble of disordered structures in solution but may adopt a definite secondary structure on interaction with cell surface. This uncertainty in regards to its structural re-conformation leads to the difficulty in imparting structural features into the design of CPPs. For example, the failure of a peptide sequence to form a definitive secondary structure may disrupt its structural amphipathicity, spatial charge distribution and the arising electrostatic potential distributions. However, it may be possible to constrain the topology of a peptide molecule with the use of D-amino acids and other non-naturally occurring amino acids [23].

The alternating occurrence of L- and D-amino acids in a peptide sequence is termed as syndiotacticity. Syndiotacticity in polypeptides was reported for the antibacterial peptide Gramicidin, which is produced by *Bacillus brevis* as a part of its natural defense mechanism [24]. The alternating L- and D-amino acids in Gramicidin lead to the formation of a $\Pi_{(L,D)}$ helical structure with 6.3 residues per turn [23, 25, 26]. This helix is thermodynamically more stable than the isotactic α-helix with an (i, i+5) hydrogen bonding pattern. Therefore, the syndiotactic backbone of Gramicidin leads to the formation of stable $\Pi_{(L,D)}$ helices. This design template in theory would provide the necessary template for designing peptides with tailored properties like spatial charge distribution, structural amphipathicity, etc. [27].

Further, the use of an achiral amino acid, 2-Amino isobutyric acid (Aib, B) promotes the formation of α-helices [28]. This non-proteogenic amino acid is the end product of pyridine metabolism and digested by a handful of bacteria [29]. It is also the component of some antibiotics of fungal origin [29, 30]. Aib is similar

to alanine in structure with an additional methyl group in place of backbone hydrogen atom, i.e. Aib has two C-β methyl groups, which makes it an achiral amino acid. The inclusion of Aib in an otherwise isotactic sequence would make the sequence atactic at the specific position. The steric hindrance from the two C-β methyl groups in Aib leads to its locking in the conformational space in the α_L region of Ramachandran Map (Figure 1.1).

The incorporation of D-amino acids and achiral amino acids, therefore, can be useful for designing peptide sequences with stable conformations and geometry [23]. A stable peptide conformation opens avenues for designing peptides with tailored features for defined applications. This is also critical for designing novel peptide sequences for drug delivery applications, which have tailored physico-chemical properties. The designability of such conformational "arrests" and their applications in drug delivery were studied for the completion of the present thesis.

In the following chapters, the evolution of three distinct peptide series/families with cell penetrative capabilities will be discussed. Based on the sequence optimization studies from a design set of over 50 peptides, the three series of peptide series named CHAPs, SARTHI and STRAPs were characterized for their cellular uptake properties. The peptides were biocompatible in human plasma and bovine serum. The cargo delivering potency of the designed peptides was also tested. The characterization of the three series of peptides provides sufficient data for the emergence of a functional design platform for future design of peptides with tailored features and consequential functions. The design platform encompasses various variables of peptide backbone design, electrostatic potential distributions and amino acid sequence optimization. Further, a set of bioinformatics tools were developed during the course of this study to supplement the design platform. The thesis is divided into four working chapters detailing the design and characterization of three peptide series, followed by details of the design platform developed for sequence optimization.

REFERENCES

[1] The Impact of Insulin Therapy on Protein Turnover in Pre-Diabetic Cystic Fibrosis Patients.

[2] Lin A, Horvath D, Afonina V, Marcou G, Reymond J-L, Varnek A. Mapping of the Available Chemical Space versus the Chemical Universe of Lead-Like Compounds. ChemMedChem 2018;13:540-54.

[3] Lau JL, Dunn MK. Therapeutic peptides: Historical perspectives, current development trends, and future directions. Bioorganic & Medicinal Chemistry 2018;26:2700-7.

[4] Fosgerau K, Hoffmann T. Peptide therapeutics: current status and future directions. Drug Discovery Today 2015;20:122-8.

[5] Morrison C. Constrained peptides' time to shine? Nature Reviews Drug Discovery 2018;17:531.

[6] Rafferty J, Nagaraj H, McCloskey AP, Huwaitat R, Porter S, Albadr A, Laverty G. Peptide Therapeutics and the Pharmaceutical Industry: Barriers Encountered Translating from the Laboratory to Patients. Current medicinal chemistry 2016;23:4231-59.

[7] Copolovici DM, Langel K, Eriste E, Langel Ü. Cell-Penetrating Peptides: Design, Synthesis, and Applications. ACS Nano 2014;8:1972-94.

[8] Brasseur R, Divita G. Happy birthday cell penetrating peptides: already 20 years. Biochimica et biophysica acta 2010;1798:2177-81.

[9] Console S, Marty C, Garcia-Echeverria C, Schwendener R, Ballmer-Hofer K. Antennapedia and HIV transactivator of transcription (TAT) "protein transduction domains" promote endocytosis of high molecular weight cargo upon binding to cell surface glycosaminoglycans. The Journal of biological chemistry 2003;278:35109-14.

[10] Agrawal P, Bhalla S, Usmani SS, Singh S, Chaudhary K, Raghava Gajendra P S, Gautam A. CPPsite 2.0: a repository of experimentally validated cell-penetrating peptides. Nucleic Acids Research 2016;44:D1098-D103.

[11] Bechara C, Sagan S. Cell-penetrating peptides: 20years later, where do we stand? FEBS Letters 2013;587:1693-702.

[12] Madani F, Lindberg S, Langel U, Futaki S, Gräslund A. Mechanisms of cellular uptake of cell-penetrating peptides. Journal of biophysics (Hindawi Publishing Corporation : Online) 2011;2011:414729-.

[13] Juks C, Padari K, Margus H, Kriiska A, Etverk I, Arukuusk P, Koppel K, Ezzat K, Langel Ü, Pooga M. The role of endocytosis in the uptake and intracellular trafficking of PepFect14–nucleic acid nanocomplexes via class A scavenger receptors. Biochimica et Biophysica Acta (BBA) - Biomembranes 2015;1848:3205-16.

[14] Brock R. The uptake of arginine-rich cell-penetrating peptides: putting the puzzle together. Bioconjugate chemistry 2014;25:863-8.

[15] LeCher JC, Nowak SJ, McMurry JL. Breaking in and busting out: cell-penetrating peptides and the endosomal escape problem. Biomolecular concepts 2017;8:131-41.
[16] Erazo-Oliveras A, Muthukrishnan N, Baker R, Wang T-Y, Pellois J-P. Improving the endosomal escape of cell-penetrating peptides and their cargos: strategies and challenges. Pharmaceuticals (Basel, Switzerland) 2012;5:1177-209.
[17] Medina SH, Miller SE, Keim AI, Gorka AP, Schnermann MJ, Schneider JP. An Intrinsically Disordered Peptide Facilitates Non-Endosomal Cell Entry. Angewandte Chemie International Edition 2016;55:3369-72.
[18] Verdurmen Wouter PR, Bovee-Geurts Petra H, Wadhwani P, Ulrich Anne S, Hällbrink M, van Kuppevelt Toin H, Brock R. Preferential Uptake of L- versus D-Amino Acid Cell-Penetrating Peptides in a Cell Type-Dependent Manner. Chemistry & Biology 2011;18:1000-10.
[19] Nguyen LT, Chau JK, Perry NA, de Boer L, Zaat SAJ, Vogel HJ. Serum Stabilities of Short Tryptophan- and Arginine-Rich Antimicrobial Peptide Analogs. PLOS ONE 2010;5:e12684.
[20] Werner HM, Cabalteja CC, Horne WS. Peptide Backbone Composition and Protease Susceptibility: Impact of Modification Type, Position, and Tandem Substitution. Chembiochem : a European journal of chemical biology 2016;17:712-8.
[21] Kim H, Jang JH, Cho JH, Kim SC. De novo generation of short antimicrobial peptides with enhanced stability and cell specificity. Journal of Antimicrobial Chemotherapy 2013;69:121-32.
[22] Hamamoto K, Kida Y, Zhang Y, Shimizu T, Kuwano K. Antimicrobial Activity and Stability to Proteolysis of Small Linear Cationic Peptides with D-Amino Acid Substitutions. Microbiology and Immunology 2002;46:741-9.
[23] Ramakrishnan V, Ranbhor R, Kumar A, Durani S. The Link between Sequence and Conformation in Protein Structures Appears To Be Stereochemically Established. The Journal of Physical Chemistry B 2006;110:9314-23.
[24] Andersen OS, Koeppe RE, 2nd. Molecular determinants of channel function. Physiological reviews 1992;72:S89-158.
[25] Urry DW. The Gramicidin A Transmembrane Channel: A Proposed $\pi_{(L,D)}$ Helix. Proceedings of the National Academy of Sciences 1971;68:672-6.
[26] Wallace B, Ravikumar K. The gramicidin pore: crystal structure of a cesium complex. Science 1988;241:182-7.
[27] Zhang Q, Gao H, He Q. Taming Cell Penetrating Peptides: Never Too Old To Teach Old Dogs New Tricks. Molecular Pharmaceutics 2015;12:3105-18.
[28] Basu G, Kuki A. Conformational preferences of oligopeptides rich in α-aminoisobutyric acid. II. A model for the 310/α-helix transition with composition and sequence sensitivity. Biopolymers 1992;32:61-71.

[29] Conlon JM, Al-Kharrge R, Ahmed E, Raza H, Galadari S, Condamine E. Effect of aminoisobutyric acid (Aib) substitutions on the antimicrobial and cytolytic activities of the frog skin peptide, temporin-1DRa. Peptides 2007;28:2075-80.

[30] Bruckner H, Graf H. Paracelsin, a peptide antibiotic containing alpha-aminoisobutyric acid, isolated from Trichoderma reesei Simmons. Part A. Experientia 1983;39:528-30.

2

Cell Penetrating Peptides: From Bench To Clinics

Selective permeability of cell membranes often restricts the exchange of molecules between the extra- and intra-cellular domains. Such a barrier coupled with poor lipophilic properties of therapeutic molecules hinders their transport to the diseased cells. Peptides with the ability to penetrate plasma membranes have been demonstrated to successfully deliver nucleic acids, proteins and small molecule entities inside the cell. The delivery of therapeutic molecules increases the bioavailability inside the cell; however, it provides no protection from the damage caused by side effects of therapeutics owing to their unspecific delivery to multiple sites. In this review, the peptides with membrane transduction properties, their mechanisms of action, specificity to diseased models, therapeutic applications and the challenges for lab to clinical application are described.

2.1 INTRODUCTION

The origins of targeted delivery can be attributed to Paul Ehrlich's concept of a "magic bullet" [1]. Though the concept has its own appeal, it remains a challenge for clinical applications. The challenge is on three tiers, discovery of a disease specific target, a drug molecule specific to the target and a stable drug carrier to transport the drug to the intended site [2-4]. Stricter norms, higher costs and a shrinking chemical universe for discovery of new therapeutic molecules further add to the woes of the pharmaceutical industry [5-7]. Given the need of new drugs and therapies to combat new diseases, multi-drug resistance and drug promiscuity, the pharmaceutical industry is relying on bio-therapeutics, drug repurposing and new delivery techniques for existing drugs. Targeted delivery increases the bioavailability of a drug at the site of action leading to better drug efficacy and reduced side effects [8, 9]. An ideal drug delivery vector should penetrate different physical and biological barriers including cell membranes.

Cell membranes restrict the transport of molecules to and from the intracellular locale. The membranes are selectively permeable to molecules recognized by various cell surface receptors. This barrier acts as an obstacle for intracellular delivery of various therapeutic molecules. Most therapeutic molecules (drugs) are chemical moieties with various levels of hydrophobicity and charge. Majority of these drugs are mimics of a natural ligand for cell surface receptors, e.g. methotrexate is the chemical mimic of folic acid and recognized by the folate receptors on the cell surface [10, 11]. The uptake of such chemi-mimics is mostly through receptor-mediated endocytosis [11]. In other cases, they may require a carrier molecule to cross the cell membranes. The use of carriers for drug encapsulation provides a variety of advantages like better drug solubility, enhanced drug stability, decreased side effects, targeted delivery, etc. in comparison to the native drug [8, 12-14].

The discovery of protein transduction properties of HIV TAT protein in late-eighties contradicted the established impression of the scientific community that the cell membrane was impermeable to hydrophilic molecules [15]. Further, a transcription factor of *Drosophila melanogaster*, Antennapedia homeodomain

was also reported to penetrate live nerve cells in 1991 [16]. Together, the transduction properties of the two proteins presented an exciting opportunity to identify the least amino acid sequence required for cellular uptake, leading to the discovery of Tat and Penetratin, the first cell penetrating peptides (CPPs) [17]. In 1997, MPG peptides were designed to transport nucleic acids, followed by Pep-1 for delivery of peptides and proteinsv[18-20]. A chimeric peptide derived from the neuropeptide galanin (Transportan) was used to transport small peptides and large proteins as a proof of concept for the *in vivo* application of CPPs [21]. A list of commonly known CPPs is given in Table 2.1.

Table 2.1. ***Well-known CPPs, their sequences and origin****. A list of well-known CPPs reported in literature with varying sources of origin.*

NAME	SEQUENCE	ORIGIN	REFERENCE
TAT (48-60)	GRKKRRQRRRPPQ	HIV	[15]
Penetratin	RQIKIWFQNRRMKWKK	*D. melanogaster*	[16]
Transportan	GWTLNSLKALAALAKKIL	Chimeric (Galanin and Mastoporan)	[21]
VP22	NAKTRRHERRRKLAIER	HSV Type 1	[22]
MPG	GALFLGFLGAAGSTMGA	Simian Virus 40	[18]
Pep-1	KETWWETWWTEWSQPKK KRKV	Simian Virus 40	[20]
pVEC	LLIILRRRIRKQAHAHSK	Murine VE-Cadherin	[23]
YTA2	YTAIAWVKAFIRKLRK	Phage Library	[24]
M918	VTVLFRRLRIRRACGPPRVRV	Human	[25]
CADY	LWRALWRLLRSLWRLLWRA	Synthetic	[20]

CPPs are short oligomeric peptides with a chain length of 5-30 amino acids, which traverse through cell membranes and can deliver a variety of molecules including proteins, nucleic acids, small molecules, etc. in the cell [26]. Naturally, given their ability to cross-over biological membranes, CPPs have been extensively studied for their drug delivery applications. CPPSite 2.0 (a database) has records of over 1800 peptides with cell-penetrative activity [27]. In the last 30 years or so, CPPs have been used from the basic research to pre-clinical studies for treatment of multiple diseases. Most often, the drug delivery applications of CPPs have been studied in the field of oncology [28]. In this review, the use of CPPs for targeted delivery to cancer cells will be emphasized.

2.2. STRENGTHS, LIMITATIONS, AND OPPURTUNITIES

The use of peptides as drug delivery vectors offers its own sets of advantages and disadvantages as advocated through various reports. Given their biological nature, peptides are comparatively more safe and tolerable for biological systems than chemi-mimics. Peptides can be designed for higher selectivity, efficacy and potency. The metabolism of peptides is more predictable than other chemical moieties. Moreover, peptides can be synthesized through standard synthetic protocols and can be conjugated with any molecule of interest through simple chemical reactions. However, peptides may sometimes require modifications due to poor chemical and physical stability in biological fluids, which may otherwise hinder their use for clinical applications. Most peptides have short plasma life leading to premature degradation in blood and thus, fast elimination. Further, the mode of administration for peptides is presently limited to intravenous routes. Many reports have described alternate modes for administration but the consensus is the same [29].

The weaknesses of peptide-based drug delivery vectors provide new avenues and opportunities for the development of novel peptide sequences to address these issues. Using the 20 naturally occurring peptides as a set of variables in a peptide sequence of sequence length 10-15, which is the length of most CPPs, a total of 20^{10}-20^{15} combinations (sequences) are possible. This signifies the vast sequence universe available for designing peptides with tailored features. The

use of unnatural amino acids as described by Kumar *et al.* can increase this available sequence universe by two-folds [30]. Further, the conjugation of peptides with different therapeutic molecules increases the number of sequential combinations available for peptide design. Moreover, peptides with multiple features can also be designed, e.g., many antimicrobial peptides share similar properties with CPPs. Overall, in the given purview, peptides do offer a great potential for development of future therapies and therapeutics [29].

2.3 CLASSIFICATION OF CELL PENETRATING PEPTIDES

There is no unified classification for CPP and they are classified on different basis. The first classification of CPPs was on the basis of their origin (Protein-derived, chimeric or synthetic). Like Tat and Penetratin, most CPPs have been identified from different protein sequences. Such CPPs have also be termed as protein transduction domains and Trojan horses due their functional characterization. Nona- and octa-arginines were among the first synthetic CPPs reported [31, 32].

CPPs, since their discovery have been classified on different basis:

a) Charge: Cationic, Neutral and Anionic.
b) Hydrophobicity: Amphipathic (Primary and Secondary) and Non-Amphipathic.
c) Linkage with Cargo: Covalent Bonded and Non-covalent bonded.
d) Intracellular Localization: Nuclear Localizing, Cytosol Localizing, etc.
e) Cell-Type Specificity: Specific and Non-specific.

For the scope of this thesis, the classification of CPPs based on their physical and chemical properties will be discussed.

2.3.1. Cationic CPPs

The first CPPs reported (TAT and Penetratin) were cationic peptides [15, 16]. Based on this criterion synthetic poly-arginine constructs were tested for their cellular uptake and it was discovered that an octa-arginine is the minimum sequence required for cellular uptake [32, 33]. Lower uptake of poly-lysine in comparison to poly-arginine suggests that charge alone is not responsible for

cellular uptake [33]. This could be explained due to the guanidium group in arginine, which facilitates the formation of hydrogen bonds [34]. The uptake of Penetratin, on the other hand is diminished by a single W14F mutation, suggesting that hydrophobic interactions also play an important role for cellular uptake of cationic peptides [35].

2.3.2. Amphipathic CPPs

Peptides consisting of specific distribution of polar and non-polar (hydrophobic) residues are termed amphipathic peptides. Amphipathicity can exist in the amino acid sequence (primary) or the secondary structure (secondary) for a given peptide.

2.3.2.1. Primary amphipathic

Primary amphipathic peptides, e.g. MPG (GLAFLGFLGAAGSTMGAWSQP-KKKRKV) and Pep-1 (KETWWETWWTEWSQPKKRKV) are chimeras of a hydrophobic and hydrophilic (KKRKV) sequences [18, 20]. Here, the KKRKV sequence is a nuclear localizing sequence which otherwise has poor cell-penetration capability. WSQP is a linker for the two cell-penetrating peptide chimeras. The hydrophobic part of the sequences improve the cellular uptake of the nuclear localizing sequence [36]. Other primary amphipathic of note is pVEC, which was derived from VE-cadherin [23].

2.3.2.2. Secondary amphipathic a-helical CPPs

α-helical conformation is the most common structural motif reportedly adopted by amphipathic CPPs [27]. Secondary amphipathic peptides have distinct regions of hydrophobic and hydrophilic amino acid clusters along their surface. Helical wheels are an important tool for visualizing the structural amphipathicity in helical peptides. However, given the probabilistic nature of an amino acid sequence adopting a helical conformation, a helical wheel may not always hold true in depicting the structural amphipathicity of peptides. The importance of amphipathicity for membrane transduction was established through studies on the model amphipathic peptide, MAP (KLALKLALKALKAALKLA) [37]. The

substitution of lysine residues with glutamine brings the overall charge of the peptide to zero but conserves its amphipathicity. The mutant MAP peptide was also cell penetrating, thereby, affirming the significance of amphipathicity on cell penetration [38, 39]. Even though many CPPs reported to date are amphipathic, it is not necessary for all amphipathic peptides to be CPPs. This has been illustrated through single point mutations of transportan and MAP peptides, which severely affected the uptake of these peptides [39, 40].

2.4. MECHANISM OF UPTAKE

The exact mechanism(s) of uptake for cell penetrating peptides vary with peptide sequence and composition [41-44]. The choice of mechanism is further dependent on the physico-chemical properties of the cargo to be delivered like size, hydrophobicity, charge, etc. However, multiple mechanisms of uptake for CPP are suggested in existing literature [41-44]. The understanding of mechanism of penetration is paramount when considering the intracellular interactions and localization of CPPs for cargo delivery applications. The fate of a CPP is dependent on the uptake mechanism it follows, e.g. if a CPP enters the cell through direct penetration, it is highly probable that it may be able to deliver the cargo directly to the cytosol and then finally to other intracellular compartments. On the other hand, a CPP entering the cell through endocytosis is more likely to be degraded in a late endosome or lysosome and may not be able to deliver the cargo to another intended target, unless it escapes the endosome/lysosome. Therefore, the choice of CPP for delivering cargoes is highly dependent on the proposed mechanism of delivery to be followed. Majority of CPPs adopt multiple pathways of internalization simultaneously [45], which presents itself as both an advantage and a disadvantage. The advantage is that a single CPP can be used for delivering cargoes to multiple locations within the cells. The disadvantage is that the cargo is also distributed to other non-intended organelles, thereby decreasing the overall delivery efficiency.

The cellular entry of a CPP can be categorized into the following steps: 1) Interaction with cell surface, 2) Crossing the cell membrane, 3) Intracellular interactions and localizations, and 4) Intracellular Degradation.

2.4.1. Interaction with cell surface

The first contact between a CPP and the cell surface is the initiation step for cell penetration. The CPP can interact with either the proteoglycans at the cell surface, extracellular receptors or the membrane phospholipids. The driving force for such biological contacts is generally attributed to electrostatic interactions.

2.4.1.1. Role of Proteoglycans:

Glycosaminoglycans (GAG's) like heparin sulphate, chondroitin sulphate, sialic acid, etc. are negatively charged and omnipresent on cell membranes. Cationic CPPs bind to these GAGs, which leads to activation of small GTPase RhoA and/or GTPase Rac1 and actin network remodelling [105.88]. This leads to an increase in membrane fluidity [46, 47] and finally the engulfment of the peptide through endocytosis. The process is similar to the uptake of other cationic molecules by the cell like poly-lysines [15, 48-50]. The proteoglycan-CPP interaction is the primary step of cellular entry for majority of peptides with L-isoforms and poly-D-isoforms of amino acids. The D-isoform amino acid containing sequences are suggested to employ other modes of first contact [51].

2.4.1.2 Role of Cellular Receptors:

Many cellular receptors are involved in the binding of natural ligands, inducing cascades of associated pathways and ligand ingestion. Similarly, peptides bind to the extracellular domain of the membrane bound receptors, leading to their ingestion. The most commonly used motif for tumor homing and penetration, RGD binds to the interleukin receptor, which activates the receptor-mediated uptake, leading to peptide intake [52-55].

2.4.1.3 Interaction with membrane phospholipids:

Plasma membrane of cells are composed of lipid bilayers, consisting of zwitterionic and negatively charged phospholipids. The composition of negatively charged lipids (POPG and POPS) is higher in bacterial cells (50%) than mammalian cells (10%) [56-58]. The distribution of negatively charged lipids is

asymmetrical between the two layers of the plasma membrane in mammalian cells, with a higher concentration in the cytosolic part of the bilayer [58]. This asymmetric distribution of anionic lipids in mammalian cells is highly regulated and known to fail during disease conditions like cancer. This loss of regulation in cancer cells brings out a higher concentration of POPS in the outer layer, thereby, making the cell surface charge more negative and reduced membrane potential [58]. The reduction in membrane potential acts as the driving force for higher accumulation of cationic CPPs on the cancer cell surface than in normal cells. As seen in the case of AMPs, cationic CPPs interact with these negatively charged phospholipids [59]. Therefore, the relative cationic charge and hydrophobicity of CPPs, just like AMPs play an important role in their membrane activity and hints for their cancer targeting ability.

The cationic amino acid residues in CPPs attract the negatively charged head groups of anionic lipids, establishing strong electrostatic contacts. This further leads to the formation of a dent on the membrane surface, lead to the internalization of CPPs. The detailed models of membrane-based penetration are discussed in the following sections.

2.4.2 Cellular internalization of CPPs

Most of the reported CPPs enter the cells through either endocytosis or direct penetration or a mix of both [41-44]. The choice of pathway for internalization of CPPs is dependent on the type of their cell surface interactions. The peptides interacting with proteoglycans or receptors follow the endocytosis route of entry. On the other hand, peptides interacting with the membrane lipids tend to penetrate through either micropinocytosis (a form of endocytosis) or various models of direct penetration. CPPs can adopt multiple pathways of cellular entry simultaneously, which are dependent on multiple factors like, temperature, pH, cargo size [41-44], CPP structure and others. Almost all CPPs partially penetrate cells through membrane-based mechanisms with higher dependency on endocytic routes of entry. As per status quo, the most prevalent form of cellular uptake for CPPs is endocytosis. The studies relating to the characterization of the cellular entry pathway are based mostly on the inhibition of certain mechanisms

pertaining to endocytosis [57]. Though these studies provide immense insights into the possible pathway(s) of entry, they discount the possible up-regulation of another pathway of entry due to the down-regulation of another. Various modes of endocytosis and direct penetration reported for CPPs (Figure 2.1) to date have been explained in the following sub-sections.

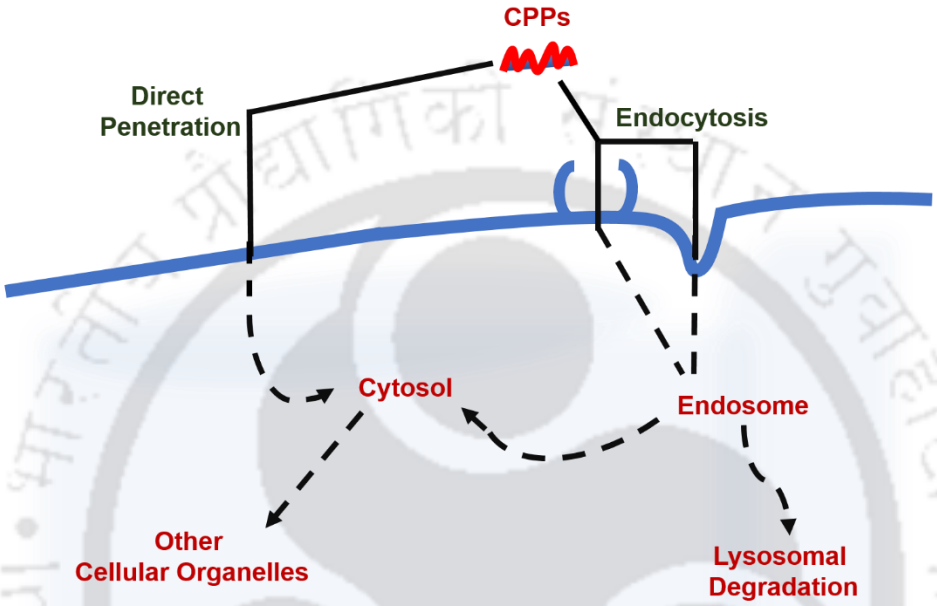

Figure 2.1. ***Mechanism of Cellular Uptake.*** *CPPs enter cells through either of the two paths of direct penetration through the cell membrane or through endocytosis. The fate of the peptide is highly dependent on the path of uptake.*

2.4.2.2 Endocytosis:

Endocytosis is the collective term for all energy dependent cellular uptake processes, characterized by vesicle formation [42, 57]. It can be broadly classified as phagocytosis and pinocytosis. Phagocytosis is majorly limited to specialized cells (Macrophages and leucocytes). Pinocytosis occurs in all cell types and can further be sub-classified into receptor mediated and non-receptor-mediated endocytosis. Receptor-mediated endocytosis is either clathrin or caveolin mediated, while non-receptor-mediated are clathrin and caveolin independent endocytosis and macropinocytosis. The choice of clathrin/caveolin mediated and independent mechanisms are dependent on the size of a molecule [60]. Vesicles

formed from clathrin mediated mechanisms are roughly 120 nm in diameter, from caveolin mediation are 70-80 nm, clathrin/caveolin independent mechanism vesicles are ~90 nm and macropinocytosis formed vesicles are 1-5 μM. Therefore, the choice of cargo is an important attribute for the choice of endocytic entry.

CPPs binding to proteoglycans can enter the cells during the recycling of proteoglycans, which is a continuous process or via clustering of proteoglycans, which initiates endocytosis through activation of intracellular pathways and actin remodelling. The clathrin and caveolin mediated pathways are also involved in the cellular uptake of peptides bound to other cellular receptors as well.

Another major form of endocytosis prevalent for cellular uptake of CPPs is macropinocytosis [61]. Macropinocytosis differs from other forms of endocytosis in terms of the size of vesicles formed (Macropinosomes) and the ruffling of membrane. The plasma membrane of cells is not a smooth surface; rather it is ubiquitous with dents (pits) and outward protrusions. Macropinosomes are formed due to the collapse of such membrane ruffles, which are actin rich protrusions of the cell surface. The size of macropinosomes is three order of magnitude more than other endocytic vesicles and thus the choice of uptake process for relatively large protein structures and other cargoes. Liposomes coated with high concentrations of oligo-arginines have been demonstrated to penetrate cells through macropinocytosis [62, 63]. However, it is not only reserved for huge cargo sizes only, Tat peptide itself is known to induce macropinocytosis without any cargo.

2.4.2.2 Direct Penetration:

Peptides interacting with membrane phospholipids follow the direct penetration mode of entry. Direct penetration through plasma membrane is an energy and temperature-independent mechanism of uptake [64, 65]. Interestingly, it was the first reported mechanism of entry for CPPs but was disregarded as an artefact arising from cell fixation [41]. Thereafter, all studies on the uptake mechanisms

of CPPs are carried out on live cells. The membrane-based uptake mechanism of CPPs is quite similar to that of AMPs, owing to similar characteristics of the two classes of membrane active peptides. The membrane interaction of these peptides is foremost dependent on the spatial electrostatic potential distribution on their surface which is complemented by the anionic lipids on membrane surface. Multiple models of direct penetration have been theorized for both CPPs and AMPs [66].

Carpet-like model as the name suggests, involves the lateral positioning of the cationic residues of peptides over the negatively charged phospholipids on the outer membrane. The accumulation of negative charge at surface and at threshold concentration of peptides, the peptides rotate about their principal axis, leading to phospholipid re-direction. This leads to the interaction of the hydrophobic residues in peptide sequences with hydrophobic tails of the phospholipids and finally cell penetration in a manner similar to a detergent – like effect [64, 67, 68].

The inverted micelle model has been proposed following the findings of Alain Prochiantz's group, using NMR imaging for the penetration of phospholipid membranes by Penetratin [69]. This model is useful in explaining the uptake of amphipathic CPPs but not others like oligoarginines, which do not contain any hydrophobic residues [70]. The primary step of this model differs from that of the carpet-like model in the non-parallel positioning of the peptides on the cell surface. The interaction of cationic peptide residues and anionic lipid headgroups leads to the formation of a micelle through the invagination of the membrane. The micelle then opens towards the cytosolic end of the membrane, thereby causing membrane permeation [71, 72].

Barrel stave model is one of the two pore-formation models proposed for CPP entry [73-75]. The peptides align perpendicular to bilayer plane, insert, associate and as a result of peptide amphipathicity, form a pore. It can be best understood as a drilling process arising from a mix of electrostatic interactions at the membrane surface and the hydrophobic interactions with the bilayer core. This model is similar to the mechanism of action proposed for the antibacterial

peptide, Gramicidin [76]. However, Gramicidin requires two end to end stacked monomers, for forming a water channel and relates to the toxicity of the peptide. In case of CPPs, the pore results from a cumulative barrel like positioning of individual peptide units in parallel.

The Toroidal pore formation model deviates from the barrel stave model in the relative positioning of peptides in the pore formed [77]. Instead of parallel positioning of peptide molecules, the peptides induce a membrane curvature local to the site of pore formed. This leads to a continuity of the outer and inner layers, such that, the two layer are indistinguishable at the site of the pore. The pore formation models discussed however, are highly dependent on the helical structure of the peptides and their amphipathicity, in summary, their spatial electrostatic distributions.

Adaptive penetration model is among the most recently proposed models for cell penetration [78, 79]. Identical to all the models discussed above, it relies on the electrostatic interactions of positively charged amino acids with anionic lipid head groups. However, it is only applicable to guanidium group containing CPPs, i.e. arginine-containing CPPs. The guanidium group of arginine forms bidentate hydrogen bonds with lipid head groups, leading to peptide charge neutralization or inversion, which is dependent upon the counterion present. This results in the phase transition of CPP from hydrophilic to more lipophilic solvability and its further insertion into the bilayer. The presence of different counterions on the cytosolic end of the bilayer reinstates the original physical properties of the peptide, leading to its release into the cytosol. The diffusion of the peptides across the bilayer is a function of membrane potential and requires a net positive charge for a CPP. The partition constant for peptides is defined as the ratio of concentrations of peptide in lipid and aqueous phases. The partition constant is indicative of the membrane disruption efficiency of AMPs but no studies have been reported on correlating it with membrane permeation efficiency of CPPs yet.

2.4.3. Cellular Localization

The intracellular localization of CPPs is highly dependent on the pathway(s) of cell penetration, which are further dependent on the type of peptide-cell surface binding interactions. As illustrated in Figure 2.1, peptides entering the cell through either of the endocytic pathways are primarily confined to vesicles, thereby, primarily localizing in the endosomes/macropinosomes. The next barrier for such peptide molecules is to escape the vesicles for intracellular delivery of cargo to other cell organelles. Therefore, endosomal escaping ability is a vital attribute for any CPP to be considered as a drug delivery vector, unless it is required to deliver the cargo to endosomes or lysosomes. After endosomal escape, the peptide localizes to the cytosol and/or further to other cellular organelles.

On the other hand, CPPs entering cells through direct translocation localize to the cytosol first and thereafter can localize to other organelles, including endosomes. Moreover, a CPP can also localize to multiple cell compartments. Though favourable in many situations, the peptide concentration distribution decreases its bioavailability to a specific organelle for effecting a cargo function, leading to higher dose requirements. However, a few CPPs in literature are reported to target mitochondria for site-directed delivery [80].

2.4.4 Transcellular Transport and Degradation

Premature degradation of CPPs hinder their applicability as drug delivery vectors, however, it also is required that the vector can be metabolized and excreted from the system. There are major barriers where a CPP may be degraded within an in vivo system. However, in the confines of mechanism of penetration, only intracellular degradation is discussed in this section. Major degradation of peptides inside cells is either in lysosomes or in cytosol. In the event that a CPP is unable to escape endosomes after penetration, it will encounter the lysosomal proteolytic degradation pathways. Lysosomal proteases comprise of more than 40 lytic enzymes.

The cytosol also comprises of numerous proteases and acts as a natural proteolytic site for cytosol localizing peptides. The ubiquitin-proteosome degradation pathway, 26S proteasome mediated degradation and cytosolic tripeptidases are among the most well documented degradation pathways in cytosol. The presence of D-amino acids have been reported to protect the CPP from pre-mature proteolytic cleavage, however, a protein cargo would effectively prone to such degradation too. Therefore, the degradation or stability of CPP in cytosol is of lesser relevance when transporting a protein-based cargo [81].

Though CPPs can be degraded in both lysosomes and cytosol, the ability of escaping endosomes is more vital than stability in cytosol, for effective transport, unless the site intended is lysosomes, as discussed above.

The penetration of cell by CPPs also opens the debate as to whether the CPPs can permeate to outside the cell too. The Tat protein is known to be released from HIV-infected cells to other non-infected cells. Therefore, it is understandable that other CPPs may as well have such a property of transcellular transport. The applications of such a property possessing CPPs can be multi-fold ranging from blood-brain barrier, epithelial barrier (skin, intestine, pulmonary) to 3D tumor penetration.

2.5. CPP PREDICTION

Predicting the cell-penetrative capability of a given amino acid sequence is a tedious task, which is further complicated by the fact that the exact mechanism of CPP uptake is still debatable [57]. As discussed in the previous section, endocytosis is the major contributor for cellular uptake of CPPs conjugated with a cargo; membrane transduction has also been indicated to be the choice of pathway adopted by specific peptides [82-85]. Further, more challenging is the question as to what is more critical for the penetrative action of an amino acid sequence. Is it the properties of the peptide or the membrane potential or the membrane composition or a combination of all or none? Given that CPPs penetrate plant, yeast and bacterial cells in addition to mammalian cells, one may assume that the properties of the peptide sequence is more important [86-90].

The elucidation of properties of peptides responsible for cell penetration is no less than a Gordian knot. Majority of CPPs are cationic, which can be attributed to arginine, lysine or histidine. As discussed in section 2.3.1., arginine residues contribute more towards the cellular uptake of CPPs than lysine residues. This may be due to the two hydrogen bond donor groups available in the guanidium group of arginine against a single hydrogen bond donor provided by the amino side-chain group in lysine. Further, the hydrophobicity and its distribution (sequential and structural) can affect the uptake of CPPs. The maintenance of structural amphipathicity in various solvents and buffers is rarely replicated under physiological conditions. The poly-L amino acid sequences exist as an ensemble of disordered structures in solutions and may or may not re-conform to helical or sheeted structures as intended in the design of their sequence [91]. The length of the peptide is also an important factor. CPPs reported in literature vary in sequence length of 5-30 amino acid residues and in the absence of a smaller range of peptide length critical for cell-penetration, it is almost impossible to identify a cell-penetrating sequence from a peptide sequence library [27]. However, despite the roadblocks mentioned above, it may still be possible to predict the cell-penetrative capability of an amino acid sequence. One mode of prediction is heuristic approach also regarded as “an educated guess” and the other is a completely predictive approach, which relies on a variety of physico-chemical properties of peptides (descriptors).

The heuristic approach is responsible for the majority of CPPs reported in literature. It is majorly based on a mechanistic sequence-activity relationship study, which includes the identification of a cationic fragment augmented by hydrophobic residues in a protein sequence. The method is laborious and time intensive given that it requires the synthesis, characterization and testing of multiple overlapping sequences. However, a number of guidelines are available for identifying a cell-penetrating sequence. These include:

a) Cationic residues are preferred and anionic residues are suggestively avoided, even when the sequence possesses more positive residues.
b) Sequences with more arginine are preferred over lysine-rich sequences.

c) Helical wheel plotting is required to check for possible structural amphipathicity in the given sequence.
d) Shorter peptides are preferred over longer sequences (>20) due to ease of synthesis and purification.
e) Highly hydrophobic sequences should be avoided due to poor water solubility, which may complicate the use of the peptide.

The predictive approach relies on a set of peptidic properties (descriptors). The use of Sandberg's z-descriptors has been demonstrated to predict CPPs from protein sequences, however, it does not take into account the amino acid sequence but only the composition [92-94]. Another approach is the use of support vector machines. Different groups have reported the use of support vector machines [95-98]. Among these, a noteworthy effort is the availability of a support vector machine based web-server, CELLPDD [99].

2.6. CELL-TYPE SPECIFICITY: TO BE OR NOT TO BE

CPPs can deliver a variety of cargoes including small molecules, proteins, nucleic acids, etc. inside any cell type [100-102]. This property makes them highly efficient in an in vitro system. However, the same property of CPP to deliver cargoes to other normal tissues in an in vivo system hinders their clinical applications [103-105]. In case of an antineoplasic cargo, the peptides can cause systemic toxicity, which in lower levels may well be acceptable but beyond a threshold may cause severe side effects [103-105]. The positive charge, a common feature of most CPPs, though advantageous for cell penetration may lead to drug delivery inefficacy due to interactions with negatively charged serum proteins, resulting in their pre-mature degradation in blood [106].

Some research groups have demonstrated that some CPPs can selectively permeate cancer cells instead of non-cancerous or normal cells [107-111]. This could be partly due to the differences in membrane composition of normal and cancer cells [66]. Cancer cells have more numbers of glycosaminoglycans and anionic phosphatidylserine on their surface than normal cells, which attract more cationic CPPs than normal cells [66, 112, 113]. Jobin et al. have previously

demonstrated that the RW16 peptide derived from penetratin interacts more with anionic liposomes than zwitterionic ones [114]. Further, tumor cells express higher levels of different receptors which can be utilized for "tumor homing" applications [66]. Apart from the membrane-based differences between cancer and healthy cells, the tumor macroenvironment factors like angiogenesis, hypoxia and inflammation can also be used for differentiating between cancer and healthy cells [115, 116]. Therefore, in the purview of anticancer therapies and targeted delivery, a CPP should have some form of cell type specificity.

2.7. CPPS FOR ANTI-CANCER DRUG DELIVERY

Cancer is an epigenetic disease characterized by unregulated cell proliferation and a major cause of death worldwide [107, 117-120]. Present chemotherapeutic strategies are synonymous with the term "a Pyrrhic victory" due to a variety of side effects. Further, the drugs sometimes are unable to penetrate the vasculature of cancer cells leading to inaction. The delivery of anticancer drugs through CPPs offers avenues for targeted delivery of drug molecules to intended site, increasing drug efficacy and resucing side effects [121]. Multiple reports in literature describe the use of peptides for cancer therapy. Some of these findings are discussed in the following sections.

2.7.1. CPPs for Targeted Delivery

The heterogeneity of cancer and healthy cells discussed in the previous section provides avenues for targeted delivery exploiting these differences in cell types. Peptides reported for cancer-specific targeting can further be classified as a) Homing Peptides (HP), b) CPPs with Homing Domains and c) Cell-Penetrating and Tumor Homing peptides (CPTHP) [122]. Homing peptides do not penetrate cells and deliver the cargo to the surface. Homing peptides conjugated with a CPP can penetrate cell membranes for intracellular drug delivery. CPTHP peptides are peptides, which selectively penetrate tumor cells without an externally conjugated homing domain.

2.7.2. Delivery of Anticancer Drugs using CPPs

Conjugation of Taxol [123], Methotrexate (MTX) [24], Doxorubicin (Dox) [124, 125] to CPPs reportedly increase their membrane permeability. The linking of taxol to octa-arginine through disulphide linkers increases its solubility in aqueous systems and pharmacokinetics. The delivery of MTX and Dox has shown to increase the cytotoxicity of the drugs and overcome multi-drug resistance. Additionally, CPPs have also been used to deliver nucleotides and therapeutic proteins to cancer cells. A detailed account of the same is beyond the scope of this study and can be found in the following reference [126].

2.8. DESIGNING CPPs

In terms of protein folding, CPPs with a poly-L backbone can adopt α-helical, β-sheet or disordered conformations in solution. The disordered CPPs can re-conform to either of the two secondary structures. In this section, I will discuss the different avenues available for the design of novel peptides with cell penetrative activity based on amino acid sequence and structural parameters.

2.8.1. Amino Acid Sequence

Proteins and peptides are polymers of different amino acid monomers. Each amino acid monomer consists of a main chain composed of backbone atoms (N, C-α, C and O) and a variable side-chain. The spatial orientation of the different side-chain array combinations provide uniqueness to each peptide molecule, which is responsible for its function. In the following sub-sections, I will discuss the effects of various amino acid properties on cell penetration.

2.8.1.1. Chirality

Most CPPs derived from natural proteins are composed of L-amino acids [27]. This makes them more susceptible to proteolytic degradation, which may lead to their inaction in an in vivo system. The use of D-stereoisomers increases the stability of peptdes against proteolytic cleavage [127]. Poly-D peptides have more stability but often have lower cellular uptake than the poly-L sequences [51, 127, 128]. The internalization efficiency of peptides is also reported to be affected

by the number of D-amino acids in a sequence [128, 129]. Multiple substitutions of L-amino acids to D-amino acids can alter the α-helix to β-sheet ratio of CPPs, thereby affecting their cellular uptake [128]. Interestingly, the use of D-Pro to conform the disordered structure of a CPP provided proteolytic stability and a non-endosomal pathway of uptake [91]. The contribution of chirality towards cell penetration remains unclear in the absence of a detailed study.

2.8.1.2. Cationic Charge

Cationic charged residues are known to promote cell penetration of CPPs [31, 130, 131]. The first CPP, TAT contains eleven cationic residues [15, 16]. Poly-arginines were among the first synthetic CPPs due to their cationicity and the ability of guanidium groups to form bidentate hydrogen bonds, critical for membrane permeation [31]. However, the length of sequence, position and number of arginines in sequence affect their cellular uptake [132, 133]. Kelley and co-workers demonstrated an interesting example of designing cationic CPPs [80]. The designed peptides were imparted with positive charge through arginine and lysine along with a lipophilic character is due to the presence of phenylalanine and cyclohexylalanine. The combination of these two characters gave the peptides the ability to selectively penetrate the mitochondria [80].

2.8.1.3. Hydrophobicity and aromaticity

Hydrophobicity in peptide sequences can be accomplished by the use of aliphatic and aromatic amino acids. Aromatic amino acids are more hydrophobic and possess favorable free energy of interaction with the lipid bilayer. Aromatic rings can form Π-Π stack with membrane proteins and may contribute to stabilization/promotion of CPPs with membranes [134]. The use of polymeric aromatic groups as peptide modifications have been reported to increase the uptake of poly-arginines [135].

2.8.2. Secondary Structure Folding and its effects on Cellular Uptake

Two interconnected parameters should be considered to study the effect of peptide folding on cellular uptake. Firstly, the affinity of the CPP for membranes

and secondly, the folding capacity of proteins in presence of membranes. Electrostatic forces, hydrophobic interactions and hydrogen bonding characterize the membrane-CPP interaction. Most CPPs adopt α-helical conformations upon membrane interaction, which provides a template for the interplay of different interaction forces [136]. Therefore, constricting the geometry of a known CPP to a helical conformation may provide the ideal structural template for re-design of novel CPPs with tailored structural amphipathicity, which in turn may help increase their cellular uptake.

Ramakrishnan et al. have previously described the role of syndiotactic backbone on the conformational locking of peptidic structures [137]. Syndiotactic peptides are capable of forming a Π(L,D) helix, which is thermodynamically more stable than the α-helix. Further, the use of unnatural amino acids can help in conforming the peptide structure in a stable configuration [137, 138]. Together, these design inputs available in literature along with other specific methods in literature can be exploited for the design of novel peptides with cell-penetrative ability.

2.9. SUMMARY

In the present chapter, the use of peptide-based drug delivery vectors for transporting different cargoes inside the cell was detailed. The use of peptides as drug delivery agents presents its own set of pros and cons. The peptides termed as protein transduction domains, Trojan horse and cell-penetrating peptides (CPPs) have the ability to traverse live cell membranes. The classification of CPPs on the basis of their physico-chemical properties provides important insights into their mechanism of action (cellular uptake). The fate of peptides inside the cell is dependent on the path of cellular uptake. Moreover, it is learnt from different reports in literature that cell-type specificity is required for the targeted delivery of anticancer agents inside the cell for future in vivo applications. This may be achieved by the inclusion of a homing domain with the cell-penetrating domain of the designed peptides. Alternately, some peptides possess the dualistic nature of CPP and HP. The design of CPPs based on various sequence and structural parameters offers new directions for the de novo design of novel CPPs with tailored features and functions.

2.10. REFERENCES

[1] Strebhardt K, Ullrich A. Paul Ehrlich's magic bullet concept: 100 years of progress. Nature Reviews Cancer 2008;8:473.
[2] Pattni BS, Torchilin VP. Targeted Drug Delivery Systems: Strategies and Challenges. In: Devarajan PV, Jain S, editors. Targeted Drug Delivery : Concepts and Design. Cham: Springer International Publishing; 2015. p. 3-38.
[3] Bae YH, Park K. Targeted drug delivery to tumors: myths, reality and possibility. Journal of controlled release : official journal of the Controlled Release Society 2011;153:198-205.
[4] Rosenholm JM, Sahlgren C, Lindén M. Towards multifunctional, targeted drug delivery systems using mesoporous silica nanoparticles – opportunities & challenges. Nanoscale 2010;2:1870-83.
[5] De Rycker M, Baragaña B, Duce SL, Gilbert IH. Challenges and recent progress in drug discovery for tropical diseases. Nature 2018;559:498-506.
[6] Gutierrez ME, Kummar S, Giaccone G. Next generation oncology drug development: opportunities and challenges. Nature Reviews Clinical Oncology 2009;6:259.
[7] Scannell JW, Bosley J. When Quality Beats Quantity: Decision Theory, Drug Discovery, and the Reproducibility Crisis. PLOS ONE 2016;11:e0147215.
[8] Singh R, Lillard JW. Nanoparticle-based targeted drug delivery. Experimental and Molecular Pathology 2009;86:215-23.
[9] Sudimack J, Lee RJ. Targeted drug delivery via the folate receptor. Advanced Drug Delivery Reviews 2000;41:147-62.
[10] Antony AC. The biological chemistry of folate receptors. Blood 1992;79:2807-20.
[11] Jansen G. Receptor-and carrier-mediated transport systems for folates and antifolates. Antifolate drugs in cancer therapy: Springer; 1999. p. 293-321.
[12] Tiwari G, Tiwari R, Sriwastawa B, Bhati L, Pandey S, Pandey P, Bannerjee SK. Drug delivery systems: An updated review. International journal of pharmaceutical investigation 2012;2:2.
[13] Gelperina S, Kisich K, Iseman MD, Heifets L. The potential advantages of nanoparticle drug delivery systems in chemotherapy of tuberculosis. American journal of respiratory and critical care medicine 2005;172:1487-90.
[14] Sastry SV, Nyshadham JR, Fix JA. Recent technological advances in oral drug delivery–a review. Pharmaceutical science & technology today 2000;3:138-45.
[15] Frankel AD, Pabo CO. Cellular uptake of the tat protein from human immunodeficiency virus. Cell 1988;55:1189-93.
[16] Joliot A, Pernelle C, Deagostini-Bazin H, Prochiantz A. Antennapedia homeobox peptide regulates neural morphogenesis. Proceedings of the National Academy of Sciences of the United States of America 1991;88:1864-8.

[17] Bechara C, Sagan S. Cell-penetrating peptides: 20years later, where do we stand? FEBS Letters 2013;587:1693-702.
[18] Morris MC, Vidal P, Chaloin L, Heitz F, Divita G. A new peptide vector for efficient delivery of oligonucleotides into mammalian cells. Nucleic acids research 1997;25:2730-6.
[19] Kang MJ, Kim BG, Eum JY, Park SH, Choi SE, An JJ, Jang SH, Eum WS, Lee J, Lee MW, Kang K, Oh CH, Choi SY, Choi YW. Design of a Pep-1 peptide-modified liposomal nanocarrier system for intracellular drug delivery: Conformational characterization and cellular uptake evaluation. Journal of drug targeting 2011;19:497-505.
[20] Morris MC, Depollier J, Mery J, Heitz F, Divita G. A peptide carrier for the delivery of biologically active proteins into mammalian cells. Nature Biotechnology 2001;19:1173.
[21] Pooga M, Hällbrink M, Zorko M, Uuml, Langel l. Cell penetration by transportan. The FASEB Journal 1998;12:67-77.
[22] Elliott G, O'Hare P. Intercellular Trafficking and Protein Delivery by a Herpesvirus Structural Protein. Cell 1997;88:223-33.
[23] Elmquist A, Lindgren M, Bartfai T, Langel Ü. VE-cadherin-derived cell-penetrating peptide, pVEC, with carrier functions. Experimental cell research 2001;269:237-44.
[24] Lindgren M, Rosenthal-Aizman K, Saar K, Eiríksdóttir E, Jiang Y, Sassian M, Östlund P, Hällbrink M, Langel Ü. Overcoming methotrexate resistance in breast cancer tumour cells by the use of a new cell-penetrating peptide. Biochemical pharmacology 2006;71:416-25.
[25] El-Andaloussi S, Johansson HJ, Holm T, Langel Ü. A Novel Cell-penetrating Peptide, M918, for Efficient Delivery of Proteins and Peptide Nucleic Acids. Molecular Therapy 2007;15:1820-6.
[26] Heitz F, Morris MC, Divita G. Twenty years of cell-penetrating peptides: from molecular mechanisms to therapeutics. British journal of pharmacology 2009;157:195-206.
[27] Agrawal P, Bhalla S, Usmani SS, Singh S, Chaudhary K, Raghava Gajendra PS, Gautam A. CPPsite 2.0: a repository of experimentally validated cell-penetrating peptides. Nucleic Acids Research 2016;44:D1098-D103.
[28] Feni L, Neundorf I. The Current Role of Cell-Penetrating Peptides in Cancer Therapy. Advances in experimental medicine and biology 2017;1030:279-95.
[29] Fosgerau K, Hoffmann T. Peptide therapeutics: current status and future directions. Drug Discovery Today 2015;20:122-8.
[30] Kumar A, Ramakrishnan V. Creating novel protein scripts beyond natural alphabets. Systems and synthetic biology 2010;4:247-56.
[31] Futaki S, Suzuki T, Ohashi W, Yagami T, Tanaka S, Ueda K, Sugiura Y. Arginine-rich peptides. An abundant source of membrane-permeable peptides

having potential as carriers for intracellular protein delivery. The Journal of biological chemistry 2001;276:5836-40.
[32] Wender PA, Mitchell DJ, Pattabiraman K, Pelkey ET, Steinman L, Rothbard JB. The design, synthesis, and evaluation of molecules that enable or enhance cellular uptake: peptoid molecular transporters. Proceedings of the National Academy of Sciences of the United States of America 2000;97:13003-8.
[33] Tunnemann G, Ter-Avetisyan G, Martin RM, Stockl M, Herrmann A, Cardoso MC. Live-cell analysis of cell penetration ability and toxicity of oligo-arginines. Journal of peptide science : an official publication of the European Peptide Society 2008;14:469-76.
[34] Herce HD, Garcia AE, Cardoso MC. Fundamental Molecular Mechanism for the Cellular Uptake of Guanidinium-Rich Molecules. Journal of the American Chemical Society 2014;136:17459-67.
[35] Prochiantz A. Getting hydrophilic compounds into cells: lessons from homeopeptides. Current opinion in neurobiology 1996;6:629-34.
[36] Oglecka K, Lundberg P, Magzoub M, Goran Eriksson LE, Langel U, Graslund A. Relevance of the N-terminal NLS-like sequence of the prion protein for membrane perturbation effects. Biochimica et biophysica acta 2008;1778:206-13.
[37] Oehlke J, Scheller A, Wiesner B, Krause E, Beyermann M, Klauschenz E, Melzig M, Bienert M. Cellular uptake of an alpha-helical amphipathic model peptide with the potential to deliver polar compounds into the cell interior non-endocytically. Biochimica et biophysica acta 1998;1414:127-39.
[38] Oehlke J, Scheller A, Janek K, Wiesner B, Krause E, Beyermann M, Bienert M. Rapid translocation of amphipathic βhelical and β-sheet-forming peptides through plasma membranes of endothelial cells. Peptide Science—Present and Future: Springer; 1999. p. 782-3.
[39] Wolf Y, Pritz S, Abes S, Bienert M, Lebleu B, Oehlke J. Structural Requirements for Cellular Uptake and Antisense Activity of Peptide Nucleic Acids Conjugated with Various Peptides. Biochemistry 2006;45:14944-54.
[40] Soomets U, Lindgren M, Gallet X, Hallbrink M, Elmquist A, Balaspiri L, Zorko M, Pooga M, Brasseur R, Langel U. Deletion analogues of transportan. Biochimica et biophysica acta 2000;1467:165-76.
[41] Richard JP, Melikov K, Vives E, Ramos C, Verbeure B, Gait MJ, Chernomordik LV, Lebleu B. Cell-penetrating peptides A reevaluation of the mechanism of cellular uptake. Journal of Biological Chemistry 2003;278:585-90.
[42] Kauffman WB, Fuselier T, He J, Wimley WC. Mechanism matters: a taxonomy of cell penetrating peptides. Trends in biochemical sciences 2015;40:749-64.
[43] Guidotti G, Brambilla L, Rossi D. Cell-penetrating peptides: from basic research to clinics. Trends in pharmacological sciences 2017;38:406-24.

[44] Guo Z, Peng H, Kang J, Sun D. Cell-penetrating peptides: Possible transduction mechanisms and therapeutic applications. Biomedical reports 2016;4:528-34.
[45] Patel LN, Zaro JL, Shen W-C. Cell penetrating peptides: intracellular pathways and pharmaceutical perspectives. Pharmaceutical research 2007;24:1977-92.
[46] Conner SD, Schmid SL. Regulated portals of entry into the cell. Nature 2003;422:37-44.
[47] Eitzen G. Actin remodeling to facilitate membrane fusion. Biochimica et biophysica acta 2003;1641:175-81.
[48] Green M, Loewenstein PM. Autonomous functional domains of chemically synthesized human immunodeficiency virus tat trans-activator protein. Cell 1988;55:1179-88.
[49] Ryser HJ, Shen WC. Conjugation of methotrexate to poly(L-lysine) increases drug transport and overcomes drug resistance in cultured cells. Proceedings of the National Academy of Sciences of the United States of America 1978;75:3867-70.
[50] Shen WC, Ryser HJ. Conjugation of poly-L-lysine to albumin and horseradish peroxidase: a novel method of enhancing the cellular uptake of proteins. Proceedings of the National Academy of Sciences of the United States of America 1978;75:1872-6.
[51] Verdurmen Wouter PR, Bovee-Geurts Petra H, Wadhwani P, Ulrich Anne S, Hällbrink M, van Kuppevelt Toin H, Brock R. Preferential Uptake of L- versus D-Amino Acid Cell-Penetrating Peptides in a Cell Type-Dependent Manner. Chemistry & Biology 2011;18:1000-10.
[52] Ruoslahti E. Targeting tumor vasculature with homing peptides from phage display. Seminars in cancer biology: Elsevier; 2000. p. 435-42.
[53] Pasqualini R, Koivunen E, Ruoslahti E. αv integrins as receptors for tumor targeting by circulating ligands. Nature biotechnology 1997;15:542.
[54] Arap W, Pasqualini R, Ruoslahti E. Cancer treatment by targeted drug delivery to tumor vasculature in a mouse model. Science 1998;279:377-80.
[55] Aoki Y, Hosaka S, Kawa S, Kiyosawa K. Potential tumor-targeting peptide vector of histidylated oligolysine conjugated to a tumor-homing RGD motif. Cancer gene therapy 2001;8:783.
[56] Fleming E, Maharaj NP, Chen JL, Nelson RB, Elmore DE. Effect of lipid composition on buforin II structure and membrane entry. Proteins: Structure, Function, and Bioinformatics 2008;73:480-91.
[57] Copolovici DM, Langel K, Eriste E, Langel Ü. Cell-Penetrating Peptides: Design, Synthesis, and Applications. ACS Nano 2014;8:1972-94.
[58] Klahn M, Zacharias M. Transformations in plasma membranes of cancerous cells and resulting consequences for cation insertion studied with molecular dynamics. Physical Chemistry Chemical Physics 2013;15:14427-41.

[59] Hazam PK, Jerath G, Kumar A, Chaudhary N, Ramakrishnan V. Effect of tacticity-derived topological constraints in bactericidal peptides. Biochimica et Biophysica Acta (BBA) - Biomembranes 2017;1859:1388-95.
[60] Fittipaldi A, Ferrari A, Zoppe M, Arcangeli C, Pellegrini V, Beltram F, Giacca M. Cell membrane lipid rafts mediate caveolar endocytosis of HIV-1 Tat fusion proteins. The Journal of biological chemistry 2003;278:34141-9.
[61] Komin A, Russell LM, Hristova KA, Searson PC. Peptide-based strategies for enhanced cell uptake, transcellular transport, and circulation: Mechanisms and challenges. Adv Drug Deliv Rev 2017;110-111:52-64.
[62] Wadia JS, Stan RV, Dowdy SF. Transducible TAT-HA fusogenic peptide enhances escape of TAT-fusion proteins after lipid raft macropinocytosis. Nat Med 2004;10:310-5.
[63] Kaplan IM, Wadia JS, Dowdy SF. Cationic TAT peptide transduction domain enters cells by macropinocytosis. J Control Release 2005;102:247-53.
[64] Ye J, Liu E, Yu Z, Pei X, Chen S, Zhang P, Shin MC, Gong J, He H, Yang VC. CPP-Assisted Intracellular Drug Delivery, What Is Next? International journal of molecular sciences 2016;17.
[65] Reissmann S. Cell penetration: scope and limitations by the application of cell-penetrating peptides. Journal of peptide science : an official publication of the European Peptide Society 2014;20:760-84.
[66] Jobin M-L, Alves ID. On the importance of electrostatic interactions between cell penetrating peptides and membranes: A pathway toward tumor cell selectivity? Biochimie 2014;107:154-9.
[67] Raucher D, Ryu JS. Cell-penetrating peptides: strategies for anticancer treatment. Trends Mol Med 2015;21:560-70.
[68] Shin MC, Zhang J, Ah Min K, Lee K, Moon C, Balthasar JP, Yang VC. Combination of antibody targeting and PTD-mediated intracellular toxin delivery for colorectal cancer therapy. J Control Release 2014;194:197-210.
[69] Derossi D, Calvet S, Trembleau A, Brunissen A, Chassaing G, Prochiantz A. Cell Internalization of the Third Helix of the Antennapedia Homeodomain Is Receptor-independent. Journal of Biological Chemistry 1996;271:18188-93.
[70] Alves ID, Goasdoué N, Correia I, Aubry S, Galanth C, Sagan S, Lavielle S, Chassaing G. Membrane interaction and perturbation mechanisms induced by two cationic cell penetrating peptides with distinct charge distribution. Biochimica et Biophysica Acta (BBA) - General Subjects 2008;1780:948-59.
[71] Joanne P, Galanth C, Goasdoué N, Nicolas P, Sagan S, Lavielle S, Chassaing G, El Amri C, Alves ID. Lipid reorganization induced by membrane-active peptides probed using differential scanning calorimetry. Biochimica et Biophysica Acta (BBA) - Biomembranes 2009;1788:1772-81.
[72] Kawamoto S, Takasu M, Miyakawa T, Morikawa R, Oda T, Futaki S, Nagao H. Inverted micelle formation of cell-penetrating peptide studied by coarse-grained

simulation: Importance of attractive force between cell-penetrating peptides and lipid head group. The Journal of Chemical Physics 2011;134:095103.
[73] Guidotti G, Brambilla L, Rossi D. Cell-Penetrating Peptides: From Basic Research to Clinics. Trends Pharmacol Sci 2017;38:406-24.
[74] Jarver P, Mager I, Langel U. In vivo biodistribution and efficacy of peptide mediated delivery. Trends Pharmacol Sci 2010;31:528-35.
[75] Lopez-Meza JE, Ochoa-Zarzosa A. Antimicrobial peptides: current and potential applications in biomedical therapies. 2015;2015:367243.
[76] Pomès R, Roux B. Molecular mechanism of H+ conduction in the single-file water chain of the gramicidin channel. Biophysical journal 2002;82:2304-16.
[77] Bechara C, Sagan S. Cell-penetrating peptides: 20 years later, where do we stand? FEBS Lett 2013;587:1693-702.
[78] Rothbard JB, Jessop TC, Lewis RS, Murray BA, Wender PA. Role of Membrane Potential and Hydrogen Bonding in the Mechanism of Translocation of Guanidinium-Rich Peptides into Cells. Journal of the American Chemical Society 2004;126:9506-7.
[79] Wender PA, Galliher WC, Goun EA, Jones LR, Pillow TH. The design of guanidinium-rich transporters and their internalization mechanisms. Advanced Drug Delivery Reviews 2008;60:452-72.
[80] Horton KL, Stewart KM, Fonseca SB, Guo Q, Kelley SO. Mitochondria-penetrating peptides. Chem Biol 2008;15:375-82.
[81] Komin A, Russell LM, Hristova KA, Searson PC. Peptide-based strategies for enhanced cell uptake, transcellular transport, and circulation: Mechanisms and challenges. Advanced Drug Delivery Reviews 2017;110-111:52-64.
[82] Guterstam P, Madani F, Hirose H, Takeuchi T, Futaki S, Andaloussi SE, Gräslund A, Langel Ü. Elucidating cell-penetrating peptide mechanisms of action for membrane interaction, cellular uptake, and translocation utilizing the hydrophobic counter-anion pyrenebutyrate. Biochimica et Biophysica Acta (BBA)-Biomembranes 2009;1788:2509-17.
[83] Rydström A, Deshayes S, Konate K, Crombez L, Padari K. Direct Translocation as Major Cellular Uptake for CADY Self-Assembling Peptide. 2011.
[84] Ezzat K, Helmfors H, Tudoran O, Juks C, Lindberg S, Padari K, El-Andaloussi S, Pooga M, Langel Ü. Scavenger receptor-mediated uptake of cell-penetrating peptide nanocomplexes with oligonucleotides. The FASEB Journal 2012;26:1172-80.
[85] Rangel R, Guzman-Rojas L, Le Roux LG, Staquicini FI, Hosoya H, Barbu EM, Ozawa MG, Nie J, Dunner Jr K, Langley RR. Combinatorial targeting and discovery of ligand-receptors in organelles of mammalian cells. Nature communications 2012;3:788.
[86] Holm T, Netzereab S, Hansen M, Langel Ü, Hällbrink M. Uptake of cell-penetrating peptides in yeasts. FEBS letters 2005;579:5217-22.

[87] Nekhotiaeva N, Awasthi SK, Nielsen PE, Good L. Inhibition of Staphylococcus aureus gene expression and growth using antisense peptide nucleic acids. Molecular Therapy 2004;10:652-9.
[88] Good L, Awasthi SK, Dryselius R, Larsson O, Nielsen PE. Bactericidal antisense effects of peptide–PNA conjugates. Nature biotechnology 2001;19:360.
[89] Nekhotiaeva N, Elmquist A, Rajarao GK, Hallbrink M, Langel U, Good L. Cell entry and antimicrobial properties of eukaryotic cell-penetrating peptides. The FASEB journal 2004;18:394-6.
[90] Mäe M, Myrberg H, Jiang Y, Paves H, Valkna A, Langel Ü. Internalisation of cell-penetrating peptides into tobacco protoplasts. Biochimica et Biophysica Acta (BBA)-Biomembranes 2005;1669:101-7.
[91] Medina SH, Miller SE, Keim AI, Gorka AP, Schnermann MJ, Schneider JP. An Intrinsically Disordered Peptide Facilitates Non-Endosomal Cell Entry. Angewandte Chemie International Edition 2016;55:3369-72.
[92] Sandberg M, Eriksson L, Jonsson J, Sjöström M, Wold S. New chemical descriptors relevant for the design of biologically active peptides. A multivariate characterization of 87 amino acids. Journal of medicinal chemistry 1998;41:2481-91.
[93] Hansen M, Kilk K, Langel Ü. Predicting cell-penetrating peptides. Advanced drug delivery reviews 2008;60:572-9.
[94] Lindgren M, Langel Ü. Classes and prediction of cell-penetrating peptides. Cell-Penetrating Peptides: Springer; 2011. p. 3-19.
[95] Sanders WS, Johnston CI, Bridges SM, Burgess SC, Willeford KO. Prediction of cell penetrating peptides by support vector machines. PLoS computational biology 2011;7:e1002101.
[96] Suhorutsenko J, Eriste E, Copolovici D-M, Langel Ü. Human Protein 53-derived Cell-penetrating peptides. International Journal of Peptide Research and Therapeutics 2012;18:291-7.
[97] Yamada T, Christov K, Shilkaitis A, Bratescu L, Green A, Santini S, Bizzarri A, Cannistraro S, Gupta T, Beattie C. p28, a first in class peptide inhibitor of cop1 binding to p53. British journal of cancer 2013;108:2495.
[98] A Dobchev D, Mager I, Tulp I, Karelson G, Tamm T, Tamm K, Janes J, Langel U, Karelson M. Prediction of cell-penetrating peptides using artificial neural networks. Current computer-aided drug design 2010;6:79-89.
[99] Gautam A, Chaudhary K, Kumar R, Raghava GPS. Computer-aided virtual screening and designing of cell-penetrating peptides. Cell-Penetrating Peptides: Springer; 2015. p. 59-69.
[100] Milletti F. Cell-penetrating peptides: classes, origin, and current landscape. Drug Discovery Today 2012;17:850-60.
[101] Temsamani J, Vidal P. The use of cell-penetrating peptides for drug delivery. Drug Discovery Today 2004;9:1012-9.

[102] Gupta B, Levchenko TS, Torchilin VP. Intracellular delivery of large molecules and small particles by cell-penetrating proteins and peptides. Advanced Drug Delivery Reviews 2005;57:637-51.
[103] Huang Y, Jiang Y, Wang H, Wang J, Shin MC, Byun Y, He H, Liang Y, Yang VC. Curb challenges of the "Trojan Horse" approach: smart strategies in achieving effective yet safe cell-penetrating peptide-based drug delivery. Advanced drug delivery reviews 2013;65:1299-315.
[104] Shi N-Q, Qi X-R, Xiang B, Zhang Y. A survey on "Trojan Horse" peptides: opportunities, issues and controlled entry to "Troy". Journal of controlled release 2014;194:53-70.
[105] Koren E, Torchilin VP. Cell-penetrating peptides: breaking through to the other side. Trends in molecular medicine 2012;18:385-93.
[106] Buyens K, De Smedt SC, Braeckmans K, Demeester J, Peeters L, van Grunsven LA, du Jeu XdM, Sawant R, Torchilin V, Farkasova K. Liposome based systems for systemic siRNA delivery: stability in blood sets the requirements for optimal carrier design. Journal of controlled release 2012;158:362-70.
[107] Farkhani SM, Valizadeh A, Karami H, Mohammadi S, Sohrabi N, Badrzadeh F. Cell penetrating peptides: efficient vectors for delivery of nanoparticles, nanocarriers, therapeutic and diagnostic molecules. Peptides 2014;57:78-94.
[108] Nakase I, Takeuchi T, Tanaka G, Futaki S. Methodological and cellular aspects that govern the internalization mechanisms of arginine-rich cell-penetrating peptides. Advanced drug delivery reviews 2008;60:598-607.
[109] Bechara C, Pallerla M, Zaltsman Y, Burlina F, Alves ID, Lequin O, Sagan S. Tryptophan within basic peptide sequences triggers glycosaminoglycan-dependent endocytosis. The FASEB Journal 2013;27:738-49.
[110] Schröder-Borm H, Bakalova R, Andrä J. The NK-lysin derived peptide NK-2 preferentially kills cancer cells with increased surface levels of negatively charged phosphatidylserine. FEBS letters 2005;579:6128-34.
[111] Papo N, Seger D, Makovitzki A, Kalchenko V, Eshhar Z, Degani H, Shai Y. Inhibition of tumor growth and elimination of multiple metastases in human prostate and breast xenografts by systemic inoculation of a host defense–like lytic peptide. Cancer research 2006;66:5371-8.
[112] Ziegler A, Seelig J. Contributions of glycosaminoglycan binding and clustering to the biological uptake of the nonamphipathic cell-penetrating peptide WR9. Biochemistry 2011;50:4650-64.
[113] Åmand HL, Rydberg HA, Fornander LH, Lincoln P, Nordén B, Esbjörner EK. Cell surface binding and uptake of arginine-and lysine-rich penetratin peptides in absence and presence of proteoglycans. Biochimica et Biophysica Acta (BBA)-Biomembranes 2012;1818:2669-78.
[114] Jobin M-L, Bonnafous P, Temsamani H, Dole F, Grélard A, Dufourc EJ, Alves ID. The enhanced membrane interaction and perturbation of a cell penetrating peptide in the presence of anionic lipids: toward an understanding of its

selectivity for cancer cells. Biochimica et Biophysica Acta (BBA)-Biomembranes 2013;1828:1457-70.
[115] Danhier F, Feron O, Préat V. To exploit the tumor microenvironment: passive and active tumor targeting of nanocarriers for anti-cancer drug delivery. Journal of controlled release 2010;148:135-46.
[116] Quail DF, Joyce JA. Microenvironmental regulation of tumor progression and metastasis. Nature medicine 2013;19:1423.
[117] Hanahan D, Weinberg RA. The hallmarks of cancer. Cell 2000;100:57-70.
[118] Hanahan D, Weinberg RA. Hallmarks of cancer: the next generation. Cell 2011;144:646-74.
[119] Pietras K, Östman A. Hallmarks of cancer: interactions with the tumor stroma. Experimental cell research 2010;316:1324-31.
[120] Pavlova NN, Thompson CB. The emerging hallmarks of cancer metabolism. Cell metabolism 2016;23:27-47.
[121] Ruoslahti E. Tumor penetrating peptides for improved drug delivery. Adv Drug Deliv Rev 2017;110-111:3-12.
[122] Svensen N, Walton JG, Bradley M. Peptides for cell-selective drug delivery. Trends in pharmacological sciences 2012;33:186-92.
[123] Dubikovskaya EA, Thorne SH, Pillow TH, Contag CH, Wender PA. Overcoming multidrug resistance of small-molecule therapeutics through conjugation with releasable octaarginine transporters. Proceedings of the National Academy of Sciences of the United States of America 2008;105:12128-33.
[124] Aroui S, Brahim S, De Waard M, Breard J, Kenani A. Efficient induction of apoptosis by doxorubicin coupled to cell-penetrating peptides compared to unconjugated doxorubicin in the human breast cancer cell line MDA-MB 231. Cancer letters 2009;285:28-38.
[125] Dawidczyk CM, Russell LM, Searson PC. Recommendations for Benchmarking Preclinical Studies of Nanomedicines. Cancer Res 2015;75:4016-20.
[126] Borrelli A, Tornesello AL, Tornesello ML, Buonaguro FM. Cell Penetrating Peptides as Molecular Carriers for Anti-Cancer Agents. Molecules (Basel, Switzerland) 2018;23:295.
[127] Pujals S, Sabido E, Tarrago T, Giralt E. all-D proline-rich cell-penetrating peptides: a preliminary in vivo internalization study. Biochemical Society transactions 2007;35:794-6.
[128] Yamada T, Signorelli S, Cannistraro S, Beattie CW, Bizzarri AR. Chirality switching within an anionic cell-penetrating peptide inhibits translocation without affecting preferential entry. Molecular pharmaceutics 2015;12:140-9.
[129] Ma Y, Gong C, Ma Y, Fan F, Luo M, Yang F, Zhang YH. Direct cytosolic delivery of cargoes in vivo by a chimera consisting of D- and L-arginine residues. J Control Release 2012;162:286-94.

[130] Takayama K, Nakase I, Michiue H, Takeuchi T, Tomizawa K, Matsui H, Futaki S. Enhanced intracellular delivery using arginine-rich peptides by the addition of penetration accelerating sequences (Pas). J Control Release 2009;138:128-33.
[131] Liu Y, Mei L, Xu C, Yu Q, Shi K, Zhang L, Wang Y, Zhang Q, Gao H, Zhang Z, He Q. Dual Receptor Recognizing Cell Penetrating Peptide for Selective Targeting, Efficient Intratumoral Diffusion and Synthesized Anti-Glioma Therapy. Theranostics 2016;6:177-91.
[132] Kawaguchi Y, Takeuchi T, Kuwata K, Chiba J, Hatanaka Y, Nakase I, Futaki S. Syndecan-4 Is a Receptor for Clathrin-Mediated Endocytosis of Arginine-Rich Cell-Penetrating Peptides. Bioconjugate chemistry 2016;27:1119-30.
[133] Mishra A, Lai GH, Schmidt NW, Sun VZ, Rodriguez AR, Tong R, Tang L, Cheng J, Deming TJ, Kamei DT, Wong GC. Translocation of HIV TAT peptide and analogues induced by multiplexed membrane and cytoskeletal interactions. Proceedings of the National Academy of Sciences of the United States of America 2011;108:16883-8.
[134] deRonde BM, Birke A, Tew GN. Design of aromatic-containing cell-penetrating peptide mimics with structurally modified pi electronics. Chemistry (Weinheim an der Bergstrasse, Germany) 2015;21:3013-9.
[135] Perret F, Nishihara M, Takeuchi T, Futaki S, Lazar AN, Coleman AW, Sakai N, Matile S. Anionic fullerenes, calixarenes, coronenes, and pyrenes as activators of oligo/polyarginines in model membranes and live cells. J Am Chem Soc 2005;127:1114-5.
[136] Kalafatovic D, Giralt E. Cell-Penetrating Peptides: Design Strategies beyond Primary Structure and Amphipathicity. Molecules (Basel, Switzerland) 2017;22.
[137] Ramakrishnan V, Ranbhor R, Kumar A, Durani S. The Link between Sequence and Conformation in Protein Structures Appears To Be Stereochemically Established. The Journal of Physical Chemistry B 2006;110:9314-23.
[138] Urry DW. The Gramicidin A Transmembrane Channel: A Proposed $\pi_{(L,D)}$ Helix. Proceedings of the National Academy of Sciences 1971;68:672-6.

3

Objectives and Research Design

3.1. OBJECTIVES

The present study was designed to address the following objectives:

1. Design and synthesize cationic amphipathic peptides of diversified stereochemistry, as possible candidates for cell-penetration and drug delivery.
2. Study the effects of reduced chain length on the cellular uptake.
3. Evaluate the drug delivery potential of syndiotactic peptides against various cell lines with efficacy and specificity as primary yardsticks.
4. Mapping the amino acid-wise side-chain preferences in protein structures.
5. Characterization of consensus electrostatic signatures for cell penetration and small molecule delivery.
6. Evolution of a backbone engineered, electrostatic signature-based computational platform for the design of new peptides with tailored functional features.

3.2. RESEARCH DESIGN

Peptides are among the most favored biomolecules for applications as drug delivery vectors. The clinical applications of peptides as drug delivery vehicles is presently limited due to the loss of function in biological fluids, because of their inherent proteolytic susceptibility [1]. This restricts the use of peptides as both therapeutics and drug delivery vectors. N-terminus acetylation has been reported to increase the proteolytic stability of antimicrobial peptides [2-6]. This may not be applicable to peptides used for drug delivery applications as the N-terminus provides a site for attachment of different cargo molecules without much affecting the peptide sequence as in the case of other modes of attachment using a linker molecule. The use of unnatural amino acids in peptide sequence increases its proteolytic stability [6-11]. Therefore, to address this problem, a set of nearly fifty peptides using a mixture of L-, D-amino acids and Aib utilizing the inputs of peptide design from literature as discussed in section 2.7 were designed. The peptides were designed with different topological constraints,

chain length and amino acid sequences to impart varying profiles of structural amphipathicity and cationic charge distribution. The peptides were then screened for their cellular uptake profiles in comparison to the TAT peptide (data not shown).

The pilot study provided us with a set of amino acid sequences, which favor cell penetration. Based on these inputs, the positively screened peptides were re-designed using stereochemical reverse engineering, which resulted in their stereochemical and amino acid inverts. This provided us with three different series of peptides capable of cell penetration. These series of peptides were annotated as SARTHI, STRAP and CHAP series of peptides, based on their individual design principles. The present study is based on a set of questions, which are required to be answered in order to develop these three series of peptides from mere amino acid sequences to cell penetrating peptides and further to peptides for drug delivery applications. The first and foremost question to be addressed was whether these peptides do hold their topology as designed. The failure of conforming to a particular designed geometry would perturb the designed physico-chemical features like spatial charge distribution and structural amphipathicity. Therefore, the structural conformation of the designed peptides was first verified.

MDA-MB-231 and HeLa cell lines as representatives of breast and cervical cancer models respectively as our test systems due to their high incidence rates in the global population [12, 13] were used. These two models provide us with similar (cancerous) yet different (cell and tissue types) test models. This further, will help us to design peptides specific to different tissue types in the future. The primary function of a cell penetrating peptide is to penetrate the cell membrane and localize inside the cell. Thus, the next step in evaluation of the designed peptides was to check their intracellular distributions, whether it was specific to single cell organelle or was the intracellular distribution non-specific. Next, I wanted to compare the cellular uptake of these peptides with a known peptide to establish the relative efficiency of the designed peptides in terms of their cell penetrating ability. Using TAT (48-60) as a positive control of cell penetration as

it is one of the most well studied peptide for cell penetration [14-18]. The next step was to understand the cellular uptake profile of the designed peptides. This is critical to the understanding the activity (cell penetration) of the designed peptides under different physico-chemically variable environments. This provided us with valuable information regarding the cellular uptake mechanism of the designed peptides, which is vital to their efficacy in delivering a specific molecule inside the cell as discussed in the previous chapter.

The next and the most important question to be answered was whether the designed peptides lose their function in the presence of biological fluids, the principle roadblock for the evolution of a cell penetrating peptide to a potential drug delivery vector. The next critical roadblock for the development of the designed peptides as potential "targeted" drug delivery vectors was whether these peptides specifically penetrate the desired cell types. From our investigations, using the two cancer models, it was observed that the uptake of the peptides was varied in the two cell types. As discussed earlier, the two model systems have a similarity of being a cancerous cell but are derived from different tissue types. Therefore, a parity in uptake in the two model systems urged us to incorporate a third model system for studying the cell-type affinity of the designed peptides. HEK-293 (Human Embryonic Kidney) cells were used as it provides a different cell (non-cancerous) and tissue type. The differences of uptake in the three test model systems would help us better understand the affinity of the designed peptides towards different cell types and lead us closer to our long-term goal of designing peptides specific to cell types. Any specificity of the designed peptides towards either of the cell types would be serendipitous, as it was never included it as a part of the design philosophy. However, our investigations did provide us with an opportunity to test this lucrative ideology. A possibility of including more test model systems (cell lines) was also considered but due to the constraints of time, I focused our study on the three model systems. Further, it was decided to include more in vitro and in vivo model systems in future studies.

The above-mentioned roadblocks for development of targeted drug delivery vectors were addressed and I came to the concluding questions, ones that prelude the two above. i) Can the peptides deliver a functional therapeutic molecule (drug) with higher efficacy than the native drug? ii) Can it help overcome the drug resistance of cancer cells? and iii) Can it lower the toxicity of the drug to the other cell type?

To answer these questions, the peptides were conjugated with methotrexate. The three model systems (cell lines) used in our study provided us with the distinct capability required to answer these questions. MDA-MB-231 and Hela cells can be used as a model to address the first question. The drug resistance of MDA-MB-231 further helps in addressing the second question and HEK-293 provides a representative of non-cancerous and kidney cells. The use of a transformed non-cancerous cell line as a representative of a normal cell can be debated. Therefore, it was used as a representative of a non-cancerous cell line and not a normal cell. Moreover, it represents the renal tissue type. Therefore, a specificity to other cell lines (MDA-MB-231 and HeLa) in theory, would provide us with a set of peptides specific to these cancer cell types. Thus, the cell viability experiments were performed using peptide-MTX conjugates, peptide-CF conjugates and MTX alone against the three cell models to answer the three concluding questions.

The three series of peptides provide new insights for the designability of stable peptide backbone conformations using sequence re-design. However, each of the discussed peptide backbone conformation is highly dependent on the array of constituent amino acid side-chains. This observation lead us to initiate another task to design a computational platform for backbone and sequence optimization. Developing a design platform requires multiple information regarding protein folding, amino acid preferences, polarity, hydrophobicity, side-chain size etc. This work addresses the geometric evolution of protein folding into distinct secondary structures, their amino acid preferences and substitutions. It may also cater to the development of specialized tools required for a variety of computational analysis pertaining to protein design and engineering.

3.3. REFERENCES

[1] Copolovici DM, Langel K, Eriste E, Langel Ü. Cell-Penetrating Peptides: Design, Synthesis, and Applications. ACS Nano 2014;8:1972-94.

[2] Drazic A, Myklebust LM, Ree R, Arnesen T. The world of protein acetylation. Biochimica et Biophysica Acta (BBA) - Proteins and Proteomics 2016;1864:1372-401.

[3] Simonsson M, Heldin C-H, Ericsson J, Grönroos E. The Balance between Acetylation and Deacetylation Controls Smad7 Stability. Journal of Biological Chemistry 2005;280:21797-803.

[4] Sang Y, Ren J, Qin R, Liu S, Cui Z, Cheng S, Liu X, Lu J, Tao J, Yao YF. Acetylation Regulating Protein Stability and DNA-Binding Ability of HilD, thus Modulating Salmonella Typhimurium Virulence. The Journal of infectious diseases 2017;216:1018-26.

[5] Caron C, Boyault C, Khochbin S. Regulatory cross-talk between lysine acetylation and ubiquitination: role in the control of protein stability. BioEssays : news and reviews in molecular, cellular and developmental biology 2005;27:408-15.

[6] Zhao Y, Zhang M, Qiu S, Wang J, Peng J, Zhao P, Zhu R, Wang H, Li Y, Wang K, Yan W, Wang R. Antimicrobial activity and stability of the D-amino acid substituted derivatives of antimicrobial peptide polybia-MPI. AMB Express 2016;6:122-.

[7] Wang Y, Ee PLR, Khara JS, Hamilton MS, Langford PR, Newton SM, Robertson BD, Uhía I, Priestman M, Krishnan N, Yang YY. Unnatural amino acid analogues of membrane-active helical peptides with anti-mycobacterial activity and improved stability. Journal of Antimicrobial Chemotherapy 2016;71:2181-91.

[8] Oliva R, Chino M, Pane K, Pistorio V, De Santis A, Pizzo E, D'Errico G, Pavone V, Lombardi A, Del Vecchio P, Notomista E, Nastri F, Petraccone L. Exploring the role of unnatural amino acids in antimicrobial peptides. Scientific Reports 2018;8:8888.

[9] Meng H, Kumar K. Antimicrobial Activity and Protease Stability of Peptides Containing Fluorinated Amino Acids. Journal of the American Chemical Society 2007;129:15615-22.

[10] Khara JS, Priestman M, Uhia I, Hamilton MS, Krishnan N, Wang Y, Yang YY, Langford PR, Newton SM, Robertson BD, Ee PL. Unnatural amino acid analogues of membrane-active helical peptides with anti-mycobacterial activity and improved stability. The Journal of antimicrobial chemotherapy 2016;71:2181-91.

[11] Gentilucci L, De Marco R, Cerisoli L. Chemical modifications designed to improve peptide stability: incorporation of non-natural amino acids, pseudo-

peptide bonds, and cyclization. Current pharmaceutical design 2010;16:3185-203.

[12] Torre LA, Islami F, Siegel RL, Ward EM, Jemal A. Global Cancer in Women: Burden and Trends. Cancer Epidemiology Biomarkers & Prevention 2017;26:444-57.

[13] Ginsburg O, Bray F, Coleman MP, Vanderpuye V, Eniu A, Kotha SR, Sarker M, Huong TT, Allemani C, Dvaladze A, Gralow J, Yeates K, Taylor C, Oomman N, Krishnan S, Sullivan R, Kombe D, Blas MM, Parham G, Kassami N, Conteh L. The global burden of women's cancers: a grand challenge in global health. Lancet (London, England) 2017;389:847-60.

[14] Ziegler A, Nervi P, Durrenberger M, Seelig J. The cationic cell-penetrating peptide CPP(TAT) derived from the HIV-1 protein TAT is rapidly transported into living fibroblasts: optical, biophysical, and metabolic evidence. Biochemistry 2005;44:138-48.

[15] Srinivasan D, Muthukrishnan N, Johnson GA, Erazo-Oliveras A, Lim J, Simanek EE, Pellois J-P. Conjugation to the cell-penetrating peptide TAT potentiates the photodynamic effect of carboxytetramethylrhodamine. PloS one 2011;6:e17732-e.

[16] Bechara C, Sagan S. Cell-penetrating peptides: 20years later, where do we stand? FEBS Letters 2013;587:1693-702.

[17] Jeong C, Yoo J, Lee D, Kim Y-C. A branched TAT cell-penetrating peptide as a novel delivery carrier for the efficient gene transfection. Biomaterials Research 2016;20:28.

[18] Richard JP, Melikov K, Vives E, Ramos C, Verbeure B, Gait MJ, Chernomordik LV, Lebleu B. Cell-penetrating Peptides: A REEVALUATION OF THE MECHANISM OF CELLULAR UPTAKE. Journal of Biological Chemistry 2003;278:585-90.

4

Experimental Methods

This chapter elaborates the in general protocol employed while performing experiments. Specific modifications adopted, were mentioned in individual chapters.

4.1. EXPERIMENTAL MATERIAL AND METHODS

4.1.1. Materials

Side-chain protected Fmoc-amino acids were purchased from Merck and Sigma-Aldrich with >95 % purity. N,N-Diisopropylethylamine, thioanisole, m-cresol, ethanedithiol, tri-fluoro acetic acid, 5(6)Carboxyfluorescein, Methotrexate, Gramicidin A and Thiazolyl Blue Tetrazolium Bromide were purchased from Sigma-Aldrich (>95 % purity). Diethly ether, Piperidine and Dimethyl Formamide (DMF) of Synthesis grade were purchased from Merck. Methanol and Dimethyl Sulfoxide of spectroscopy grade were purchased from Merck. DMEM-F12 media was purchased from HyClone. Phosphate buffer saline, trypsin, antibiotic solutions and fetal bovine serum were purchased from Himedia laboratories. All other reagents used for the study were >95 % pure.

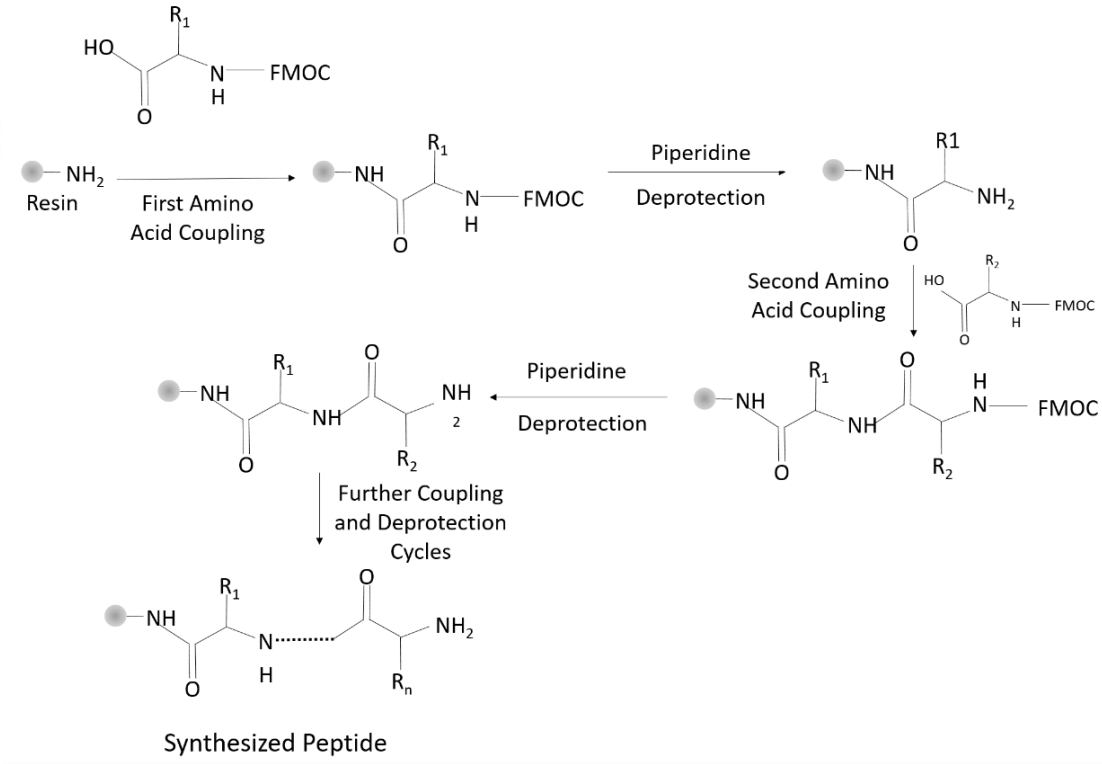

Figure 4.1. ***Peptide synthesis.*** *Peptides were synthesized from C to N position using a rink amide resin. The amino acids were attached sequentially with alternating cycles of Fmoc deprotection using piperidine and amino acid coupling.*

4.1.2. Peptide Synthesis

Peptides were synthesized by solid phase peptide synthesis using Fmoc chemistry on a rink amide resin (Figure 4.1). The peptides were synthesized from the C to N-terminus direction. The Fmoc deprotection was done in single cycle of 20 minutes with 30% piperidine. After Fmoc removal, piperidine was washed off with DMF. Amino acids were added in a threefold molar excess along with Hydroxybenzotriazole, 2-(1H-benzotriazol-1-yl)-1,1,3,3-tetramethyluronium hexafluorophosphate and N,N-Diisopropylethylamine. Subsequent amino acids, 5(6)Carboxyfluorescein and Methotrexate were attached to the N-terminus of the peptide using the same procedure (Figure 4.2). After completion, peptide was cleaved from the resin by using a cocktail of deprotection mixture comprising of thioanisole, m-cresol, ethanedithiol and tri-fluoro acetic acid. Cleaved peptides were precipitated in ice-cold diethyl ether and washed several times to remove the components of the deprotection mixture.

4.1.3. Peptide Purification and Primary Characterization

Peptides, thus extracted were purified by semi-preparative reverse-phase HPLC (Shimadzu) with a C-18 column using a 10-100% gradient of acetonitrile in water with 0.1% TFA by monitoring at 210 nm, 280 nm and 460 nm. Elutes from purification step were subjected to mass spectrometry using MALDI-TOF to characterize the synthesized peptide.

4.1.4. Circular Dichroism Spectroscopy

Peptides were dissolved in 1 mL of water to attain 10 µM solutions of peptides in water. To counter the solubility issues of Gramicidin A, it was dissolved in ethanol to a 5 mM stock concentration. The solution was further diluted in water to 10 µM concentration (1 mL total volume). The CD spectra was recorded using Jasco 700 CD spectropolarimeter with a quartz cuvette of path length 1 mm at 25 °C between 190 and 300 nm at a 1 nm interval. Mean residue molar ellipticity was calculated by the following equation:

$$\theta\ (\mathrm{deg.cm^2.dmol^{-1}}) = \frac{Ellipticity\ (mdeg).10^6}{Pathlength\ (mm).\ [Peptide](\mu M).\ n}$$

where, θ is the mean residue molar ellipticity, n is the number of peptide bonds and Ellipticity is the raw data collected by the instrument.

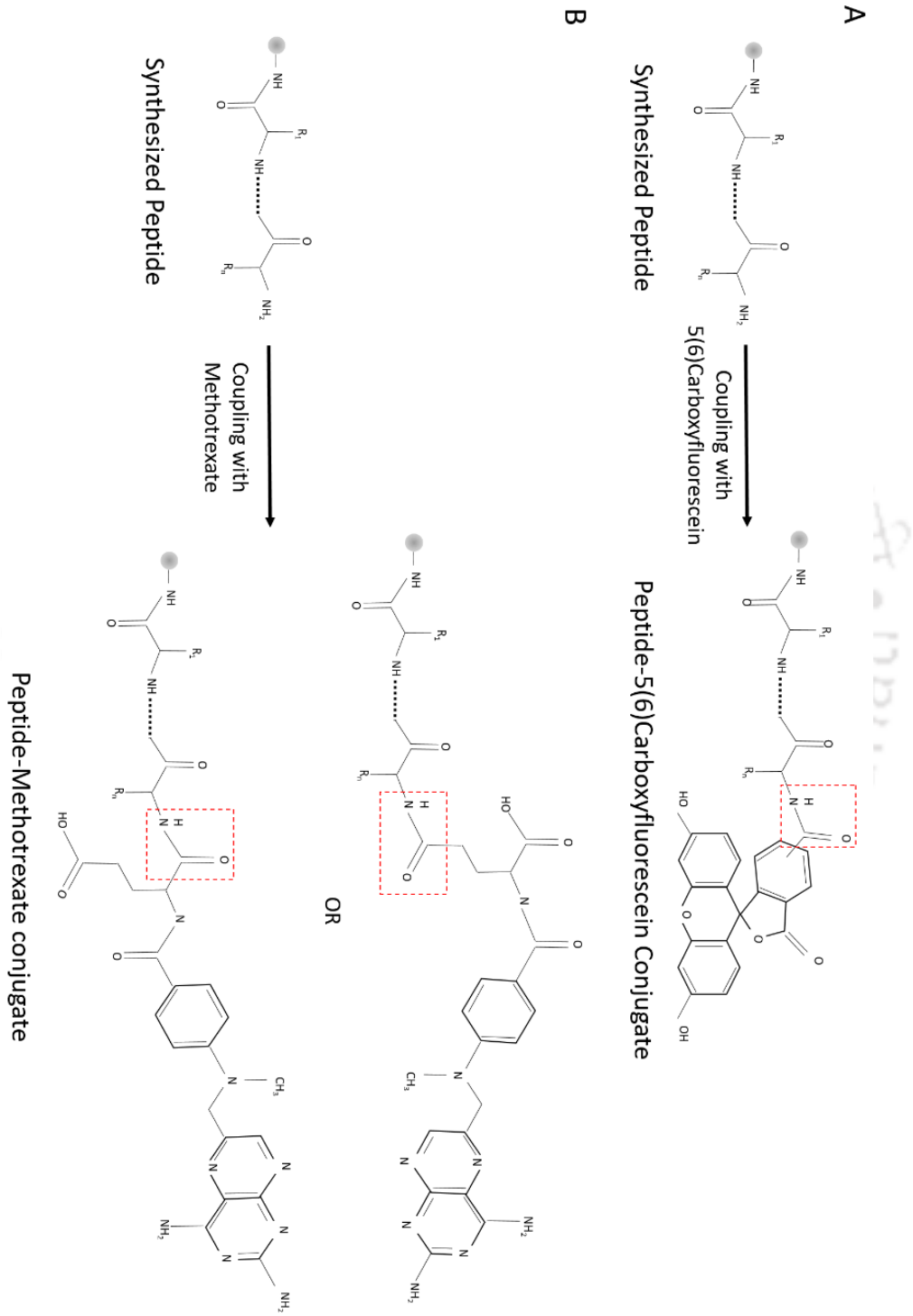

Figure 4.2. ***Conjugation of 5(6)Carboxyfluorescein and Methotrexate.*** *The N-terminal of synthesized peptides on resin was conjugated to the carboxyl group of*

5(6)Carboxyfluorescein (A) and Methotrexate (B) as per the illustration to form peptide-CF and peptide-MTX conjugates respectively.

4.1.5. Cell Culture

HeLa (Cervical cancer), HEK-293 (Human Embryonic Kidney) and MDA-MB-231(triple negative breast cancer) cells were grown as monolayer cultures in 1:1 DMEM-F12 medium supplemented by 10% Fetal Bovine Serum and 1% of antibiotics (Streptomycin and Penicillin). The cells were maintained at 37 °C and 5 % CO_2.

4.1.6. Fluorescence Microscopy

Ten thousand cells/well were seeded in 96-well plates and incubated them overnight at 37 °C with 5% CO_2. The cells were treated with peptide-CF conjugates in serum-free media and incubated for 4 hours. Untreated cells were taken as negative control in the experiment. The cells were then washed twice with 1X PBS and treated with 50 µL of 0.04 % Trypan Blue in 1X PBS for 5 minutes. Cells were washed twice and treated with 50 µL of 0.005 mg/ml Hoechst 33342 for 5 minutes to stain the nuclei of live cells. Following nuclei staining, cells were washed twice to remove any excess stain and viewed under Confocal Laser Scanning Microscope for imaging the uptake of peptide-CF conjugates. The contrast of the output images were adjusted for best viewing and therefore all results of microscopy are qualitative.

4.1.7. Flow Cytometry

Forty thousand cells/well were seeded in 24-well plates and incubated them overnight at 37 °C with 5% CO_2, followed by treatment with peptide-CF conjugates and incubated at 37 °C with 5 % CO_2 for 4 hour duration. Cells were washed with PBS and treated with 400 µL of 0.04% Trypan Blue in 1X PBS for 5 minutes to quench extracellular fluorescence followed by washing with 400 µL of PBS three times. Cells were lifted from wells by treating with 50 µL of 0.06 % EDTA in 1X PBS for 5 minutes. These extracts were suspended in 400 µL of PBS and kept on ice until analysis. Flow Cytometry analysis was done on a Becton Dickinson FACS CALIBUR.

4.1.8. Fluorescence Spectroscopy

Ten thousand cells/well were seeded in 96-well plates and incubated overnight at 37 °C with 5% CO_2. Cells were treated with peptide-CF conjugates for four hours followed by treatment with 50 µL of 0.005 mg/ml Hoechst 33342 for 5 minutes and subjected to Fluorescence Spectroscopy analysis using multimode microplate reader. Intracellular fluorescence of peptide-CF conjugates (ex 489 nm/ em 517 nm) and Hoechst 33342 (ex 346 nm / em 460 nm) were recorded. Intracellular intensity for carboxyfluorescein was corrected for accounting the differential number of cells by dividing it with Hoechst fluorescence intensity and multiplying the resulting value by 1000 to give "corrected fluorescence units" [1].

4.1.9. Mechanism of cellular uptake

The dependence of cellular uptake on various physico-chemical parameters were tested for the designed peptides. Dependence on temperature was studied by comparing the uptake of cells at 4 °C and 37 °C. Cells were pre-incubated for one hour at 4 °C. All peptide concentrations were prepared and stored at 4 °C for thirty minutes prior to treatment. The cells were washed with ice-cold PBS and treated with the refrigerated peptide concentrations in serum-free media at 4 °C. The energy requirements for cellular uptake were investigated by treating the cells with 0.1% sodium azide for one hour prior to peptide treatment [2, 3]. For blocking clathrin-mediated endocytosis, the cells were treated with hypermolar concentration of sucrose (0.45 M) in serum free media for one hour. The remaining procedures and post treatment analysis were the same as explained in section 4.1.8.

4.1.10. Serum Stable activity of peptides

The peptides were treated with equal volume of Human plasma or Bovine serum at 37 °C for one hour. The same stock solutions were used for treating HeLa cells for four hours at 37 °C. Post treatment cells were washed with 400 µL of 0.04 % Trypan Blue in PBS, followed by three washes with 400 µL of PBS to wash excess staining solution. Further procedure and analysis were the same as explained in section

4.1.8. The uptake in test conditions was compared with the uptake of untreated peptides.

4.1.11. MTT Assay for cell viability

The exponentially growing cells were seeded in 96-well plates at a density of 10,000 cells and grown overnight in medium containing 10% FBS. The cells were treated with varying concentrations of MTX(0, 0.25, 0.5, 1, 2, 4, 5, 8, 10, 20, 30, 40, 50, 100 and 200 µM), peptide-CF(0, 10, 20, 30, 40 and 50 µM) and peptide-MTX conjugates (0, 0.05, 0.1, 0.25, 0.5, 1, 2, 4, 5, 8, 10, 20, 30, 40 and 50 µM) in serum-free media at 37 °C for 72 hours. The cells were washed after the treatment with 1X PBS and 100 µL of 0.5 mg/mL MTT in PBS was added to each well. The cells were incubated for 4 hours, washed with PBS and 100 µL of DMSO was added. The plates were incubated for 10 minutes and then measured spectrophotometrically at 540 and 660 nm.

4.1.12. Haemolytic Assay

2 ml of fresh blood was drawn from a healthy individual and mixed with 3.4 mg of EDTA to prevent coagulation. The plasma was separated by centrifuging the mixture at 1000 r.p.m. for five minutes. The RBCs were washed three times with saline using the same centrifugation process. The RBCs were diluted in saline to form a 10% haematocrit. 100 µL of haematocrit was taken in a micro-centrifuge tube and the cells were treated with 100 µL of saline mixed with varying concentrations of peptide-CF and peptide-MTX conjugates. 100 µL of water was added as a positive control and 100 µL of saline was added to the blank samples. The resultant 5 % haematocrit was then incubated at 37 °C for four hours. The cells were then centrifuged at 1000 r.p.m. for five minutes and the supernatant was extracted into a 96-well plate. The absorbance for the supernatant was recorded at 540 nm and 660 nm. The percent haemolysis was calculated by taking the positive control as a reference for 100 % lysis. All samples were taken in six replicas for statistical significance.

4.2. COMPUTATIONAL METHODS

4.2.1. Molecular Modelling Tools

A number of computational and bioinformatics tools were used during the course of this study. The tools used, their utility and availability have been listed in Table 4.1

Table 4.1: ***List of Bioinformatics and Computational tools.***

Tools / Databases	Usage
PyMol [4]	Visualization tool for PDB structures
VMD [5]	Tool for analysis of MD Simulation Trajectories
PROSS	Determining dihedral angles of protein structures
RIBOSOME	Construction of PDB coordinate files
PDB [6]	Database for Protein Structures
DELPHI [7]	Tool to calculate electrostatic potential
Other in-house tools and programs	Shell scripts for automation and analysis

4.2.2. Molecular Dynamics Simulations

All Molecular Dynamics simulations were performed using GROMACS [8, 9]. The setup of MD simulations varied with the focus of individual experiments; i) For studying the stability of the peptide structures in water systems, and ii) For studying the interactions of peptides with lipid bilayers, mimicking the interactions of peptides with plasma membranes.

4.2.2.1. MD Simulations for studying the structural stability of designed peptide structures.

Peptide Structure co-ordinate files were generated using Ribosome software provided by George D. Rose. All Molecular Dynamics (MD) simulations were performed on GROMACS 4.6.5, [8, 9] a molecular dynamics simulation suite with GROMOS 96 43a1 force field, [10] for 10 ns at 300 K under standard NVT conditions. The structures were first energy minimized in vacuum and further in

a water solvated system, using the steepest descent algorithm. A production run of 10 ns was completed with an integration step of 2 fs. Bond lengths were constrained with 10^{-4} geometrical accuracy with the LINCS algorithm and non-bonded interactions were spaced at 0.8-1.1 nm. Berendsen thermostat was used for temperature coupling of the peptide and initial velocities were calculated as per the Maxwell distribution at 300K.

4.2.2.2. MD Simulations for insights into membrane-peptide interactions

A 128 membered POPG lipid bilayer was constructed using the MemBuilder server [11]. GROMOS 53a6 force field parameters were used in combination with Berger lipds force field [12, 13]. POPC and POPG forcefield parameters were taken from Kukol et al. [14] 4 peptide molecules were added near one end of the bilayer followed by solvation of the system and energy minimization. The system was further calibrated in NVT conditions for 100 ps followed by a 1 ns NPT equilibration. The system now comprising of 4 peptide molecules, 128 membered POPG bilayer and water (solvent) molecules was then simulated for 200 ns. Post-simulation, the system was analyzed using GridMat for the bilayer thickness followed by density mapping of the phospholipid headgroups through the course of simulation [15].

4.2.3. Electrostatic profiling of peptide molecules in water

The peptide structures were constructed using the Ribosome software provided by George D Rose's lab. Electrostatic potential at each atomic position was calculated by solving finite distance Poisson Bolttzmann equation using DelPhi [7]. The potential for each side-chain was summed to express the cumulative electrostatic potential at each amino acid position. Further, this electrostatic potential was mapped using the peptide backbone architecture, which gives rise to unique electrostatic fingerprints of the designed peptides. The designed backbone structures conform to either α or Π helical conformations for each series of peptides designed. All helices essentially have a cylindrical geometry. Therefore, the three-dimensional electrostatic fingerprints for each peptide can be represented as the curved surface of a cylinder.

4.3. REFERNECES

[1] Jha D, Mishra R, Gottschalk S, Wiesmüller K-H, Ugurbil K, Maier ME, Engelmann J. CyLoP-1: A Novel Cysteine-Rich Cell-Penetrating Peptide for Cytosolic Delivery of Cargoes. Bioconjugate Chemistry 2011;22:319-28.

[2] Cascales L, Henriques ST, Kerr MC, Huang Y-H, Sweet MJ, Daly NL, Craik DJ. Identification and Characterization of a New Family of Cell-penetrating Peptides: CYCLIC CELL-PENETRATING PEPTIDES. Journal of Biological Chemistry 2011;286:36932-43.

[3] Drin G, Cottin S, Blanc E, Rees AR, Temsamani J. Studies on the Internalization Mechanism of Cationic Cell-penetrating Peptides. Journal of Biological Chemistry 2003;278:31192-201.

[4] The {PyMOL} Molecular Graphics System, Version~1.3r1. 2010.

[5] Humphrey W, Dalke A, Schulten K. VMD: Visual molecular dynamics. Journal of Molecular Graphics 1996;14:33-8.

[6] Gilliland G, Berman HM, Weissig H, Shindyalov IN, Westbrook J, Bourne PE, Bhat TN, Feng Z. The Protein Data Bank. Nucleic Acids Research 2000;28:235-42.

[7] Li L, Li C, Sarkar S, Zhang J, Witham S, Zhang Z, Wang L, Smith N, Petukh M, Alexov E. DelPhi: a comprehensive suite for DelPhi software and associated resources. BMC Biophysics 2012;5:9.

[8] Abraham MJ, Murtola T, Schulz R, Páll S, Smith JC, Hess B, Lindahl E. GROMACS: High performance molecular simulations through multi-level parallelism from laptops to supercomputers. SoftwareX 2015;1-2:19-25.

[9] David VDS, Erik L, Berk H, Gerrit G, E. MA, C. BHJ. GROMACS: Fast, flexible, and free. Journal of Computational Chemistry 2005;26:1701-18.

[10] van Gunsteren WF. Biomolecular Simulation: The GROMOS96 Manual and User Guide: Biomos ; Zürich; 1996.

[11] Ghahremanpour MM, Arab SS, Aghazadeh SB, Zhang J, van der Spoel D. MemBuilder: a web-based graphical interface to build heterogeneously mixed membrane bilayers for the GROMACS biomolecular simulation program. Bioinformatics (Oxford, England) 2014;30:439-41.

[12] Berger O, Edholm O, Jähnig F. Molecular dynamics simulations of a fluid bilayer of dipalmitoylphosphatidylcholine at full hydration, constant pressure, and constant temperature. Biophysical Journal 1997;72:2002-13.

[13] Chris O, Alessandra V, E. MA, F. VGW. A biomolecular force field based on the free enthalpy of hydration and solvation: The GROMOS force-field parameter sets 53A5 and 53A6. Journal of Computational Chemistry 2004;25:1656-76.

[14] Kukol A. Lipid Models for United-Atom Molecular Dynamics Simulations of Proteins. Journal of Chemical Theory and Computation 2009;5:615-26.

[15] J. AW, A. LJ, R. BD. GridMAT-MD: A grid-based membrane analysis tool for use with molecular dynamics. Journal of Computational Chemistry 2009;30:1952-8.

5

Syndiotactic Peptides for Targeted Delivery

Lack of cell-type specificity and proteolytic susceptibility have long been the major bottlenecks for the development of peptide-based biomaterials for targeted drug delivery. Though a poly-L backbone provides the adaptability to re-conform the peptide structure to bind to a receptor, it also makes the peptide more susceptible to proteolytic cleavage. It was attempted to address this issue by designing a set of syndiotactic peptides de novo, with alternating L- and D-amino acids in succession. The designed peptides have higher rates of cellular uptake than the Tat (48-60) peptide in breast and cervical cancer cells. The uptake is independent of concentration, temperature and endocytosis (clathrin mediated). Importantly, the peptides are stable in both plasma and serum. The peptide-drug conjugates are much less toxic to the non-cancerous cells than cancer cells. The designed peptides are a step forward towards the development of targeted drug delivery vectors on peptide templates.

An article based on this chapter is; Jerath *et al.*, Syndiotactic Peptides for Targeted Delivery. *Acta Biomaterialia*. (2019) **87**:130-139.

5.1. INTRODUCTION

The toxic side effects of chemotherapy drugs due to non-specificity have necessitated the need for the design of targeted delivery systems. The hydrophobic nature of cell membranes regulates the influx of bioactive molecules like drugs, peptides, proteins etc. The development of peptide-based biomaterials for drug delivery have gained momentum since the discovery of membrane transduction properties of HIV-derived TAT peptide [1, 2]. Peptides are small, bio-derived, and easy to synthesize molecular systems that can conjugate to practically any molecule of interest [3]. Cell penetrating peptides (CPPs) are usually short cationic sequences with the ability to translocate in multiple cell-types. Multiple mechanisms of CPP uptake including endocytosis (clathrin and caveolae mediated) and direct translocation (inverse micelle, pore formation, carpet and membrane thinning models) have been described [4]. The choice of mechanism is dependent on the peptide sequence, cell type and other physiological conditions. Interestingly, a CPP can simultaneously adopt multiple pathways for cellular entry. [5]

Significant advances have been made in developing multiple peptide based biomaterial conjugates such as hydrogels, liposomes, nanocomplexes, nanowires etc. for drug delivery applications [6-11]. However, the role of peptide component as the principal charioteer in such biomaterial conjugates has been a major bottleneck for the development of targeted delivery vectors [12, 13]. Although, there are more than 1800 CPPs presently registered in the CPP-site database, incompatibility of CPP in biological fluids and lack of cell-type specificity remain as the principal roadblocks for their clinical use [14]. Proteolytic susceptibility of peptides is primarily due to the presence of L-chiral amino acids in their sequences [15]. These poly-L sequences can be recognized by a variety of receptors and enzymes leading to the confinement in endosomes (receptor-mediated endocytosis) and proteolytic cleavage respectively [5]. In the present study, the aim is to address the issues of peptide stability in biological fluids and lack of cell type specificity, for their further development as peptide based biomaterials or biomaterial conjugates for targeted drug delivery.

Chapter 5
Syndiotactic Peptides for Targeted Delivery

In this chapter, *de novo* design of syndiotactic peptides for drug delivery applications is presented. Tacticity in polymer chemistry refers to the stereochemical sequence of successive monomers in a polymer chain. Isotactic peptides have only one form of stereoisomers, poly L or poly D. Heterotactic peptides have a mixture of both stereoisomers, L and D at random. Syndiotactic peptides are sequences with alternating stereoisomers (LDLD or DLDL). For a 12 amino acid sequence, a peptide can have 4096 (2^{12}) stereochemical combinations, of which only two are syndiotactic.

The structure of Gramicidin, a syndiotactic antibacterial peptide was first proposed in 1971 by Urry and crystal structure was solved in 1988 [16, 17]. The sequential syndiotacticity in Gramicidin results in an unique $\Pi_{(L,D)}$ helical structure with 6.3 residues per turn. In such $\Pi_{(L,D)}$ helices, the C=O and N-H bond vectors and their resulting dipoles are oriented in an anti-parallel direction. Such an arrangement makes the structure energetically stable. Moreover, barring the ends, all residues in a $\Pi_{(L,D)}$ helix have hydrogen bonds, further adding to the stability of the structure [16]. Such a helix would require a set of phi and psi backbone angles in the β-region for L-amino acids and its complementing angle distributions for D-amino acids of the Ramachandran plot (Figure 5.1).

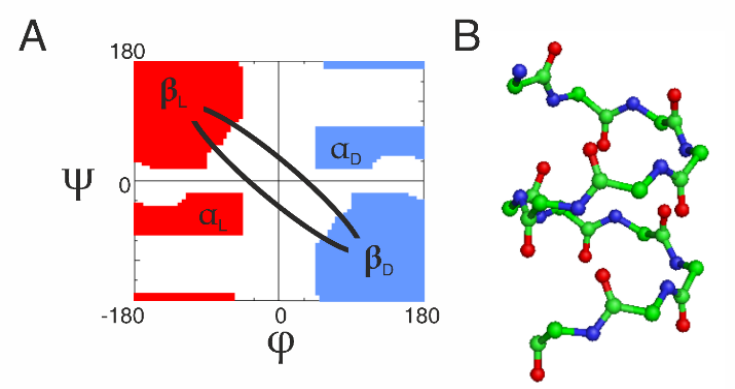

Figure 5.1: ***Design philosophy for SARTHI peptides.*** *(A) The sterically allowed regions of Ramachandran plot for L- and D-amino acids forming a $\Pi_{(L,D)}$ helix. (B) A syndiotactic Gramicidin-like $\Pi_{(L,D)}$ helix formed from the φ, ψ distributions in the β-region of successive L- and D-amino acids.*

In one of the published studies, the statistical analysis of backbone and side-chain dihedral angle distributions in over 21, 000 non-redundant protein structures has been reported [18]. This analysis when extended to amino acid-wise distribution of dihedral angles, revealed the statistical distribution of amino acid dihedral angles in protein structures. The amino acids with energetically favorable conformation in the β-region of the Ramachandran plot were taken into account. Assuming that a syndiotactic stereochemical sequence results in the formation of Gramicidin-like $\Pi_{(L,D)}$ helix, a set of syndiotactic peptides were designed. About 50 peptides to optimize the amino acid sequence for a syndiotactic backbone with cell permeating capability were tested(data not shown). The positively screened amino acid sequence and their sequence inverts were re-designed into a set of four syndiotactic 12-mer peptides. These Stereo-chemical Amphipathic chaRged Tumor Homing and Internalizing (SARTHI) peptides have identical amino acid composition. The sequence SARTHI-1 and SARTHI-3 are stereochemical inverse of each other, whereas SARTHI-2 and SARTHI-4 are the amino acid side-chain sequence inverse of SARTHI-1 and SARTHI-3 respectively.

The peptides were synthesized and fluorescently labelled with 5(6)-Carboxyfluorescein (CF). These peptides were tested for their cell-penetrative capability, cellular uptake profile and biocompatibility. Further, peptides were conjugated with an anticancer drug, methotrexate (MTX) for evaluating their drug delivery potential. The cytotoxicity of MTX increases towards cancer cells when conjugated with the designed peptides with lowered cytotoxicity towards non-cancerous cells. Moreover, peptide-MTX conjugates were able to overcome the resistance of MDA-MB-231 cells towards MTX.

5.2. RESULTS

5.2.1. Peptide Synthesis

The fluorophore-tagged peptides were synthesized by solid-phase peptide synthesis protocol using Fmoc-chemistry. The peptides were purified by reverse-phase liquid chromatography followed by MALDI-TOF, for identification and

estimation of the designed sequence. The amino acid sequences and their respective masses are given in Table 5.1.

Table 5.1. ***Designed Sequences and Mass Observed.*** *The designed peptide sequences are given. D-amino acids are shown as underlined characters. The peptides conjugated with 5(6) carboxyfluorescein and methotrexate had expected masses of 1875.29 and 1931.98 Da respectively.*

Sample	Sequence	Mass Observed	
		5(6)Carboxyfluorescein	Methotrexate
SARTHI-1	K R K I F L R C K I L V	1875.11	1931.89
SARTHI-2	V L I K C R L F I K R K	1875.43	1932.31
SARTHI-3	K R K I F L R C K I L V	1874.28	1932.06
SARTHI-4	V L I K C R L F I K R K	1875.24	1932.43

5.2.2. Peptide Structure Conformation

The conformation of the designed peptides was evaluated using CD Spectroscopy. 10 µM SARTHI-CF conjugates were dissolved in water and ellipticity was measrured in a CD spectrophotometer.

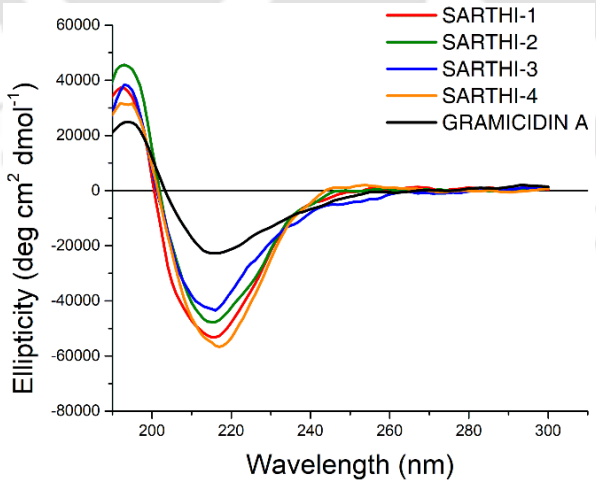

Figure 5.2. ***CD Spectroscopy of SARTHI peptides.*** *The CD spectra of SARTHI peptides in water at 10 µM concentration was compared with Gramicidin A. The spectra of SARTHI peptides is similar to that of Gramicidin A, suggesting that the SARTHI peptides are forming $\Pi_{(L,D)}$ helix.*

The conformation of peptides were compared with Gramicidin A under similar conditions (Figure 5.2). The CD spectra of the designed peptides and Gramicidin A were similar. This suggests that the designed SARTHI peptides and Gramicidin A have similar structures.

5.2.3. Cellular Uptake

To assess the cell permeating potential of the designed peptides, cervical cancer cells (HeLa) were treated with 10 μM of peptide-CF conjugates for four hours at 37 °C. The intracellular distribution of the peptide-CF conjugates in HeLa cells was observed under the confocal microscope (Figure 5.3). SARTHI-1 and SARTHI-3 were majorly distributed throughout the cell and also present in nucleus as can be seen through the merged images. SARTHI-2 and SARTHI-4 showed both vesicular and diffused uptake in cells. This suggests that all the designed peptides, though identical in amino acid composition, have varied cellular uptake profiles [19, 20].

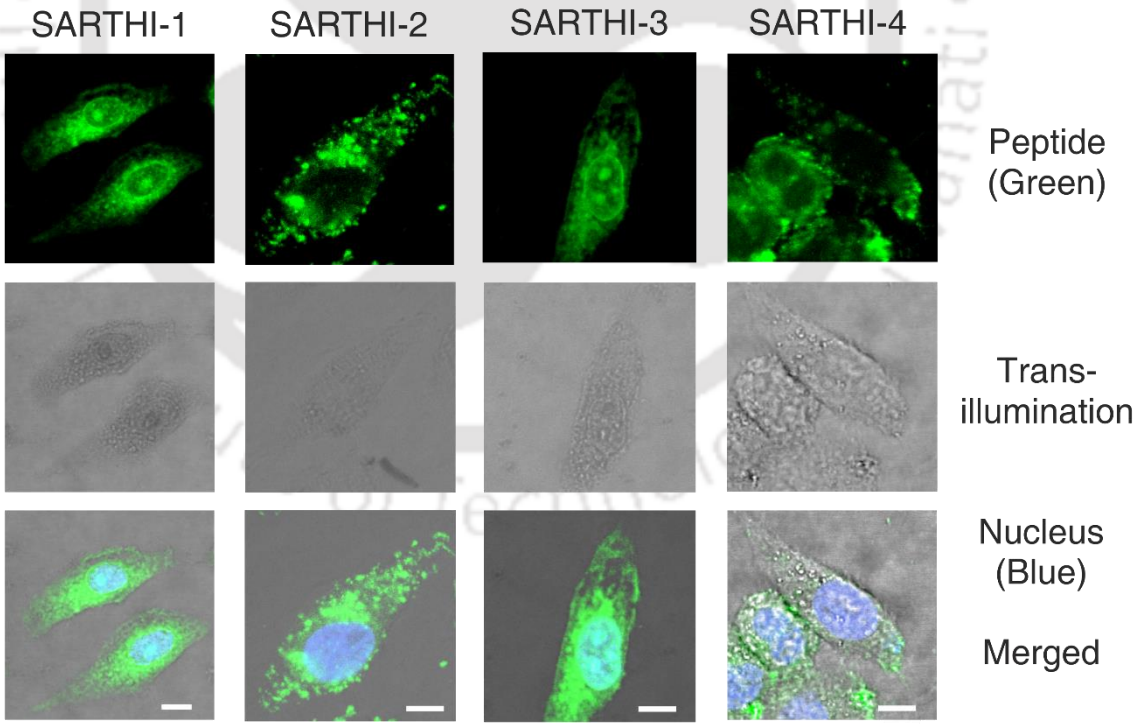

Figure 5.3. ***Cellular Uptake of SARTHI peptides in Cervical Cancer Cells.*** *HeLa cells were treated with 10 μM of SARTHI-CF conjugates for four hours under standard conditions. Post peptide treatment, cells were treated with Hoechst 33342 to label the nuclei of live cells. The photomicrographs were taken in the green*

channel (peptide signal), blue channel (nuclei) and trans-illumination. SARTHI peptides had both diffused and vesicular uptake profile suggesting both cytosolic and vesicular localizations. Scale bar corresponds to 10 µm.

Further, thecompared uptake of the designed peptides in HeLa cells with the TAT peptide using flow cytometry (Figure 5.4). The uptake of SARTHI peptides was 10-100 folds more than the TAT peptide at the same concentration of treatment (10 µM). This observation points to the potential of SARTHI peptides in penetrating cell membrane with higher efficiency than the standard TAT peptide.

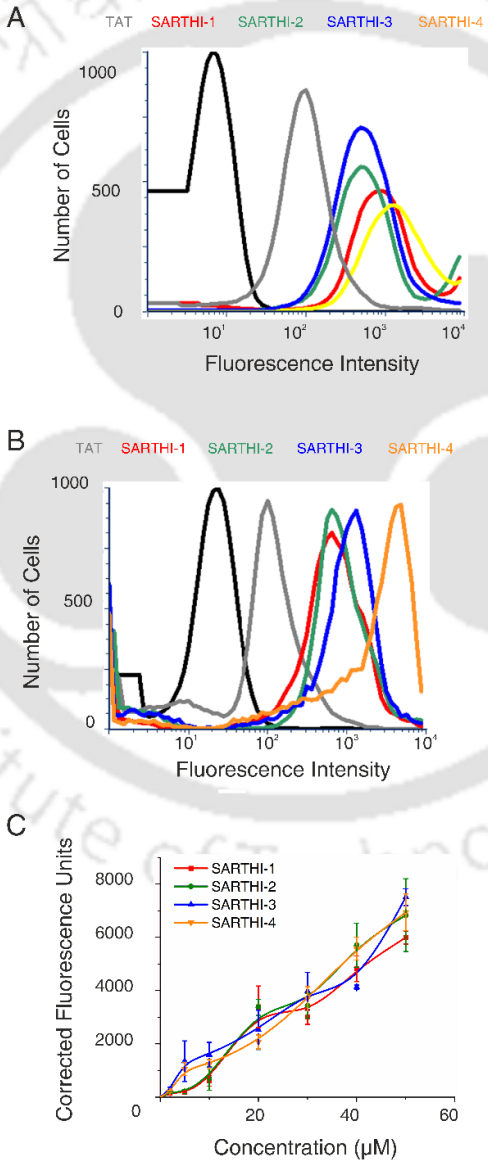

Figure 5.4. ***Comparative uptake of SARTHI peptides.*** *MDA-MB-231(A) and Hela (B) cells were treated with 10 µM of TAT and SARTHI peptides for four hours. The uptake was measured through flow cytometry for assessment of uptake*

comparative to the standard TAT peptide. (C) Concentration titration for the cellular uptake of SARTHI peptides in HeLa cells over four hours of treatment. Corrected fluorescence units correspond to fluorescence per unit cell.

Through fluorescence spectroscopy based concentration titration experiments, it was observed that the cellular uptake of peptides in HeLa cells increased linearly with increasing peptide concentrations (Figure 5.4C). This observation indicates that the cellular uptake of SARTHI peptides is independent of the concentration of peptides and provides suggestive indications against a receptor-based uptake mechanism [20].

5.2.4. Mechanism of Cellular Uptake

The entry of CPPs in cells is primarily through either endocytosis or direct translocation [4, 5]. However, a peptide may also penetrate through multiple routes of entry simultaneously. Further, it has also been observed that the route of cellular uptake of CPPs varies with cell types. Therefore, the uptake route for the designed peptides was tested under different physico-chemical conditions and cell lines to evaluate the mode of entry using fluorescence spectroscopy. HeLa, MDA-MB-231 and HEK-293 cells were treated with 10 μM of peptide-CF conjugates for one hour at 4 °C [21]. The uptake of peptides at 4 °C was similar to the cellular uptake at 37 °C in HeLa and MDA-MB-231 cells, except for SARTHI-4 (Figure 5.5).

The uptake of SARTHI-4 reduced to about 50 % of the uptake, compared to the control. However, the uptake of peptides was significantly reduced at 4 °C in the case of HEK-293 cells to 25-50 % (Figure 5.5). The reduction in cellular uptake at 4 °C is usually attributed to the blocking of energy dependent uptake, mainly endocytosis, but is also known to be due to reduced dynamics of the system (peptides, membrane and fluid) [22, 23].

Therefore, the cells were treated with 0.1 % sodium azide to block the energy dependent pathways of entry [21]. Similar uptake in both test and control conditions of the designed peptides in HeLa and MDA-MB-231 cells suggest towards a passive pathway of cellular uptake in both these cell lines. In HEK-293

cells, the uptake of the cells decreased to about 50 %, which is characteristic of employing multiple energy dependent and energy independent pathways of CPP entry (5.5). Clathrin-mediated endocytosis is a major route of receptor-mediated CPP uptake in cells.

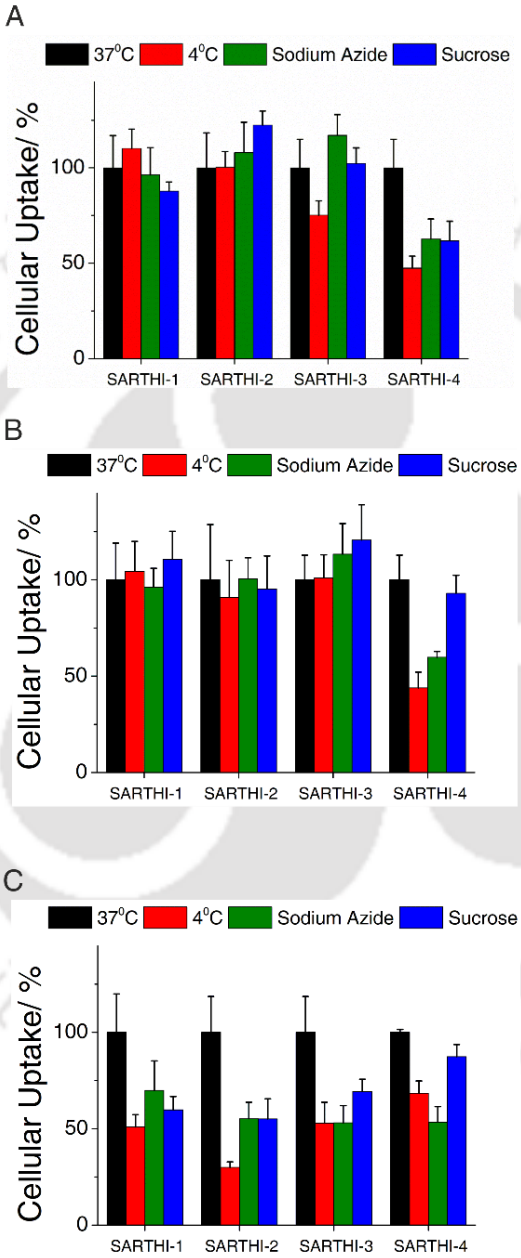

Figure 5.5. ***Cell-type dependent pathway of uptake.*** *The cellular uptake of SARTHI peptides under different conditions; temperature, energy availability and hyper molar sucrose in HeLa (A), MDA-MB-231 (B) and HEK-293 (C) cells. The cellular uptake of SARTHI-1, SARTHI-2 and SARTHI-3 is independent of temperature, ATP and clathrin-mediated endocytosis in HeLa and MDA-MB-231*

cells. However, the uptake of these peptides in HEK-293 cells is partly dependent on the above-mentioned parameters. The uptake of SARTHI-4 is partly dependent on temperature, ATP and endocytosis in the three cell types.

So, the dependence of clathrin-mediated endocytosis process on the uptake of peptides in the three cell types was tested by blocking the pathway using hypermolar concentration of sucrose in treatment media [24]. No reduction in cellular uptake for SARTHI-1, SARTHI-2 and SARTHI-3 was observed in HeLa and MDA-MB-231 cells, while the uptake of SARTHI-4 was similar to the uptake in ATP-depleted conditions. In HEK-293 cells, the uptake of all SARTHI peptides reduced to 50-70 %. Therefore, the results collectively suggest towards passive modes of cellular uptake of SARTHI-1, SARTHI-2 and SARTHI-3 in HeLa and MDA-MB-231 cells. Further, multiple modes of entry for SARTHI peptides were observed for HEK-293 cells. SARTHI-4, on the other hand, has a mixed profile of energy-dependent and energy-independent modes of uptake in all the three cell types (HeLa, MDA-MB-231 and HEK-293).

5.2.5. Cell-type Dependent Cellular Uptake

While studying the dependence of cell type on the uptake mechanism of entry for SARTHI peptides, it was observed that the uptake of the designed peptides was lower in the non-cancerous origin HEK-293 cells than the cervical cancer cell line, HeLa. Therefore, the two cell-types were treated with 10 μM of peptide-CF conjugates for four hours and compared their uptake through fluorescence spectroscopy (Figure 5.6). The estimated uptake of SARTHI-1, SARTHI-2 and SARTHI-3 were much lower in HEK-293 cells than the HeLa cells at test concentration. On the other hand, the uptake of SARTHI-4 was similar in the two cell-types. This suggests towards cell-type dependency on both the cellular uptake and the mode of uptake for SARTHI-1, SARTHI-2 and SARTHI-3. The observation is based on the set of fluorescence-based study and therefore, suggestive. The primary reason for the suggestive nature of this observation is the endosomal uptake of SARTHI peptides in HEK-293 cells. The acidic pH of endosomes can lead to a loss/decrease in signal of carboxyfluorescein.

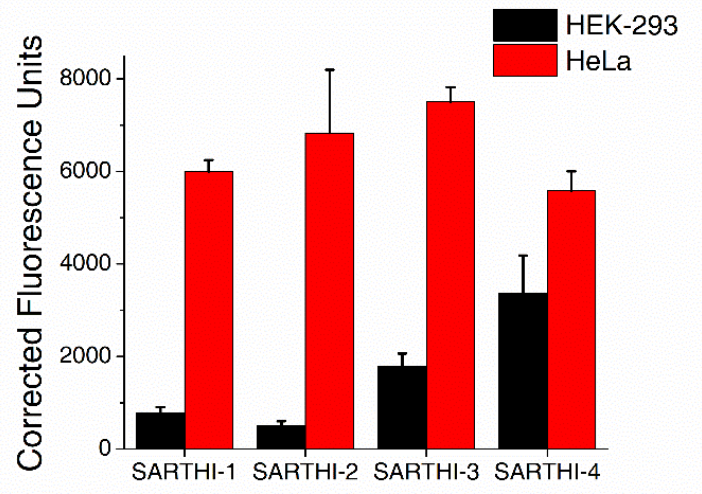

Figure 5.6. ***Cell Type dependent uptake of SARTHI peptides.*** *The comparative uptake of SARTHI peptides at 10 µM concentration, in HEK-293 and HeLa cells.*

5.2.6. Interaction of SARTHI peptides with POPG bilayers in water: A Molecular Dynamics study

The results discussed in the previous sections indicate membrane-based mode of cellular entry for SARTHI peptides. To study the interaction of SARTHI peptides with the lipid bilayer, a Molecular Dynamics simulation experiments of SARTHI peptides with POPG bilayer in water was done. All MD simulations were performed in GROMACS using GROMOS96 force field with 53a6 parameter set, along with Berger lipids parameters [25, 26]. Four peptide molecules were placed near one side of the POPG bilayer in a water system. The system was equilibrated, followed by a 100ns production run under NPT conditions.

After the 100 ns production run, each of the SARTHI peptides were evaluated for the maintenance of the designed structure during the course of the simulation through Root Mean Square Deviations and Radius of Gyration distributions (Figure 5.7).The P4 molecule of SARTHI-1 showed higher magnitude of RMSD, when compared to other molecules of SARTHI-1. To understand the extent of deviation, the backbone trace of the individual peptide molecules was analyzed throughout the simulation (Figure 5.8).

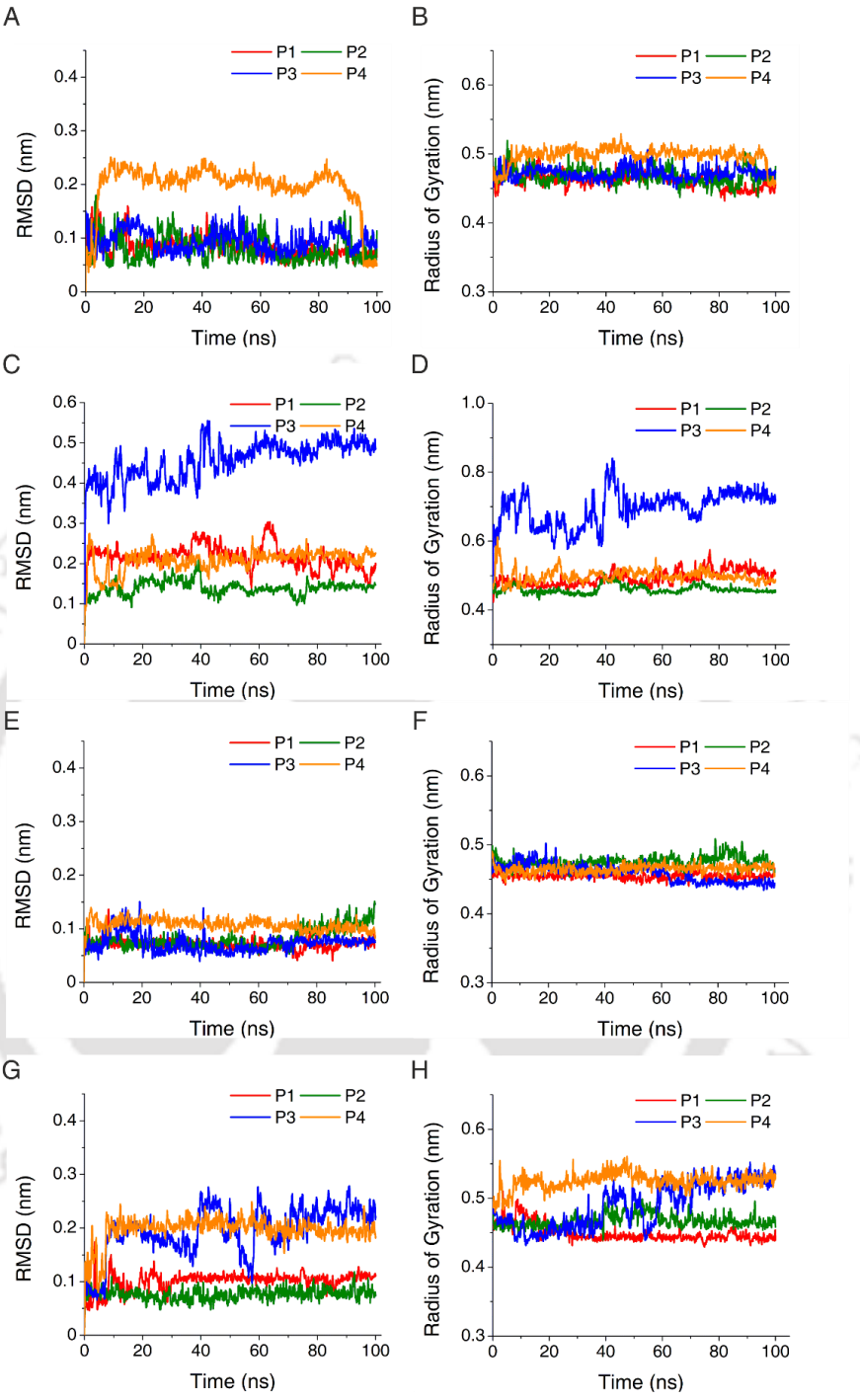

Figure 5.7. ***Backbone Stability of SARTHI Peptides on Interaction with POPG bilayer.*** *Four molecules of SARTHI-1(P1-P4) were introduced near one side of the POPG bilayer in water. The stability of SARTHI-1 peptide molecules was evaluated through the stable distributions of RMSD (A) and Radius of Gyration (B) during the course of the simulation. P4 molecule exhibited higher RMSD values than P1-P3. (C). At the end of 100 ns production run, the peptide molecules were embedded within*

the POPG bilayer (D). The distribution of the POPG headgroups, SARTHI-1 molecules and water at the start and end of the simulation further support the observation that the peptide molecules were successful in penetrating the outer layer of the POPG bilayer (E). Moreover, the thinning of the POPG bilayer was observed and is shown as a heat map indicating the membrane thickness distribution in the X-Y plane (F).

The terminal residue of P4 showed deviations from the original structure, which can be attributed to the absence of intra-molecular hydrogen bonds for the terminal residues in a syndiotactic $\Pi_{(L,D)}$ helix. The peptide molecules maintain their backbone structure throughout the simulation.

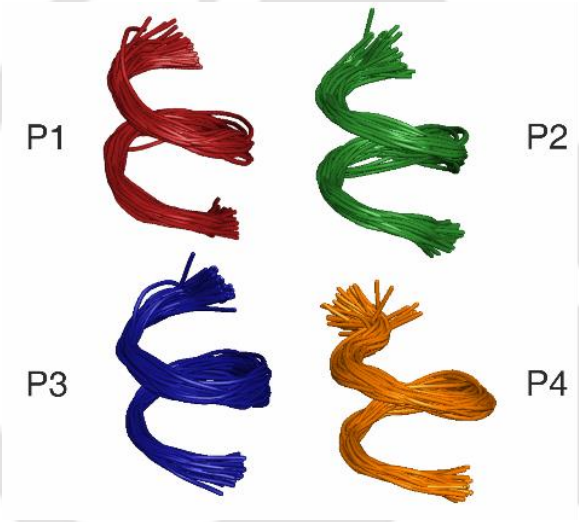

Figure 5.8. ***Backbone Trace of SARTHI-1. .****A backbone trace of the four molecules for the simulation reveals that the backbone structure was conserved throughout the production run.*

This indicates that the $\Pi_{(L,D)}$ helical structure for a syndiotactic backbone is stable in the tested conditions. However, in the case of SARTHI-2, one of the peptide molecule was observed to have deviated from the original structure. This leads to an observation that the syndiotactic backbone is semi-rigid i.e. even though the syndiotactic backbone maintains the $\Pi_{(L,D)}$ helical structure in different solvents, it can adopt other conformations as well, during membrane interaction.

The peptides penetrated the outer layer of the lipid bilayer within the 100 ns run. The penetration of the POPG bilayer at the end of the production run was observed by visualizing the simulation using VMD. The peptides were able to penetrate the outer layer of the POPG bilayer within the 100 ns of production run (Figure 5.9).

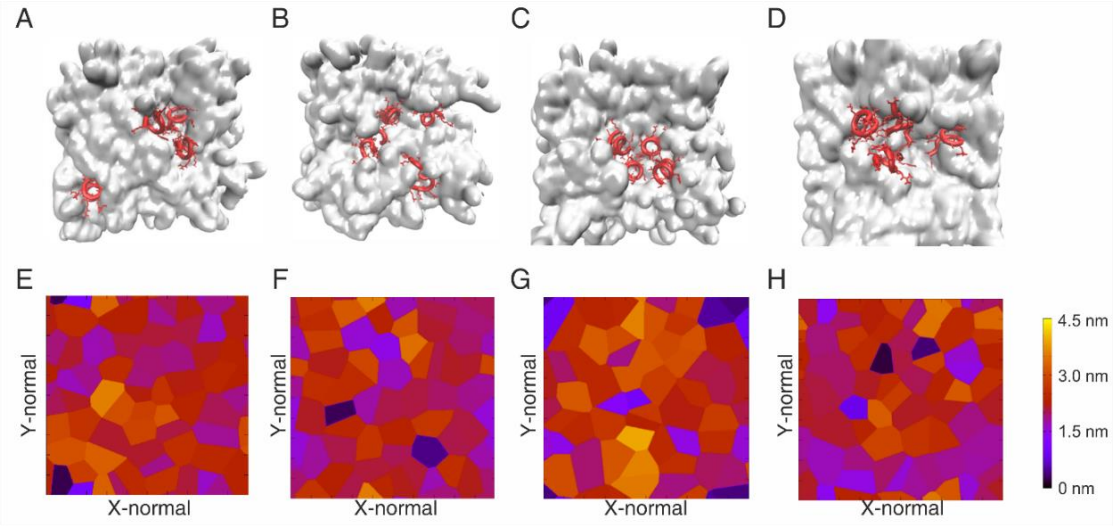

Figure 5.9. ***Penetration of POPG bilayer by SARTHI peptides.*** *The designed peptides were successfully able to penetrate the outer layer of the POPG bilayer as seen by membrane embedding of peptides (A) and membrane thickness distribution of POPG bilayer (B).*

The position of peptide molecules was within the boundary of the lipid bilayer. A heat map indicating the thickness of the lipid bilayer at the end of 100 ns, shows that the regions of membrane thinning are due to the penetration of SARTHI peptides (Figure 5.9). Additionally the water molecules had entered the lipid bilayer through the channels formed by peptide insertion. The formation of water channels due to the peptide penetration are similar to various water pore formation models reported for uptake of CPPs in literature [27].

5.2.7. Compatibility in Biological Fluids

Though the biological origin of peptides present an advantage over other modes of drug delivery, loss of activity of CPPs in biological fluids remains a major roadblock to their development as drug delivery vectors. Therefore, to study the compatibility of the designed peptides in biological fluids, the peptide-CF

conjugates were pre-treated with bovine serum and human plasma for one hour prior to treating HeLa cells with the same peptide stock solutions. Cellular uptake was observed using flow cytometry (Figure 5.10).

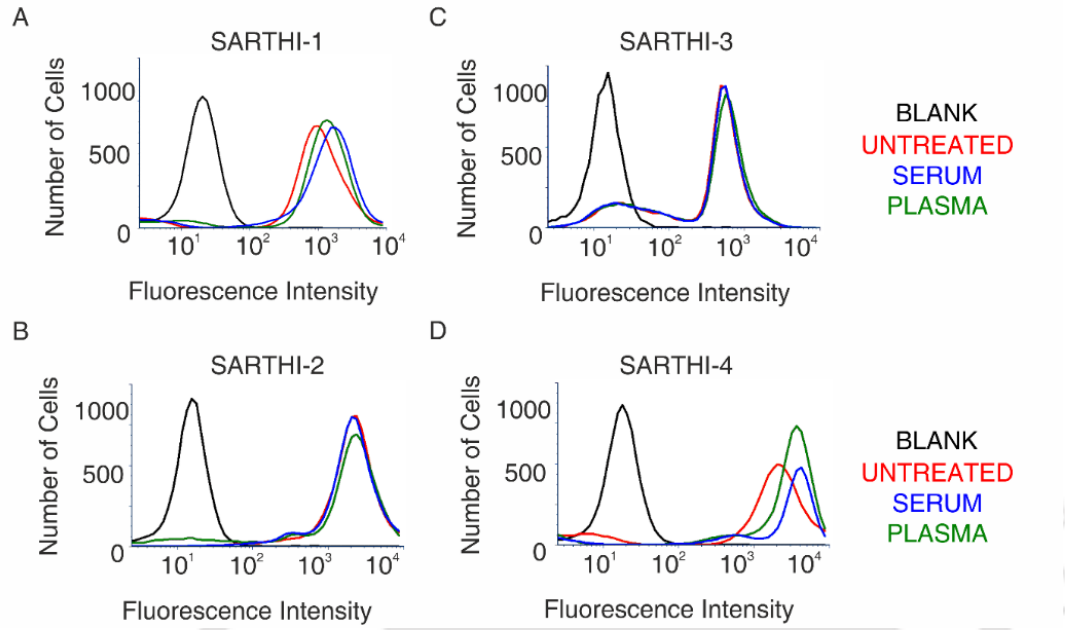

Figure 5.10: ***Biocompatibility of SARTHI peptides.*** *The serum and plasma stability of SARTHI peptides was tested by pre-treating the peptide stock solutions with Bovine Serum and Human Plasma. HeLa cells were treated with 5 μM of SARTHI peptides (pre-incubated with serum and plasma) for four hours. Blank represents cells treated with buffer and Untreated refers to the cells treated with peptides not treated with either bovine serum or human plasma. Cellular uptake of SARTHI peptides in the above-mentioned treatment conditions were compared with the untreated peptides (control) and show no decrease of uptake in either of the two test conditions.*

The cellular uptake for SARTHI peptides in the test conditions was compared to the uptake of untreated peptide-CF conjugates (control) under similar conditions. The cellular uptake in the test and control sets were similar and no loss of activity was observed, suggesting that the peptides are both serum and plasma stable. Additionally, the cells were treated with 10 μM of peptide-CF conjugates in serum-free and serum-containing media, with no reduction in cellular uptake in the presence of serum was observed. The presence of D-amino

acids in peptide sequences is known to increase their stability in biological fluids [15, 20].

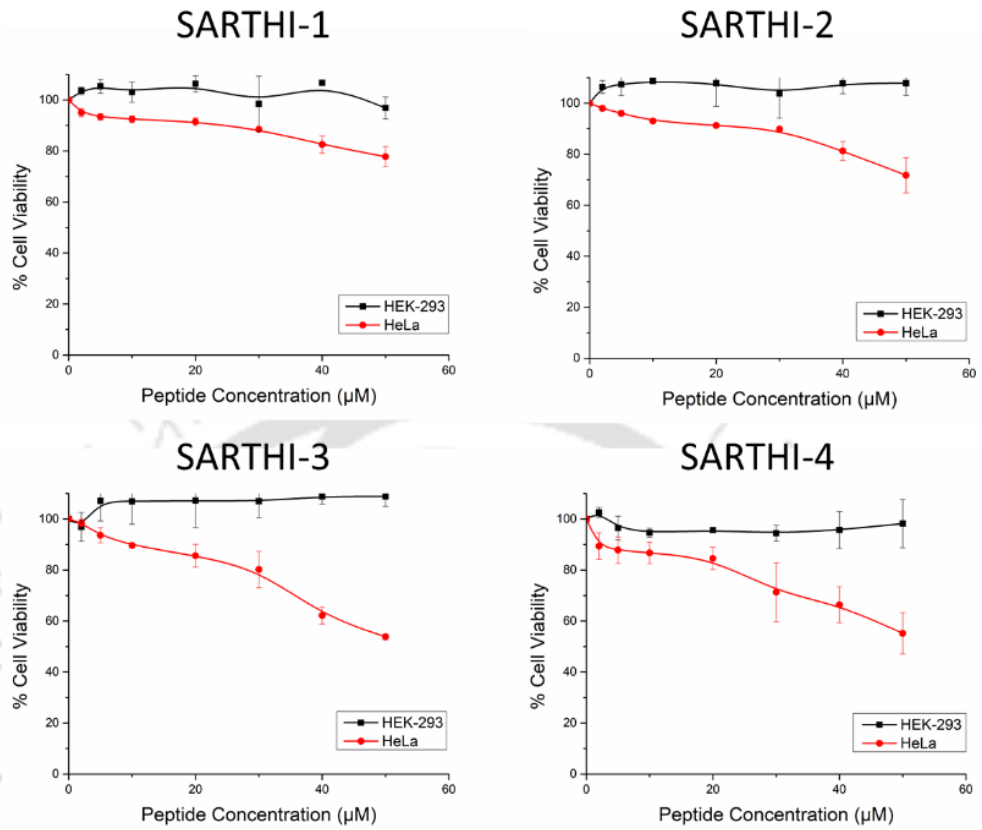

Figure 5.11: ***Cytotoxicity of SARTHI peptides.*** *MDA-MB-231 and HEK-293 cells were treated with increasing concentration of SARTHI-CF conjugates for 72 hours in serum-free media at 37 °C. The peptides showed minimal levels of toxicity towards the two cell lines.*

5.2.8. Cytotoxicity of SARTHI-CF Conjugates

MDA-MB-231 and HEK-293 cells were treated with varying concentrations (0, 2, 5, 10, 20, 30, 40 and 50 μM) of SARTHI-CF conjugates. Cell viability was assessed using the MTT assay. The peptide-CF conjugates had minimal toxicity towards HEK-293 cells. However, SARTHI-4-CF and SARTHI-3-CF conjugates showed some extent of toxicity towards MDA-MB-231 cells at >40 μM concentrations (Figure 5.11).

5.2.9. Drug Delivery Potential of SARTHI Peptides

Delivery of a functionally active molecule is the primary function of a drug delivery vector. Therefore, the efficiency of SARTHI peptides to deliver

functionally intact Methotrexate (MTX) into cells was tested. The drug was covalently conjugated to the N-terminus of each peptide through an amide linkage, similar to the fluorophore tagging of the peptides. HeLa cells were treated with peptide-CF conjugates for 72 hours to check the toxicity of the peptide-CF conjugates. Cell viability was assessed using MTT assay.

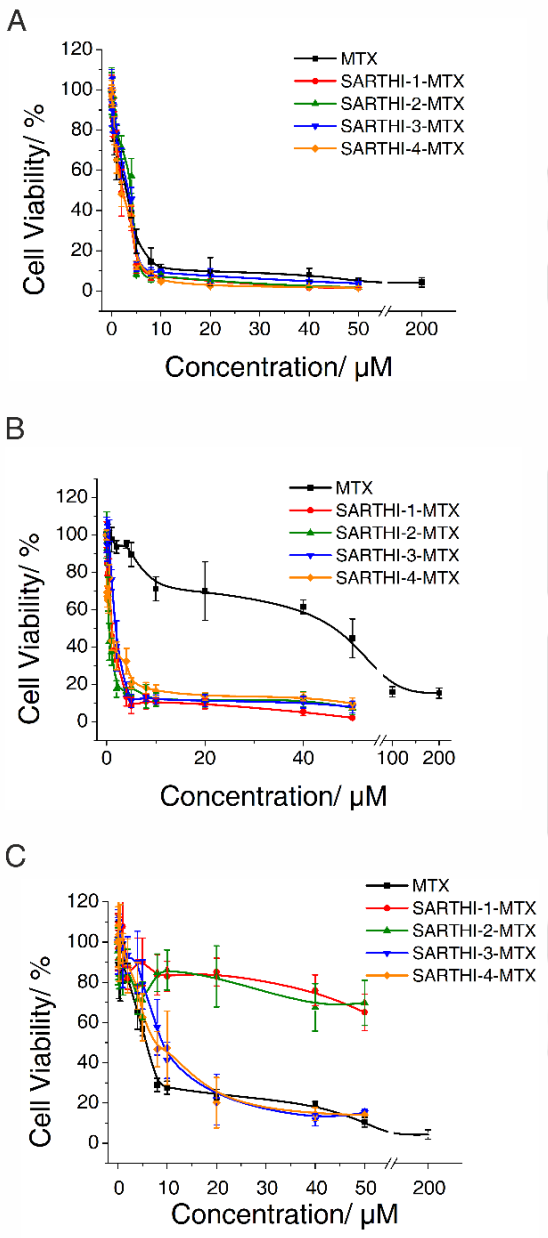

Figure 5.12: ***Small-molecule delivery potential of SARTHI peptides.*** *The cytotoxicity of MTX and SARTHI-MTX conjugates was evaluated using the MTT assay. HeLa (A), MDA-MB-231 (B) and HEK-293 (C) cells were treated with varying concentrations of MTX and SARTHI-MTX conjugates for 72 hours. The cytotoxicity*

of the tested compounds were similar in HeLa cells. SARTHI-MTX conjugates were able to overcome the drug resistance of MDA-MB-231 cells against MTX. The cytotoxicity of SARTHI-1-MTX and SARTHI-2-MTX was lower than the cytotoxicity of MTX, SARTHI-3-MTX and SARTHI-4-MTX towards the non-cancerous HEK-293 cells.

Table 5.2: ***IC_{50} values for peptide-MTX conjugates against cancer and non-cancerous cells.*** *The peptide-MTX conjugates had higher toxicity levels than methotrexate (MTX) against cancer cells. On the other hand, the toxicity of SARTHI-1-MTX and SARTHI-2-MTX conjugates towards HEK-293 cells was lesser than the toxicity of MTX, SARTHI-3-MTX and SARTHI-4-MTX.*

SAMPLE	IC_{50} ± Standard Deviation (μM)		
	HeLa	MDA-MB-231	HEK-293
Methotrexate (MTX)	4.99 ± 0.45	> 40	3.67 ± 0.21
SARTHI-1-MTX	1.55 ± 0.17	0.93 ± 0.10	> 50
SARTHI-2-MTX	1.82 ± 0.11	0.57 ± 0.07	> 50
SARTHI-3-MTX	1.76 ± 0.18	1.74 ± 0.13	10.46 ± 1.17
SARTHI-4-MTX	1.58 ± 0.16	0.47 ± 0.11	9.28 ± 1.07

Next, HeLa cells were treated with MTX and peptide-MTX conjugates. The cytotoxicity of MTX and peptide-MTX conjugates was comparable towards HeLa cells (Figure 5.12A). Further, MDA-MB-231 cells known to be resistant against the action of MTX, were treated with peptide-MTX conjugates [28]. The delivery of MTX as peptide-MTX conjugates increased the toxicity of the drug molecule towards MDA-MB-231 cells (Figure 5.12B). This could be due to the increased bioavailability of MTX inside the cell, as drug efflux is one of the many pathways of drug-resistance in cancer cells [28]. HEK-293 cells were treated with MTX and peptide-MTX conjugates. The cytotoxicity of MTX was comparable to the toxicity of SARTHI-3-MTX and SARTHI-4-MTX conjugates (Figure 5.12C).

On the other hand, SARTHI-1-MTX and SARTHI-2-MTX conjugates were significantly less toxic to HEK-293 cells. This suggests that SARTHI-1 and SARTHI-2 possess cell-type specificity towards cancerous cells over non-cancerous cells. The IC_{50} values for peptide-MTX conjugates against the three cell lines are given in Table 5.2.

All SARTHI peptides show varying levels of cell type specificity towards breast (MDA-MB-231) and cervical (HeLa) cells with low IC_{50} values towards these cancer cells than HEK-293 cells. Even SARTHI-3 and SARTHI-4 peptides have a higher IC_{50} value against HEK-293 cells than MTX. This suggests that these peptides do have some level of specificity towards the cancer cells. A possible explanation for such a phenomenon is that the mechanism of cellular uptake for these two peptides is pre-dominantly membrane-based. Cancer cells have higher presence of Phospho-Serines on the outer cell membrane layer than non-cancerous cells [29, 30]. This leads to higher overall negative charge on the cell surface of a cancer cell and more negative membrane potential than a normal cell [30-32]. This negative potential attracts the positively charged peptides, which in turn leads to cell-type specificity observed in various reported anti-cancer peptides [33-35].

5.3. DISCUSSION

Peptides capable of transducing the cell membrane (CPPs) have long been envisaged as the choice of future drug delivery vectors [5]. Multiple studies on peptide-based biomaterials and their conjugates have demonstrated their ability to deliver various cargoes into cells [2, 6-10]. However, lack of cell-type specificity and proteolytic susceptibility of peptides has been major roadblocks for their clinical applications [5]. Majority of CPPs are isotactic with a poly-L backbone, leading to their interaction with various cellular receptors and proteolytic enzymes. This issue was addressed by designing a set of syndiotactic peptides with alternating L- and D- stereoisomers, mimicking the stereochemical sequence of Gramicidin. This incorporation of D-amino acids protects the peptide from premature cleavage by serum and plasma proteases. At the same time, a syndiotactic stereochemical sequence promotes the formation of a Π(L,D) helix

[23]. This provides the necessary template for incorporating other design features into the peptide sequence.

The amino acid side chain sequence was optimized through a series of point mutations in a set of nearly fifty peptide sequences. These peptides were screened for their cell penetrating potential and the best performing sequence was used for the design of SARTHI peptides. The amino acid side-chain of all SARTHI peptides is predominantly the same, though their chain stereochemistry sequence and amino acid sequence vary. Different stereochemical sequences for the peptides give rise to different electrostatic signatures. With electrostatic interactions being the most primary mode of contact in biomolecules, the incorporation of syndiotacticity has thus, resulted in formation of different peptides from the same amino acid side-chain sequence [36]. The observations reported in the results section clearly indicate the varying properties of cell penetration and cell-type specificity arising from the differential electrostatic signatures. The cell-type specificity arising from the electrostatic signatures was therefore consequential. As explained and discussed elaborately in the results section of this manuscript, all possible in vitro studies to verify the hypothesis and design rationale, pertaining to cell penetration and cell type specificity have been completed.

5.4. CONCLUSION

A novel class of syndiotactic peptides, capable of cell penetration with cell-type specificity and drug-delivery potential is presented here. The study emphasizes on the design of peptides for cellular delivery by reverse engineering of a syndiotactic backbone. The stereochemically-engineered peptides have identical amino acid side-chain sequences. However, the reversal of the amino acid and stereochemical sequences gives rise to differentiating electrostatic fingerprints to each of the designed peptides. The designed peptides have been shown to have a high cellular uptake profile, dependent on cell type, are compatible in both serum and human plasma without any loss of activity. Moreover, the peptides are capable of delivering a functionally active molecule to the cells while maintaining their cancer cell type specificity. Further, the peptide-mediated delivery of the

drug molecule could overcome drug-resistance of triple-negative breast cancer cells. The differences in the activity profiles for each peptide can be attributed to their respective electrostatic fingerprints. However, it was opted to concentrate the efforts in designing novel peptide based delivery vehicles with a design directive primarily guided by electrostatics, and hence did not further pursue a mechanistic investigation. The results offer new potential candidates for delivery of small molecules and also provide new directions in the generation of novel cell-type specific drug delivery vectors designed on stereochemically diversified peptide templates.

5.5. REFERENCES

[1] Brasseur R, Divita G. Happy birthday cell penetrating peptides: Already 20years. Biochimica et Biophysica Acta (BBA) - Biomembranes 2010;1798:2177-81.

[2] Steinbach JM, Seo Y-E, Saltzman WM. Cell penetrating peptide-modified poly(lactic-co-glycolic acid) nanoparticles with enhanced cell internalization. Acta Biomaterialia 2016;30:49-61.

[3] Bechara C, Sagan S. Cell-penetrating peptides: 20years later, where do we stand? FEBS Letters 2013;587:1693-702.

[4] Heitz F, Morris MC, Divita G. Twenty years of cell-penetrating peptides: from molecular mechanisms to therapeutics. British Journal of Pharmacology 2009;157:195-206.

[5] Copolovici DM, Langel K, Eriste E, Langel Ü. Cell-Penetrating Peptides: Design, Synthesis, and Applications. ACS Nano 2014;8:1972-94.

[6] Zhang P, Cheetham AG, Lin Y-a, Cui H. Self-Assembled Tat Nanofibers as Effective Drug Carrier and Transporter. ACS Nano 2013;7:5965-77.

[7] Yang J, Shimada Y, Olsthoorn RCL, Snaar-Jagalska BE, Spaink HP, Kros A. Application of Coiled Coil Peptides in Liposomal Anticancer Drug Delivery Using a Zebrafish Xenograft Model. ACS Nano 2016;10:7428-35.

[8] Boeneman K, Delehanty JB, Blanco-Canosa JB, Susumu K, Stewart MH, Oh E, Huston AL, Dawson G, Ingale S, Walters R, Domowicz M, Deschamps JR, Algar WR, DiMaggio S, Manono J, Spillmann CM, Thompson D, Jennings TL, Dawson

PE, Medintz IL. Selecting Improved Peptidyl Motifs for Cytosolic Delivery of Disparate Protein and Nanoparticle Materials. ACS Nano 2013;7:3778-96.

[9] Karagiannis ED, Urbanska AM, Sahay G, Pelet JM, Jhunjhunwala S, Langer R, Anderson DG. Rational Design of a Biomimetic Cell Penetrating Peptide Library. ACS Nano 2013;7:8616-26.

[10] Wan Y, Dai W, Nevagi RJ, Toth I, Moyle PM. Multifunctional peptide-lipid nanocomplexes for efficient targeted delivery of DNA and siRNA into breast cancer cells. Acta Biomaterialia 2017;59:257-68.

[11] Asai D, Kanamoto T, Takenaga M, Nakashima H. In situ depot formation of anti-HIV fusion-inhibitor peptide in recombinant protein polymer hydrogel. Acta Biomaterialia 2017;64:116-25.

[12] Kamei N, Bech Nielsen EJ, Nakakubo T, Aoyama Y, Rahbek UL, Pedersen BL, Takeda-Morishita M. Applicability and Limitations of Cell-Penetrating Peptides in Noncovalent Mucosal Drug or Carrier Delivery Systems. Journal of Pharmaceutical Sciences 2016;105:747-53.

[13] Reissmann S. Cell penetration: scope and limitations by the application of cell-penetrating peptides. Journal of Peptide Science 2014;20:760-84.

[14] Agrawal P, Bhalla S, Usmani SS, Singh S, Chaudhary K, Raghava Gajendra PS, Gautam A. CPPsite 2.0: a repository of experimentally validated cell-penetrating peptides. Nucleic Acids Research 2016;44:D1098-D103.

[15] Verdurmen Wouter PR, Bovee-Geurts Petra H, Wadhwani P, Ulrich Anne S, Hällbrink M, van Kuppevelt Toin H, Brock R. Preferential Uptake of L- versus D-Amino Acid Cell-Penetrating Peptides in a Cell Type-Dependent Manner. Chemistry & Biology 2011;18:1000-10.

[16] Urry DW. The Gramicidin A Transmembrane Channel: A Proposed π_(L,D) Helix. Proceedings of the National Academy of Sciences 1971;68:672-6.

[17] Wallace B, Ravikumar K. The gramicidin pore: crystal structure of a cesium complex. Science 1988;241:182-7.

[18] Jerath G, Hazam PK, Shekhar S, Ramakrishnan V. Mapping the Geometric Evolution of Protein Folding Motor. PLOS ONE 2016;11:e0163993.

[19] Jha D, Mishra R, Gottschalk S, Wiesmüller K-H, Ugurbil K, Maier ME, Engelmann J. CyLoP-1: A Novel Cysteine-Rich Cell-Penetrating Peptide for Cytosolic Delivery of Cargoes. Bioconjugate Chemistry 2011;22:319-28.

[20] Medina SH, Miller SE, Keim AI, Gorka AP, Schnermann MJ, Schneider JP. An Intrinsically Disordered Peptide Facilitates Non-Endosomal Cell Entry. Angewandte Chemie International Edition 2016;55:3369-72.

[21] Cascales L, Henriques ST, Kerr MC, Huang Y-H, Sweet MJ, Daly NL, Craik DJ. Identification and Characterization of a New Family of Cell-penetrating Peptides: CYCLIC CELL-PENETRATING PEPTIDES. Journal of Biological Chemistry 2011;286:36932-43.

[22] Lewis HD, Husain A, Donnelly RJ, Barlos D, Riaz S, Ginjupalli K, Shodeinde A, Barton BE. Creation of a novel peptide with enhanced nuclear localization in prostate and pancreatic cancer cell lines. BMC Biotechnology 2010;10:79.

[23] Drin G, Cottin S, Blanc E, Rees AR, Temsamani J. Studies on the Internalization Mechanism of Cationic Cell-penetrating Peptides. Journal of Biological Chemistry 2003;278:31192-201.

[24] Mäger I, Eiríksdóttir E, Langel K, El Andaloussi S, Langel Ü. Assessing the uptake kinetics and internalization mechanisms of cell-penetrating peptides using a quenched fluorescence assay. Biochimica et Biophysica Acta (BBA) - Biomembranes 2010;1798:338-43.

[25] Abraham MJ, Murtola T, Schulz R, Páll S, Smith JC, Hess B, Lindahl E. GROMACS: High performance molecular simulations through multi-level parallelism from laptops to supercomputers. SoftwareX 2015;1-2:19-25.

[26] Oostenbrink C, Villa A, Mark AE, Van Gunsteren WF. A biomolecular force field based on the free enthalpy of hydration and solvation: The GROMOS force-field parameter sets 53A5 and 53A6. Journal of Computational Chemistry 2004;25:1656-76.

[27] Herce HD, Garcia AE. Molecular dynamics simulations suggest a mechanism for translocation of the HIV-1 TAT peptide across lipid membranes. Proceedings of the National Academy of Sciences 2007;104:20805-10.

[28] Worm J, Kirkin AF, Dzhandzhugazyan KN, Guldberg P. Methylation-dependent Silencing of the Reduced Folate Carrier Gene in Inherently Methotrexate-resistant Human Breast Cancer Cells. Journal of Biological Chemistry 2001;276:39990-40000.

[29] Klähn M, Zacharias M. Transformations in plasma membranes of cancerous cells and resulting consequences for cation insertion studied with molecular dynamics. Physical Chemistry Chemical Physics 2013;15:14427-41.

[30] Riedl S, Rinner B, Asslaber M, Schaider H, Walzer S, Novak A, Lohner K, Zweytick D. In search of a novel target — Phosphatidylserine exposed by non-apoptotic tumor cells and metastases of malignancies with poor treatment efficacy. Biochimica et Biophysica Acta (BBA) - Biomembranes 2011;1808:2638-45.

[31] Cruciani RA, Barker JL, Zasloff M, Chen HC, Colamonici O. Antibiotic magainins exert cytolytic activity against transformed cell lines through channel formation. Proceedings of the National Academy of Sciences 1991;88:3792-6.

[32] Gurtovenko AA, Vattulainen I. Membrane Potential and Electrostatics of Phospholipid Bilayers with Asymmetric Transmembrane Distribution of Anionic Lipids. The Journal of Physical Chemistry B 2008;112:4629-34.

[33] Rothbard JB, Jessop TC, Lewis RS, Murray BA, Wender PA. Role of Membrane Potential and Hydrogen Bonding in the Mechanism of Translocation of Guanidinium-Rich Peptides into Cells. Journal of the American Chemical Society 2004;126:9506-7.

[34] Aronson MR, Simonson AW, Orchard LM, Llinás M, Medina SH. Lipopeptisomes: Anticancer peptide-assembled particles for fusolytic oncotherapy. Acta Biomaterialia 2018.

[35] Lin Y-C, Lim YF, Russo E, Schneider P, Bolliger L, Edenharter A, Altmann K-H, Halin C, Hiss JA, Schneider G. Multidimensional Design of Anticancer Peptides. Angewandte Chemie International Edition 2015;54:10370-4.

[36] Jobin M-L, Alves ID. On the importance of electrostatic interactions between cell penetrating peptides and membranes: A pathway toward tumor cell selectivity? Biochimie 2014;107:154-9.

Chapter 5
Syndiotactic Peptides for Targeted Delivery

6

Stereochemically Re-engineered and Functionally Optimized Syndiotactic Peptides for Small Molecule Delivery

The utilization of peptide-based drug delivery systems has been sub-optimal due to proteolytic susceptibility, poor cell permeability and limited tumor homing capabilities. In the present study, a series of peptides (STRAPs) with a syndiotactic polypeptide backbone (LDLD or DLDL stereochemical sequence) that can potentially form a spatial array of cationic group; an important feature that facilitate cellular uptake in tumor cells were designed. The peptides showed higher rates of transduction compared to the standard TAT peptide with an uptake profile independent of concentration, temperature and ATP. Furthermore, the cellular uptake of peptides was cell type dependent, with higher affinity for cancerous cells, than their non-cancerous counterparts. The designed peptides successfully delivered methotrexate, an anti-cancer drug to the cancerous cells with minimal toxicity to normal cells.

6.1 INTRODUCTION

The discovery of protein transduction domains (PTDs) from Antennapedia homeoprotein and HIV-1 transactivator TAT has paved the way for the identification of novel polypeptides capable of membrane permeation [1-3]. These cell-penetrating peptides (CPPs) are usually short, cationic sequences with the ability to internalize into various cell types. More than 1800 CPPs are presently recorded in the CPPSite 2.0 database [4]. Naturally, CPPs have been vastly studied for their prospective drug delivery application. Lack of stability in biological environment like proteolytic susceptibility and non-specific cellular targeting are the major roadblocks for limiting their use as drug delivery vehicles [5]. Herein, a novel class of de novo designed CPPs which are both proteolytically stable and cell-type specific is described.

Structure based design efforts so far were advocating two rather contrasting ideas. The first idea focus on providing enough flexibility to the peptide backbone, describing a rugged energy landscape with multiple minima (e.g. by introducing alkyl spacers), and the second one is forcing the molecule to a singular minimal energy conformation adopting methods like cyclization [6-8]. This work attempts to try a hybrid approach by designing an amphipathic sequence on a syndiotactic chain, yet short enough (7 amino acids long) to provide the necessary conformational flexibility. In the previous chapter, we discussed the re-designing of a stable syndiotactic backbone for cell penetrating applications. The designed SARTHI peptides had a chain length of 12 amino acids (12-mer). Peptide chain length is known to affect the cellular uptake of CPPs [9]. Therefore, a set of novel 7-mer peptides to study the effects of chain length on cell penetration potential of syndiotactic peptides were designed. A 7-mer syndiotactic peptide in principle would complete a single turn of the syndiotactic helix discussed in previous chapter. Other properties of 12-mer peptides i.e. cationicity, amphipathicity and stereochemical sequence were conserved in the designed 7-mer peptides.

6.2 RESULTS

6.2.1 PEPTIDE DESIGN and SYNTHESIS

The designed SyndioTactic Re-engineered Amphipathic Peptides (STRAPs) were tested for their ability to penetrate cell and deliver small molecules. The amino acid constitutions of STRAP-1, STRAP-2, STRAP-3 and STRAP-4 are same. STRAP-2 is the stereochemically reversed STRAP-1; similarly STRAP-4 is the stereochemically reversed STRAP-3 (Table 6.1). The designed peptides were synthesized by solid phase peptide synthesis using Fmoc chemistry [10]. A fluorophore (5(6)-Carboxyfluorescein) was conjugated to the N-terminus of the synthesized peptides for cellular uptake studies. The peptides were purified with semi-preparative reverse-phase HPLC and characterized by mass spectrometry using MALDI-TOF (Table 6.1).

Table 6.1. Peptide Sequences and Mass Characterization. *The sequences for the designed STRAP peptides are given in the following table. D-amino acids are shown as underlined characters. The expected masses for the designed sequences with N-terminus labelled with 5(6) Carboxyfluorescein (CF) and Methotrexate (MTX) were 1264.85 and 1343.07 respectively. The observed mass corresponds to the mass observed from MALDI-TOF analysis of the purified peptide products.*

Peptide	Sequence	Mass Observed
5(6) Carboxyfluorescein (CF) peptide conjugates		
STRAP-1-CF	CF- K R K I F C L	1265.82
STRAP-2-CF	CF- K R K I F C L	1265.59
STRAP-3-CF	CF- K R K F I C L	1265.72
STRAP-4-CF	CF- K R K F I C L	1265.74
Methotrexate (MTX) peptide conjugates		
STRAP-1-MTX	MTX- K R K I F C L	1343.64
STRAP-2-MTX	MTX- K R K I F C L	1343.71
STRAP-3-MTX	MTX- K R K F I C L	1343.79
STRAP-4-MTX	MTX- K R K F I C L	1343.88

6.2.2 PEPTIDE CONFORMATION

The conformation of the designed peptides were evaluated using CD Spectroscopy. The peptides were dissolved at 20 µM concentration in water and analyzed in the spectrophotometer (Figure 6.1). The conformation of peptides in both solvents was similar to SARTHI peptides and Gramicidin A (Figure 5.1), suggesting a similarity to Gramicidin conformation.

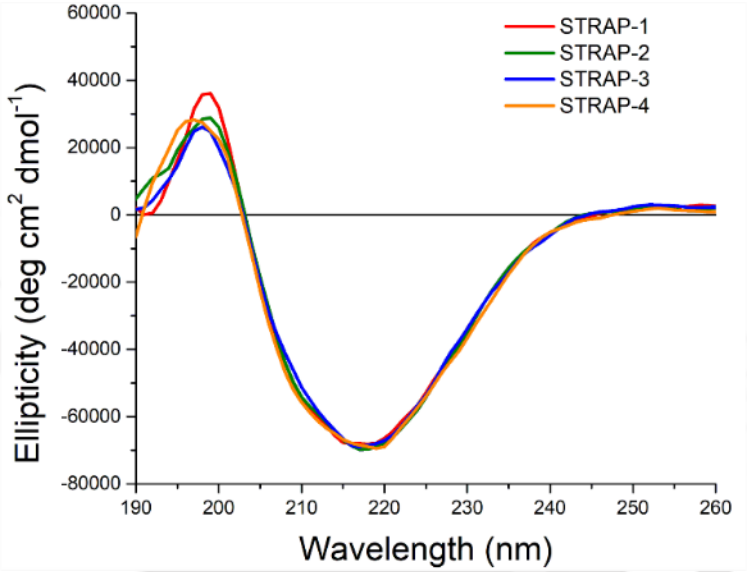

Figure 6.1. ***CD Spectra for STRAPs.*** *The CD spectra for STRAPs in water.*

6.2.3 CELLULAR UPTAKE OF STRAP PEPTIDES

Triple negative breast cancer cells (MDA-MB-231) were treated with 10 µM fluorophore tagged peptides for four hours at 37 °C in serum free media. The cells were visualized using a confocal laser scanning microscope to check for peptide internalization. The uptake of all the designed peptides was intracellular (Figure 6.2). The intracellular localization of all STRAP peptides was non-specific with both diffused and vesicular fluorescence signals. This suggests that the peptides are not selective towards any itracellular organelle. Such patterns of fluorescence are usually representation of a membrane-based cellular uptake mechanism [6]. The uptake of peptides through a membrane-based mechanism leads to the immediate bioavailability of CPPs in the cytosol from where the peptides may or may not localize in different cellular compartments [9]. Due to the non-specificity of intracellular localization of STRAP peptides, no further studies pertaining to intracellular localization were undertaken.

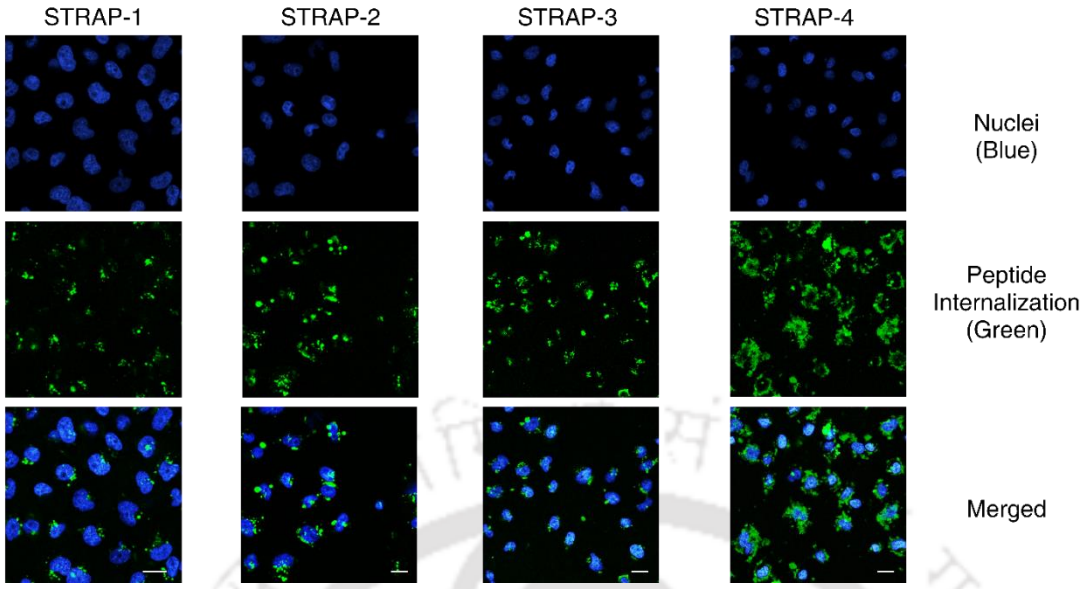

Figure 6.2. ***Cellular Uptake of STRAPs****. The cellular uptake of STRAP peptides was imaged after a four hour incubation of cells with 10 μM of peptides at 37 °C in serum-free conditions. Scale bar corresponds to 10 μm.*

6.2.4 COMPARATIVE CELLULAR UPTAKE OF STRAP PEPTIDES

The uptake of STRAP peptides was compared to the widely studied TAT peptide in breast cancer cells (MDA-MB-231) through flow cytometry. The designed peptides presented higher levels of cellular uptake than the TAT peptide under similar conditions of treatment (Figure 6.3). The uptake of STRAP peptides was 10-100 folds more than the TAT peptide similar to the previously discussed SARTHI peptides in MDA-MB-231 cells.

Further, the cellular uptake of STRAPs was studied with varying peptide concentrations (0, 2, 5, 10, 20, 40 and 50 μM) for a four-hour incubation period in breast cancer cells using fluorescence spectroscopy. The cellular uptake of peptides in breast cancer cells increased with incrementing concentrations (Figure 6.3). The corrected fluorescence units correspond to cell associated fluorescence measured per unit cell as discussed in section 4.1.8.

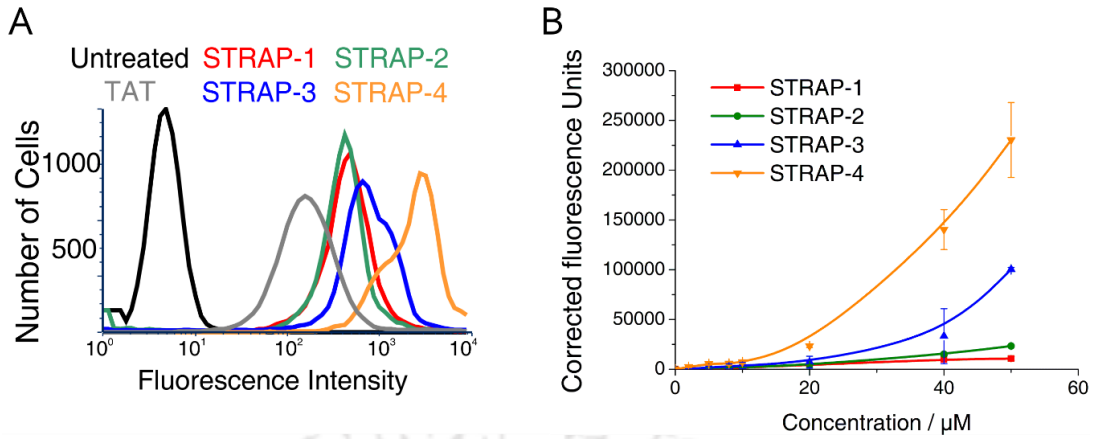

Figure 6.3. ***Comparative Uptake of STRAPs.*** *A) MDA-MB-231 cells were treated with 10 µM of STRAP-1-STRAP-4 and TAT peptides for four hours at 37 °C. Cells were analyzed for cell-associated fluorescence using flow cytometry. The uptake of STRAP peptides was 10-100 fold that of TAT peptide. B) MDA-MB-231 cells were treated with increasing concentrations (0, 2, 5, 10, 20, 40 and 50 µM) of STRAP-1-STRAP-4 for four hours at 37 °C. The cells were analyzed using fluorescence spectroscopy.*

6.2.5 MECHANISM OF CELLULAR UPTAKE FOR STRAP PEPTIDES

The mechanism of uptake for CPPs is majorly through endocytosis and/ or membrane translocation [9, 11]. However, the choice of mechanism(s) for cellular uptake of CPPs is affected by various factors including temperature, energy availability of the cell, cargo size and cell type [9]. The uptake of a peptide at a low temperatures (< 10 °C) is majorly due to membrane translocation. The uptake at phsiological temperature (37 °C) is generally attributed to both endocytosis and membrane translocation. Moreover, endocytosis is an energy dependent process, therefore, in an energy depleted condition, the uptake of peptides is mainly due to the passive membrane translocation process. However, the blocking of a single pathway can also lead to an increase in uptake of peptide through another channel [9], i.e. blocking of endocytosis may lead to an increased influx of peptides into the cells through membrane associated pathways.

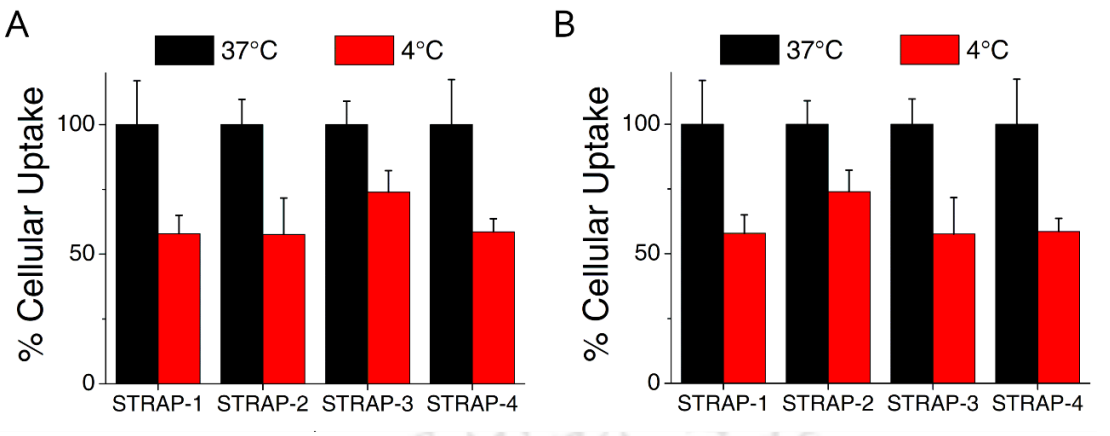

Figure 6.4. ***Temperature dependent uptake of STRAPs.*** *MDA-MB-231 (A) and HeLa (B) cells were treated with 10 μM of STRAP peptides at 4 °C for one hour. The cellular uptake of peptides was compared with their uptake at 37 °C. The uptake of STRAP peptides reduced to about 50 % at 4 °C.*

The mechanism(s) of cellular uptake of the designed peptides was studied by comparing the uptake of peptides under different conditions of temperature and energy availability. Both MDA-MB-231 and HeLa cells were treated with 10 μM of peptide-CF conjugates at 4 °C and 37 °C (Figure 6.4). The cellular uptake was evaluated using fluorescence spectroscopy. A reduced cellular uptake was observed for all the designed peptides at a lower temperature. The deficit of cellular uptake was nearly 40 % for STRAP-1, STRAP-2 and STRAP-4. On the other hand, the uptake of STRAP-3 was reduced by 25 % at 4 °C. The decreased uptake of CPPs at lower temperatures is due to the inhibition of energy dependent endocytic processes [12]. However, it can also arise from the reduced dynamics of the system which can affect membrane permeability [9, 13, 14].

Next, MDA-MB-231 and HeLa cells were treated with 0.1 % sodium azide for one hour at 37 °C which reduces the energy available to the cells [15]. The cells were then treated with 10 μM of peptide-CF conjugates for four hours at 37 °C. The cellular uptake of peptide-CF conjugates under the test conditions of sodium azide treatment was compared with the uptake in cells not treated with sodium azide (control). The cellular uptake of STRAP peptides was reduced by nearly 25 % in cells pre-treated with sodium azide in the two cell lines (Figure 6.5). This indicates that the cellular uptake of the designed peptides occurs through

multiple paths of endocytosis and membrane transduction simultaneously. The combination of pathways involved results in multiple localization sites for the peptide in the cells which was observed in the previous sections.

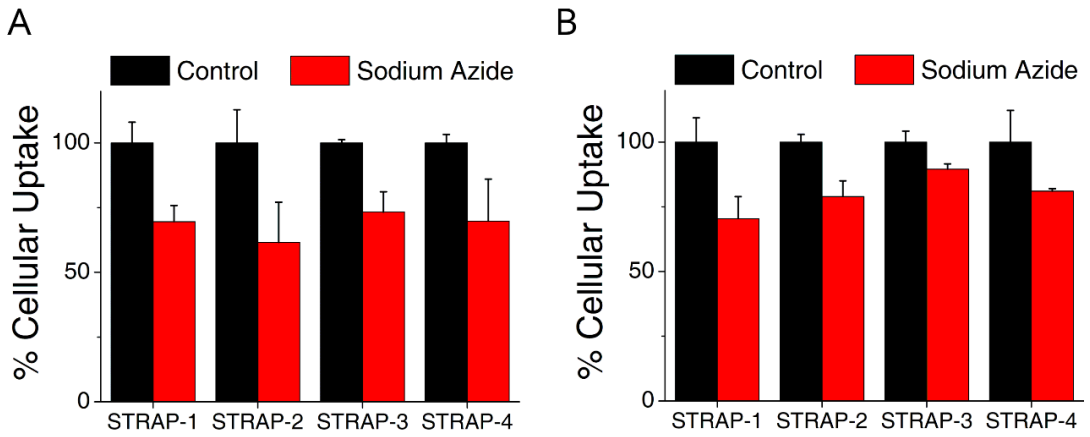

Figure 6.5. ***Energy dependent uptake of STRAPs.*** *MDA-MB-231 (A) and HeLa (B) cells were treated with 0.1 % of Sodium azide for one hour prior to treatment with 10 µM of STRAP peptides at 37 °C for one hour. The cellular uptake of peptides was compared with their uptake at 37 °C in cells without any sodium azide treatment. The uptake of STRAP peptides reduced to 70-90 % under test conditions.*

6.2.6 INTERACTION OF STRAP PEPTIDES WITH MODEL LIPID BILAYERS: An *in silico* study

The cellular uptake of STRAP peptides, as discussed in the previous sections suggests that, it is majorly through membrane transduction mechanisms. Therefore, an *in silico* experiment was designed for studying the interactions of the designed peptides with model lipid bilayers. The peptide molecules were simulated in a water system consisting a 128 membered POPG bilayer for 100 ns. The peptide structures were generated using a modified version of Ribosome software to incorporate D-amino acids, which was further verified using ProChiral [16]. The POPG bilayer was constructed using MemBuilder [17] and oriented in the x-y plane with its thickness in the z-direction. Four peptide molecules were added near to one side of the lipid bilayer along the Z-normal. The system was calibrated under NPT conditions for 1 ns followed by a production run of 100 ns.

At the end of the production run, the system was analyzed specifically for:

a) Visual signs of membrane penetration
b) Thickness of bilayer upon penetration
c) Depth of lipid bilayer penetration by peptides

The trajectory files for the production run was loaded in the VMD software for visualization of the simulation. All STRAP peptides were observed to have penetrated into the POPG bilayer at the end of the production run (Figure 6.6). The peptides have been represented in red, POPG bilayer as a white transparent surface and water as ice blue transparent surface.

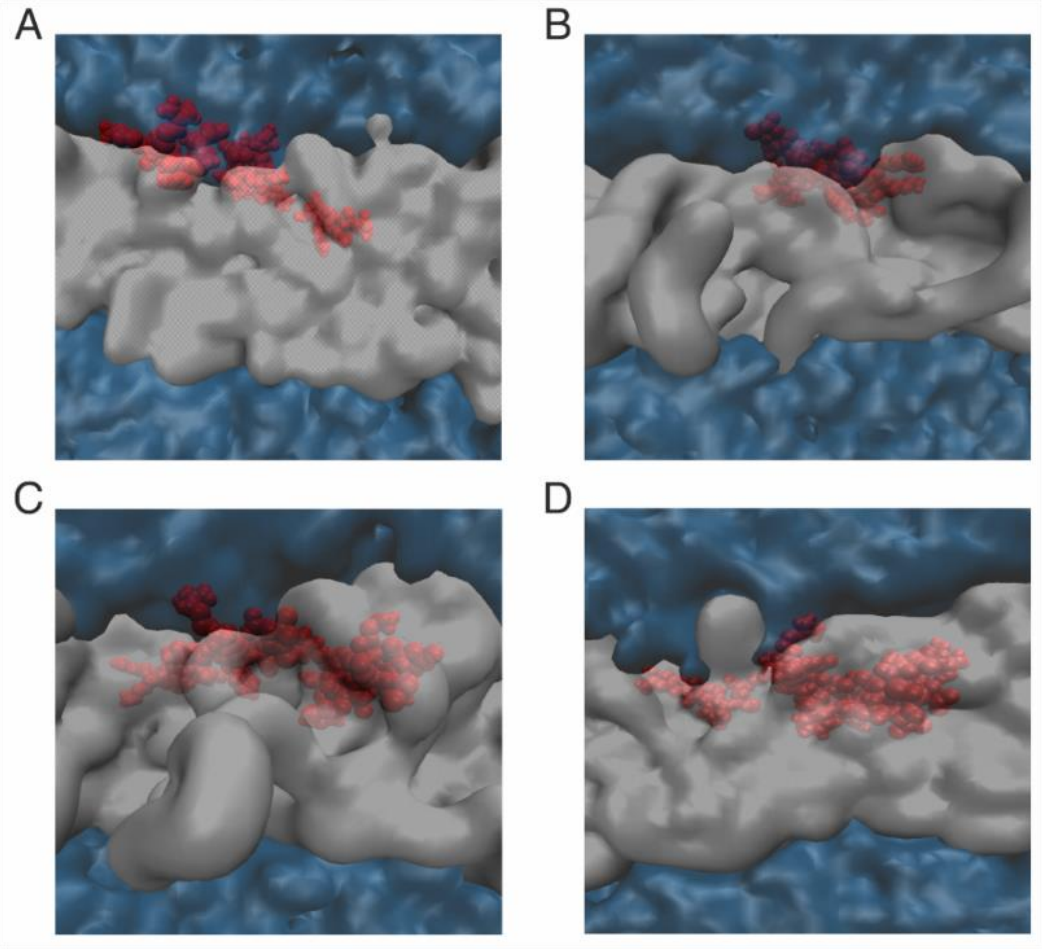

Figure 6.6. ***POPG Bilayer Penetration by STRAP Peptides.*** *Four molecules of STRAP-1-STRAP-4 (A-D respectively) were introduced near one layer of POPG bilayer in water. The penetration of POPG bilayer at the end of 100 ns run was*

visualized using VMD. The peptide molecules are shown in red, POPG bilayer as a white transparent surface and water as blue transparent surface.

The thickness of the bilayer was analyzed using GridMat software [18] at the end of the 100 ns run. The bilayer thickness was plotted as colored heat maps using GNUplot. A thinning of bilayer was observed at the sites of penetration by STRAP peptides (Figure 6.7). Similar observations have been previously reported for other CPP models studied by MD simulations [19].

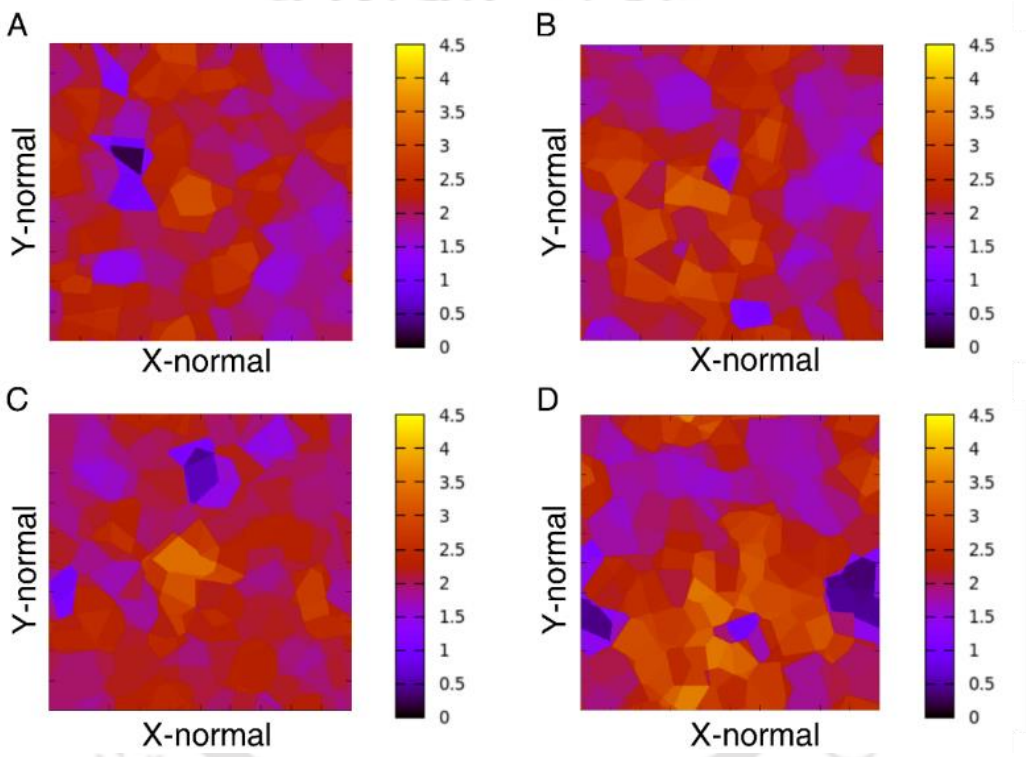

Figure 6.7. ***POPG Bilayer Thickness After Penetration by STRAP Peptides.*** *Four molecules of STRAP-1-STRAP-4 (A-D respectively) were introduced near one layer of POPG bilayer in water. The thickness of the POPG bilayer was calculated using GridMAT at the end of 100 ns run. The bilayer thickness is shown as a heat map with the bilayer thickness indicated as per the color bar.*

Next, the positions of the STRAP peptide molecules, POPG bilayer and water along the z-normal were analyzed(Figure 6.8). This would give us an insight towards the depth of penetration achieved by STRAP peptides. The positions of the peptide, POPG bilayer and water after 100 ns were compared to their positions at the beginning of the simulation. The depth of penetration for each of

the STRAP peptides were different with maximum penetration achieved by STRAP-4. This is in concordance with the earlier experimental observations discussed, wherein STRAP-4 showed maximum uptake in MDA-MB-231 and HeLa cells, among the STRAP peptide series.

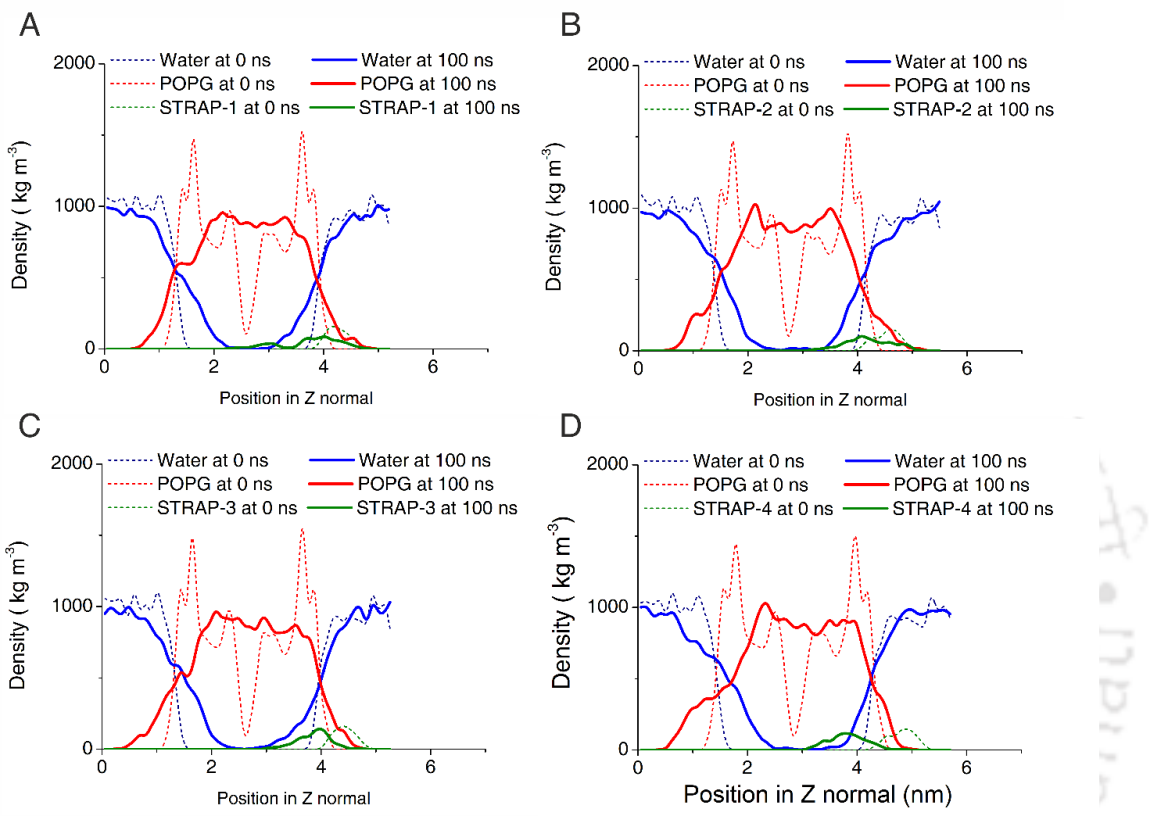

Figure 6.8. ***Relative Positioning of STRAP Peptides, POPG Bilayer and Water.*** *The positions of STRAP-1-STRAP-4 (A-D), POPG bilayer and water was mapped using the g_density function of GROMACS. The density of particle along the z-axis at the start (dotted) and end (solid) of 100 ns simulation indicates the extent of POPG bilayer penetration by STRAP peptides.*

6.2.7 BIOCOMPATIBLE CELLULAR UPTAKE OF STRAPs

Lack of proteolytic stability (biocompatibility) is a major roadblock for the development of CPPs as drug delivery vehicles. Therefore, the cellular uptake of the designed peptides was tested in serum containing media (10 % fetal bovine serum) using flow cytometry. MDA-MB-231 cells were treated with 10 μM of STRAP-CF conjugates for four hours under standard conditions. The cellular

uptake of STRAP peptides under test conditions was compared with their uptake in serum-free media. The cellular uptake of the designed peptides, except STRAP-3 was similar in both serum-positive and serum-free media (Figure 6.9).

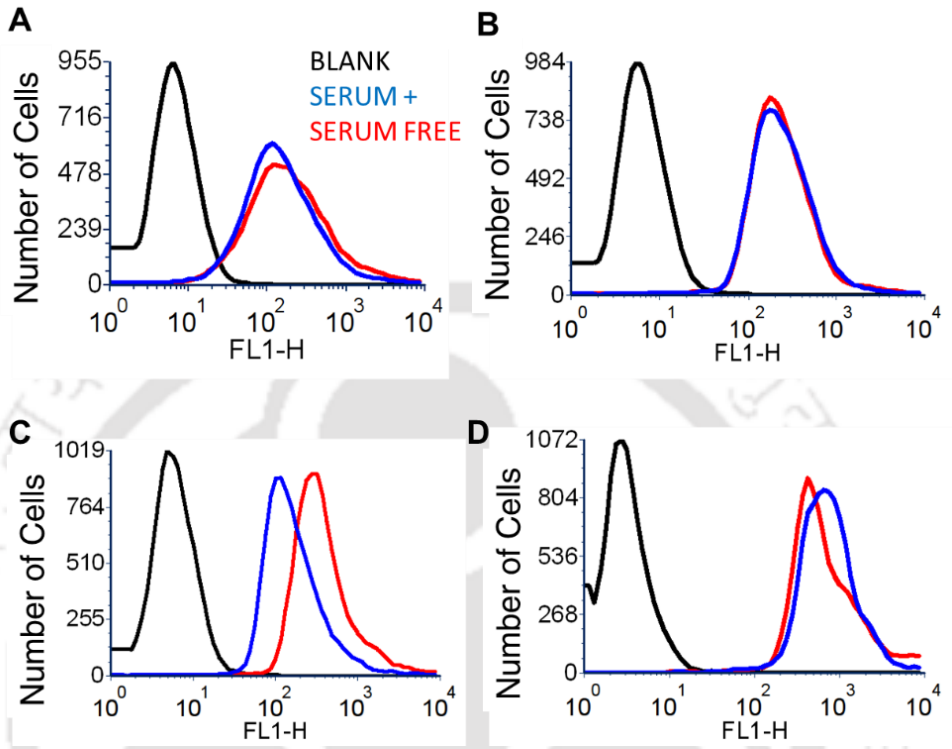

Figure 6.9. ***Cellular Uptake of STRAPs in serum presence.*** *MDA-MB-231 cells were treated with 10 μM of STRAPs for 4 hours in serum containing and serum-free conditions. All peptides showed similar penetrative capability in the two conditions suggesting that the serum presence in the medium does not hamper their activity.*

The above observation indicates that the activity of the designed peptides is conserved even in the presence of serum in treatment media. However, the presence of serum in treatment media may lead to artefacts due to increased cell proliferation and/or kinetics. Therefore, another experiment was designed for evaluating the biocompatible activity of the designed peptides. Peptide stocks were treated with equal volumes of human plasma and bovine serum for one hour at 37 °C. MDA-MB-231 cells were treated with the peptide stocks pre-treated with plasma or serum for four hours under standard conditions. The uptake of peptides under these test conditions was compared with the uptake of peptides which were not treated with either human plasma or bovine serum.

Cellular uptake was measured through flow cytometry. The uptake of STRAP-1, STRAP-2 and STRAP-4 was similar in both test and control conditions (Figure 6.10). The uptake of STRAP-3 was reduced when treated with bovine serum but showed similar uptake on treatment with human plasma. This suggests that the cell penetration efficacy of STRAP-1, STRAP-2 and STRAP-4 is stable in the presence of biological fluids and thus biocompatible. On the other hand, reduction in cellular uptake of STRAP-3 indicates partial serum susceptibility.

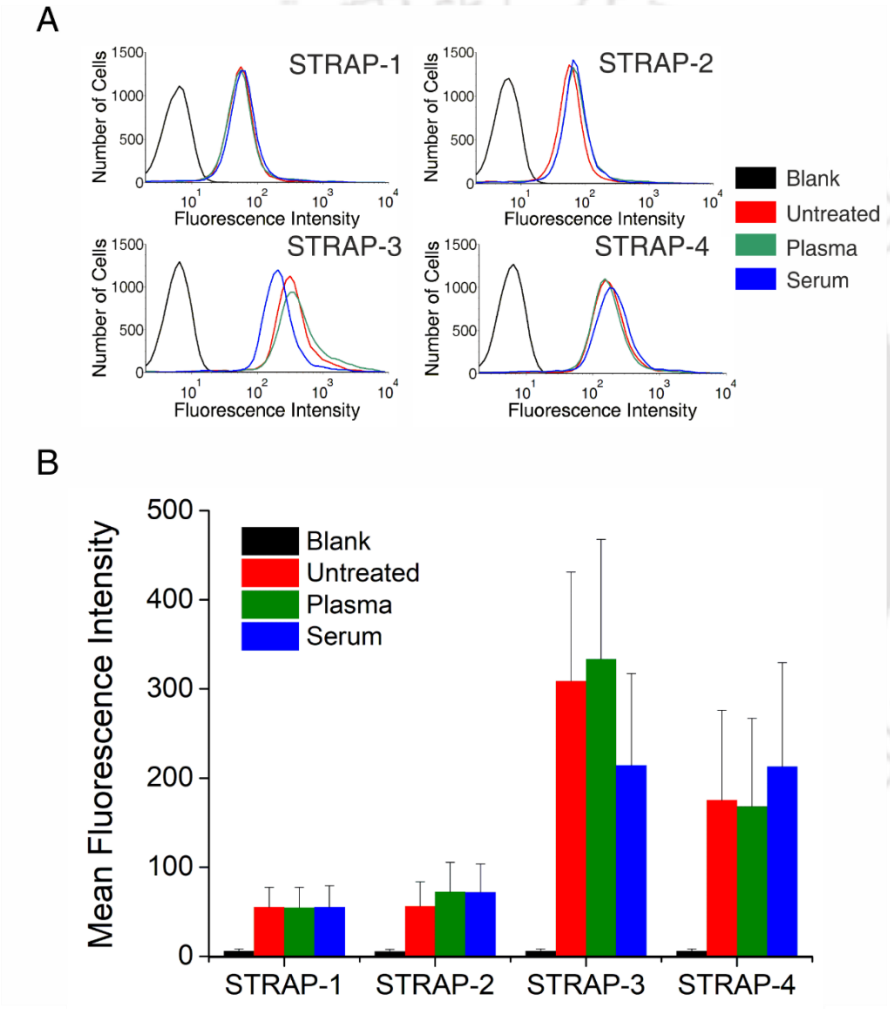

Figure 6.10. ***Biocompatibility of STRAPs.*** *Biocompatibility of STRAP peptides was evaluated in bovine serum and human plasma. The peptides were pre-treated with bovine serum and human plasma for one hour at 37 °C. MDA-MB-231 cells were treated with the same peptide stocks and their uptake was compared with the uptake of untreated peptide stocks using flow cytometry. A) Histograms signify cell-associated fluorescence under different pre-treatment conditions for STRAPs.*

Blank represents cells not treated with any peptide solution and untreated refers to cells treated with peptides (without any pre-treatment). B) Mean fluorescence computed from the histograms shown in panel A for the varied treatment conditions.

6.2.8 CELLULAR UPTAKE IN CANCEROUS vs NON-CANCEROUS CELLS

To evaluate the cell type specificity of the designed peptides, breast cancer, cervical cancer and non-cancerous origin (transformed HEK-293) cells were treated with 10 μM of STRAP peptides. The cellular uptake in the three cell lines was compared for each of the designed peptides (Figure 6.11). The uptake of peptides was maximum in breast and cervical cancer cells compared to HEK-293. This observation was based on the comparative assessment of fluorescence-based uptake studies and is therefore suggestive [20-24].

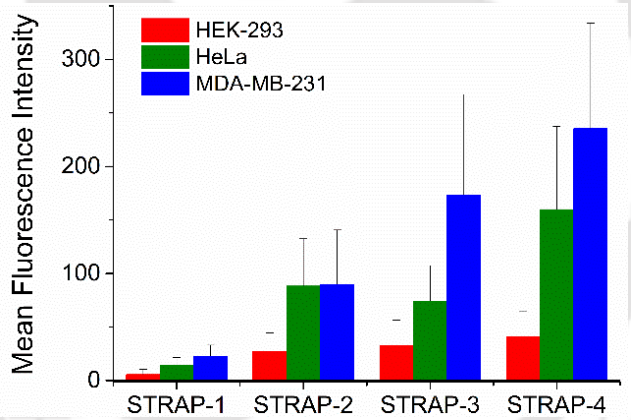

Figure 6.11. ***Cell-Type Specificity of STRAPs.*** *Comparative uptake of STRAPs in cancerous (MDA-MB-231, HeLa) and non-cancerous (HEK-293) cell lines was evaluated through flow cytometry. The relative uptake represented in histograms are shown as per the color bar associations for each cell type.*

6.2.9 CARGO DELIVERY EFFICIENCY OF STRAPs

The purpose of a drug delivery vehicle is to "deliver" a functional molecule to the cells. The delivery vehicle can be conjugated to the drug molecule through ionic, hydrogen or covalent bonds. Size and hydrophobicity of the cargo effects cellular uptake of CPPs delivering the cargo. Therefore, methotrexate (MTX) was used

and conjugated to the N-terminus of STRAPs (Table 6.1) to evaluate their cargo/drug delivery potential. The size and hydrophobicity of MTX is similar to those of CF and thus makes it an ideal candidate for evaluating a peptide's cargo/ drug delivery potential. The peptides were tested for their capability to deliver the active drug molecule in breast and cervical cancer cells. HeLa, MDA-MB-231 and HEK-293 cells were treated with varying concentrations of STRAP-CF, MTX and STRAP-MTX conjugates for 72 hours. Cell viability was assessed using MTT assay.

Table 6.2. ***IC_{50} values****. The inhibitory concentration to kill 50 % cells in 72 hours (IC_{50}) against MDA-MB-231, HeLa and HEK-293 cells is given for the peptide-CF and peptide-MTX conjugates. Peptide-CF conjugates had no significant toxicity till the maximum concentration tested (50 μM).*

Peptide	IC_{50} (μM)*		
	MDA-MB-	HeLa	HEK-293
5(6) Carboxyfluorescein (CF) peptide conjugates			
STRAP-1-CF	> 50	> 50	> 50
STRAP-2-CF	> 50	> 50	> 50
STRAP-3-CF	> 50	> 50	> 50
STRAP-4-CF	> 50	> 50	> 50
Methotrexate (MTX) peptide conjugates			
STRAP-1-MTX	2.26 ± 0.31	1.63 ± 0.28	> 50
STRAP-2-MTX	1.82 ± 0.24	11.8 ± 2.28	> 50
STRAP-3-MTX	1.79 ± 0.31	1.22 ± 0.18	> 50
STRAP-4-MTX	1.34 ± 0.19	1.01 ± 0.22	> 50

*IC_{50} for Methotrexate in MDA-MB-231, HeLa and HEK-293 cells was > 40 μM, 3.3 ± 0.9 μM and 2.4 ± 0.4 μM respectively.

The delivery of MTX by STRAP peptides would in principle increase its bioavailability in the cell given poor permeating property of MTX. This should lead to an increase in the cytotoxicity of MTX when delivered as peptide-MTX conjugates. The cytotoxicity of MTX towards HeLa cells increased when delivered as peptide-MTX conjugates, except for STRAP-2-MTX (Figure 6.12A).

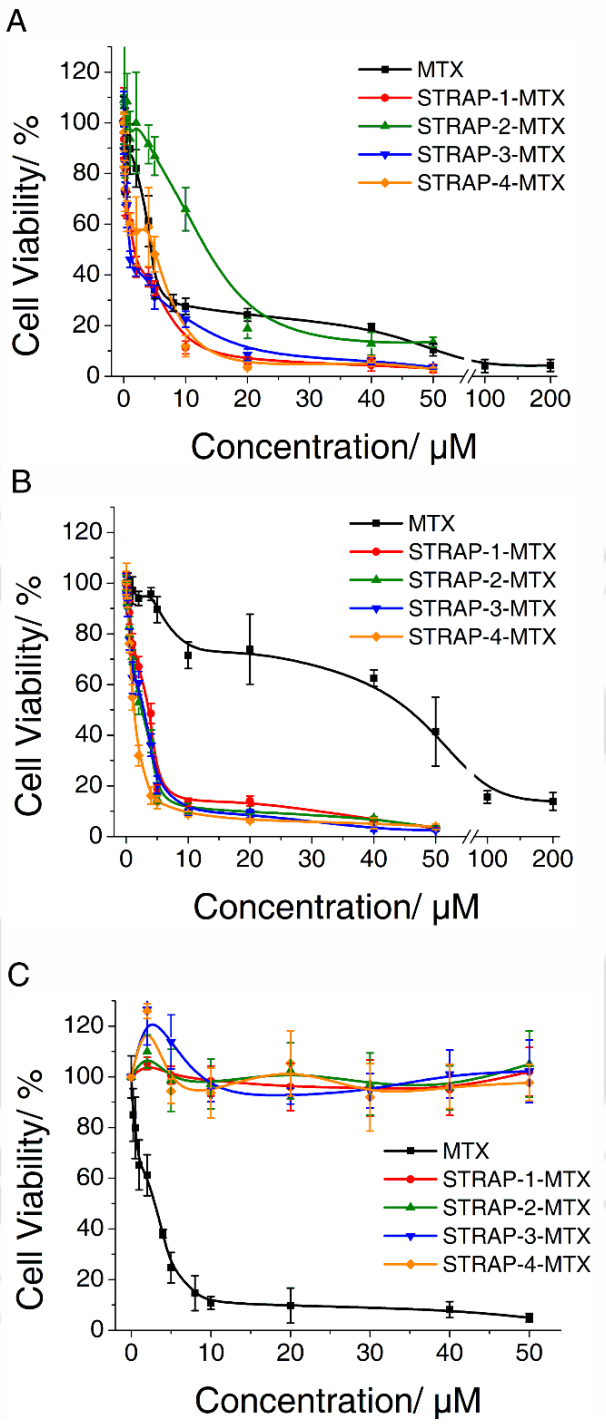

Figure 6.12. ***Small Molecule delivery efficiency of STRAPs.*** *A)-D) MDA-MB-231 cells were treated with varying concentrations of STRAP-MTX conjugates and MTX for 72 hours in serum-free conditions. The toxicity of STRAP-MTX conjugates was more than the toxicity of MTX. The dose-response curve for peptide-drug conjugates against MDA-MB-231 and HeLa cells are shown as per their respective color associations.*

The increase in cytotoxicity is evident from reduction in inhibitory concentrations to kill 50 % of cells (IC_{50}) for STRAP-MTX conjugates in comparison to MTX alone (Table 6.2). The MTX-resistance for MDA-MB-231 cells is well-established [25, 26]. However, the delivery of MTX through STRAP peptides lead to overcoming of the mentioned drug resistance of MDA-MB-231 cells (Figure 6.12B). The IC_{50} for STRAP-4-MTX in MDA-MB-231 cells was the least among all STRAP peptides (Table 6.2).

The peptide-drug conjugates showed no significant toxicity to the HEK-293 cells under the tested conditions, thereby, affirming the previous observation of higher uptake rates in cancerous cells (Figure 6.12C). The peptide-CF conjugates were not cytotoxic to either of the cell types. The IC_{50} values of STRAP-CF and STRAP-MTX conjugates against the tested cell lines is given in Table 6.2.

6.3. DISCUSSION

A novel approach to design syndiotactic cell-penetrating peptides has been discussed. The effect of peptide length on cell penetration potential of peptides was evaluated. The physicochemical properties of the designed STRAP peptides was similar to the previously described SARTHI peptides in terms of relative charge per unit length, structural amphipathicity and stereochemical sequence. The peptide length of STRAP peptides is seven (7-mer) in comparison to the 12-mer SARTHI peptides. The designed peptide structures were evaluated in water and ethanol using CD spectroscopy. The designed peptides showed similar CD spectra to Gramicidin and SARTHI peptides in water (Figure 6.1 and Figure 5.1). This indicates the stability of the syndiotactic backbone structure to form $\Pi_{(L,D)}$ helix irrespective of the length of the sequence.

The intra-cellular distribution of STRAP peptides showed both diffused and vesicular profiles. A diffused pattern relates to their localization in the cytosol, while a vesicular distribution suggests localization to other cell organelles. Therefore, the intracellular localization of STRAP peptides is non-specific. Further, STRAP peptides employ multiple routes of cellular entry for their cellular uptake. The mechanism of cellular uptake of STRAP peptides was studied

by treating MDA-MB-231 and HeLa cells with peptides at lower temperatures and under energy depleting conditions. Both conditions are inhibitors of endocytosis and therefore, the uptake under these test conditions signifies the membrane-based route of cellular uptake for STRAP peptides. Conversely, the reduction in uptake which varies for each peptide in either of the test conditions, suggests the presence of an endocytic route for cellular uptake as well. Therefore, the uptake of STRAP peptides occurs through multiple routes simultaneously.

MD simulations using POPG lipid bilayers in water as a test system were performed to study the interactions of STRAP peptides with lipid bilayer. The peptides were introduced in the system and simulated for 100 ns. The lipid bilayer penetration by peptides was evaluated on three parameters: visual observation, membrane thickness and relative positions. The peptides penetrated the outer layer of the POPG bilayer. The penetration of the lipid bilayer lead to a thinning of the bilayer near the site of penetration. This is in concordance with the observations of previously published studies, which have postulated the bilayer thinning as an early event of cell penetration through membrane-based pathways. Further, the formation of pores in the membrane due to penetration of STRAP peptides also correlates to other pore formation models for cell penetration.

The peptides are biocompatible with both serum and human blood plasma. An interesting observation is that the designed peptides are suggestively specific for cancer cells. The drug/small molecule delivery of the designed peptides has also been demonstrated. The delivery of the drug as peptide-drug conjugates, increases the intracellular bioavailability of the drug. The peptide-drug conjugates significantly increase the toxicity of the drug molecule against the diseased cells, with minimum damage to other cell types. The observation is, therefore, supportive towards re-programming of existing drug molecules with novel peptide-based drug delivery vehicles as a future therapeutic option.

6.4. CONCLUSION

Cellular uptake at micromolar concentrations coupled with lower levels of cytotoxicity and hemolytic activity are the hallmarks of an ideal delivery vehicle, which offers immediate access to cytoplasm. A consensual structural fingerprint with the desired levels of target specificity has not yet been achieved. The sub-optimal use of peptides as a possible solution was primarily due to poor serum stability and permeability. Through the design of 7-mer STRAP series peptides, the aim is to address these limitations, adopting a balanced approach in design with a long term objective of generating a CPP fingerprint based on electrostatics, for each cell type.

6.5. REFERENCES

[1] Brasseur R, Divita G. Happy birthday cell penetrating peptides: already 20 years. Biochimica et biophysica acta 2010;1798:2177-81.

[2] Heitz F, Morris MC, Divita G. Twenty years of cell-penetrating peptides: from molecular mechanisms to therapeutics. British journal of pharmacology 2009;157:195-206.

[3] Bechara C, Sagan S. Cell-penetrating peptides: 20 years later, where do we stand? FEBS Letters 2013;587:1693-702.

[4] Agrawal P, Bhalla S, Usmani SS, Singh S, Chaudhary K, Raghava Gajendra PS, Gautam A. CPPsite 2.0: a repository of experimentally validated cell-penetrating peptides. Nucleic Acids Research 2016;44:D1098-D103.

[5] Verdurmen WP, Bovee-Geurts PH, Wadhwani P, Ulrich AS, Hallbrink M, van Kuppevelt TH, Brock R. Preferential uptake of L- versus D-amino acid cell-penetrating peptides in a cell type-dependent manner. Chemistry & biology 2011;18:1000-10.

[6] Medina SH, Miller SE, Keim AI, Gorka AP, Schnermann MJ, Schneider JP. An Intrinsically Disordered Peptide Facilitates Non-Endosomal Cell Entry. Angewandte Chemie International Edition 2016;55:3369-72.

[7] Nischan N, Herce HD, Natale F, Bohlke N, Budisa N, Cardoso MC, Hackenberger CPR. Covalent Attachment of Cyclic TAT Peptides to GFP Results in Protein Delivery into Live Cells with Immediate Bioavailability. Angewandte Chemie International Edition 2015;54:1950-3.

[8] Wu H, Mousseau G, Mediouni S, Valente ST, Kodadek T. Cell-Permeable Peptides Containing Cycloalanine Residues. Angewandte Chemie International Edition 2016;55:12637-42.

[9] Copolovici DM, Langel K, Eriste E, Langel Ü. Cell-Penetrating Peptides: Design, Synthesis, and Applications. ACS Nano 2014;8:1972-94.

[10] Hazam PK, Jerath G, Kumar A, Chaudhary N, Ramakrishnan V. Effect of tacticity-derived topological constraints in bactericidal peptides. Biochimica et biophysica acta 2017;1859:1388-95.

[11] Heitz F, Morris MC, Divita G. Twenty years of cell-penetrating peptides: from molecular mechanisms to therapeutics. British Journal of Pharmacology 2009;157:195-206.

[12] Cascales L, Henriques ST, Kerr MC, Huang Y-H, Sweet MJ, Daly NL, Craik DJ. Identification and Characterization of a New Family of Cell-penetrating Peptides: CYCLIC CELL-PENETRATING PEPTIDES. Journal of Biological Chemistry 2011;286:36932-43.

[13] Lewis HD, Husain A, Donnelly RJ, Barlos D, Riaz S, Ginjupalli K, Shodeinde A, Barton BE. Creation of a novel peptide with enhanced nuclear localization in prostate and pancreatic cancer cell lines. BMC Biotechnology 2010;10:79.

[14] Drin G, Cottin S, Blanc E, Rees AR, Temsamani J. Studies on the Internalization Mechanism of Cationic Cell-penetrating Peptides. Journal of Biological Chemistry 2003;278:31192-201.

[15] Mäger I, Eiríksdóttir E, Langel K, El Andaloussi S, Langel Ü. Assessing the uptake kinetics and internalization mechanisms of cell-penetrating peptides using a quenched fluorescence assay. Biochimica et Biophysica Acta (BBA) - Biomembranes 2010;1798:338-43.

[16] Jerath G, Hazam PK, Ramakrishnan V. bPE toolkit: toolkit for computational protein engineering. Systems and synthetic biology 2014;8:337-41.

[17] Ghahremanpour MM, Arab SS, Aghazadeh SB, Zhang J, van der Spoel D. MemBuilder: a web-based graphical interface to build heterogeneously mixed membrane bilayers for the GROMACS biomolecular simulation program. Bioinformatics (Oxford, England) 2014;30:439-41.

[18] J. AW, A. LJ, R. BD. GridMAT-MD: A grid-based membrane analysis tool for use with molecular dynamics. Journal of Computational Chemistry 2009;30:1952-8.

[19] Herce HD, Garcia AE. Molecular dynamics simulations suggest a mechanism for translocation of the HIV-1 TAT peptide across lipid membranes. Proceedings of the National Academy of Sciences 2007;104:20805-10.

[20] Myrberg H, Zhang L, Mäe M, Langel Ü. Design of a Tumor-Homing Cell-Penetrating Peptide. Bioconjugate Chemistry 2008;19:70-5.

[21] Teesalu T, Sugahara K, Ruoslahti E. Tumor-Penetrating Peptides. Frontiers in Oncology 2013;3.

[22] Mäe M, Myrberg H, El-Andaloussi S, Langel Ü. Design of a Tumor Homing Cell-Penetrating Peptide for Drug Delivery. International Journal of Peptide Research and Therapeutics 2009;15:11-5.

[23] Myrberg H, Zhang L, Mae M, Langel U. Design of a tumor-homing cell-penetrating peptide. Bioconjugate chemistry 2008;19:70-5.

[24] Teesalu T, Sugahara KN, Kotamraju VR, Ruoslahti E. C-end rule peptides mediate neuropilin-1-dependent cell, vascular, and tissue penetration. Proceedings of the National Academy of Sciences 2009;106:16157-62.

[25] Depau L, Brunetti J, Falciani C, Scali S, Riolo G, Mandarini E, Pini A, Bracci L. Coupling to a cancer-selective heparan-sulfate-targeted branched peptide can by-pass breast cancer cell resistance to methotrexate. Oncotarget 2017;8:76141-52.

[26] Wu Z, Shah A, Patel N, Yuan X. Development of methotrexate proline prodrug to overcome resistance by MDA-MB-231 cells. Bioorganic & Medicinal Chemistry Letters 2010;20:5108-12.

7

Topologically Constrained Peptides for Targeted Drug Delivery

Cell Penetrating peptides (CPPs) are short oligomeric peptides capable of translocating across the cell membrane while simultaneously employing multiple mechanisms of entry. Most CPPs exist as disordered structures in solution and may adopt a helical conformation on interaction with cell membrane, vital to their penetrative capability. Herein, a series of cationic helical amphipathic peptides (CHAPs) which are topologically constrained is reported. The peptides were tested against cervical and breast cancer cells for their cell penetration and drug delivery potential. The cellular uptake of CHAP peptides is independent of temperature and energy availability. The activity of the peptides is biocompatible in bovine serum. CHAPs delivered functional methotrexate (MTX) inside the cell as CHAP-MTX conjugates, which was more toxic to cancer cells than MTX alone. Significantly, the CHAP-MTX conjugates were less toxic to HEK-293 cells than the cancer cells suggesting higher affinity towards breast and cervical cancer cells.

7.1. INTRODUCTION

Development of novel targeted drug delivery systems has gained momentum in the last decade [1]. Multiple polymer, nano-assembly, liposome, nucleic acid and peptide based materials have been reported with varying efficiencies of drug delivery [2-6]. Peptides are small bio-derived molecules with the capacity to link a molecule of choice through established chemical reactions. Since the discovery of Tat and Penetratin, numerous peptides with cell permeation capability have been reported in past couple of decades as potential drug delivery vehicles [7-11]. Varying insights for CPP design like cationic charge, sequence length, amino acid composition and amphipathicity have been widely reported [12]. However, the clinical applications of CPPs as delivery vectors are limited due to their proteolytic instability and lack of cell type specificity [10, 12].

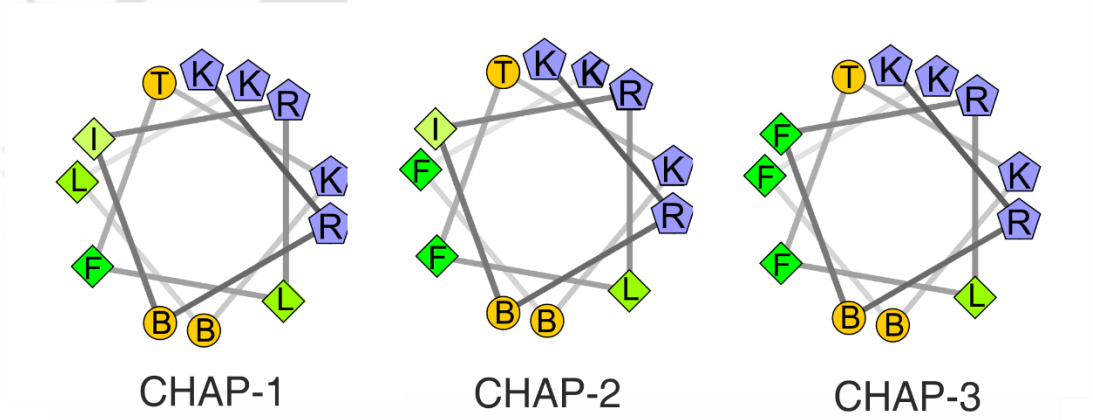

Figure 7.1. ***Helical wheels for CHAP peptides.*** *The helical wheels for the designed peptide sequences show distinct polar and hydrophobic regions. Blue denotes polar or hydrophilic residues. Green signifies hydrophobic residues, with a darker shade for more hydrophobic residues. Yellow denotes residues.*

Most CPPs are poly-L in terms of stereochemistry and exist as an ensemble of disordered structures in solution [13, 14]. Though disordered peptides can also penetrate live cell membranes, however, many CPPs including penetratin re-structure to form alpha helices upon their interaction with cell membranes [15]. Helical structures may or may not be retained in physiological conditions. The inability of a peptide to form an alpha helix can alter the structural

amphipathicity and other design features in the peptide sequence [16]. The poly-L nature of CPPs also contributes to their proteolytic instability. Additionally, poly-L peptides have more tendency to be recognized by endocytic receptors on cell surface leading to their uptake by endocytosis. Though, it works positively for CPPs in terms of cell penetration, it may also lead to their entrapment in endosomes and lysosomes, which can hinder their use drug delivery vehicles [11].

In this chapter, a peptidomimetic approach was used for designing CPPs with defined conformation. An "unnatural" amino acid, 2-Amino isobutyric acid (Aib, B) was used to constrain the topology of the peptide molecule. Aib has been known to predominantly form alpha helices and is often a constituent of many fungal based antibacterial peptides [17-19]. Antimicrobial peptides share multiple common features with CPPs and present a template for designing novel CPPs [20]. About 50 peptides designed on various design paradigms and amino acid compositions were tested to optimize the amino acid side-chain sequence for cell-penetration. The amino acid sequence for CHAP-1 was thus identified. The sequences, CHAP-2 and CHAP-3 were designed with sequential mutations at positions 11 (L->F) and 4 (I->F) respectively (Figure 7.1). The peptides CHAP-1, CHAP-2 and CHAP-3 were imparted with two molecules of Aib at 3rd and 10th amino acid positions to constrain the structure in alpha helical conformation. The designed sequences have an integral structural amphipathicity with distinct region of polar and hydrophobic residue clusters as shown by their helical wheels. However, this only holds true if the incorporation of Aib constricts the topology of the peptides in an α-helical conformation only [21-23]; the failure of which would lead to perturbations in the structural amphipathicity of the designed peptides which may compromise their ability to penetrate live membranes.

7.2. RESULTS and DISCUSSIONS

7.2.1. Peptide Structure Conformation

The helical conformation of the designed peptides were experimentally verified. 10 μM peptide-CF conjugates were dissolved in water and analyzed using CD

Spectroscopy (Figure 7.2). The CD spectra for the designed peptides showed positive peak at 193 nm and negative peaks at 208 and 222 nm, characteristic of alpha helices [24, 25]. The presence of these peaks confirm the alpha helical conformation of the designed peptides. The percent helicity of the designed sequences was calculated using the K2D3 server [26]. The peptides showed different measures of helicity, usually expressed as percentage helicity as deduced from the CD spectra. CHAP-1, CHAP-2 and CHAP-3 had 55, 78 and 95 % helicity respectively. This indicates the possible effects of variable amino acid side-chains on the topological constriction of designed peptides.

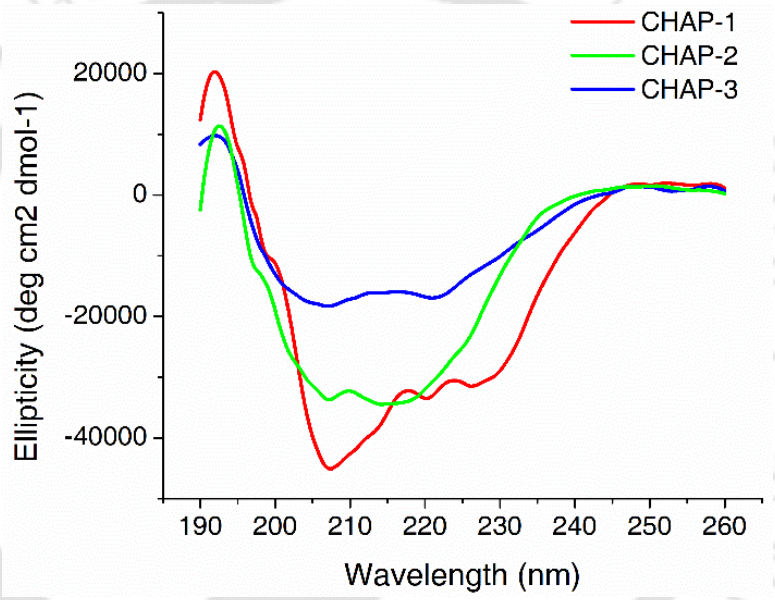

Figure 7.2. ***CD Spectra of CHAP Peptides.*** *CD spectra for 10 μM CHAP peptides in water. Positive peak at 193 nm and negative peaks at 208 and 222 nm are representative of alpha helices*

7.2.2. Cellular Uptake of CHAP peptides

To study the cell penetrative capability of CHAP peptides, HeLa cells were treated with 10 μM of peptide-CF conjugates for four hours. Post-treatment, nuclei of live cells was labelled with Hoechst 33342. The cells were viewed under a confocal microscope. The uptake of CHAP peptides showed similar distribution. The internalized peptides showed diffused and vesicular uptake profiles (Figure 7.3). This suggests that the peptide uptake was non-organelle specific. Further, the

cellular uptake of CHAP peptides was compared to the standard TAT peptide using flow cytometry.

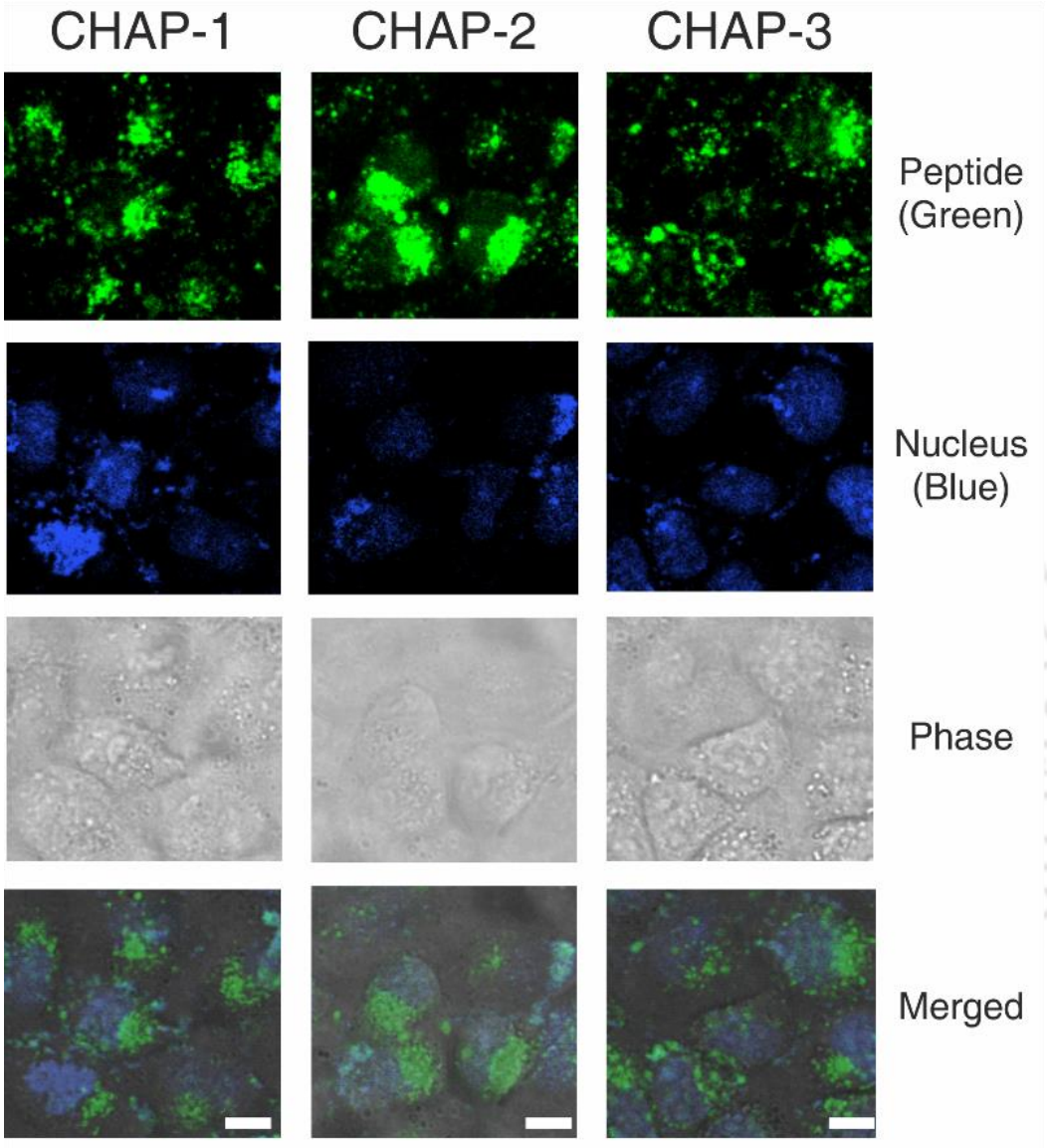

Figure 7.3. ***Intracellular Localization of CHAP Peptides.*** *Cell line derived from cervical cancer cells (HeLa) was treated with 10 μM of CHAP-CF conjugates for four hours at 37 °C. Nuclei of live cells were labelled with Hoechst 33342. The cellular uptake profile of CHAP peptides was both diffused and vesicular, indicating their non-specific intracellular localization.*

Cervical (HeLa) and breast cancer cells were treated with 10 μM of CHAP-CF and TAT-CF conjugates for four hours at 37 °C. The uptake of CHAP peptides was relatively more than that of the TAT peptide, indicating increased levels of uptake

of CHAP peptides compared to TAT (Figure 7.4A-7.4B). Among the CHAP peptides, CHAP-3 showed maximum levels of cellular uptake in the two cancer cell lines (MDA-MB-231 and HeLa). These observations illustrate the effect of changes in electrostatic potential distribution on the cell penetration capability of the designed peptides.

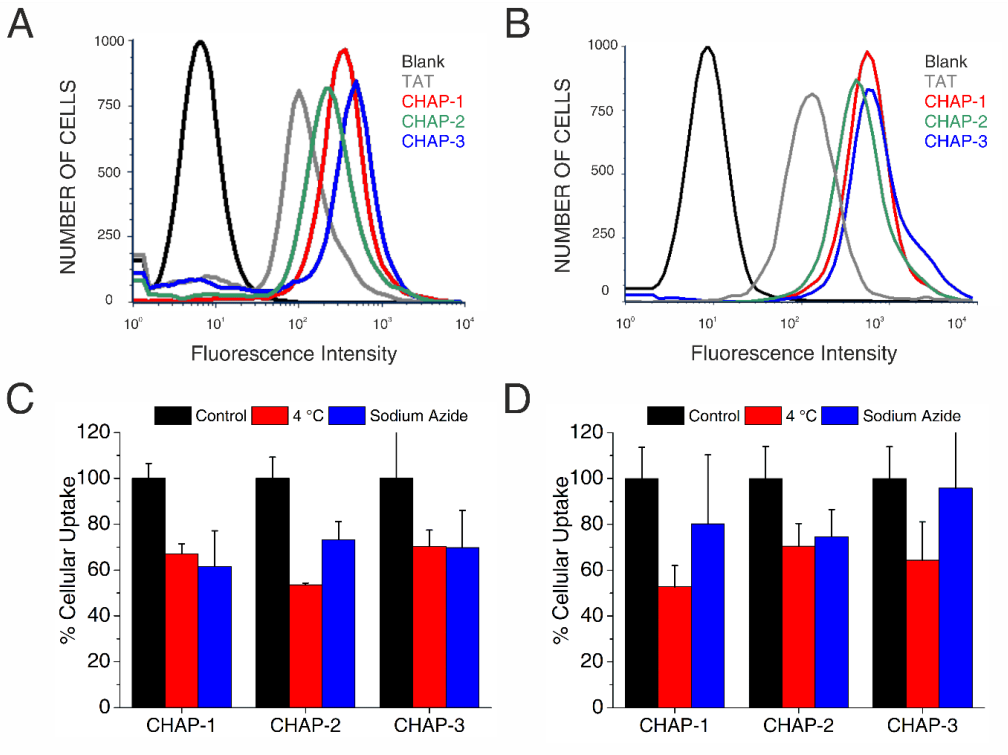

Figure 7.4. ***Cellular Uptake of CHAP Peptides.*** *A) Breast (MDA-MB-231) and B) cervical cancer (HeLa) were treated with 10 µM of CHAP-CF conjugates for four hours at 37 °C. Cell associated fluorescence was measured by flow cytometry. MDA-MB-231 (C) and HeLa (D) cells were treated with 10 µM CHAP peptides for one hour under differing conditions of temperature and in presence of sodium azide. The cellular uptake of CHAP peptides reduced to about 50-70 % at lower temperature in the two cell lines. However, the uptake in presence of sodium azide was 60-80 % of the control.*

7.2.3. Dependence on Temperature and Energy availability on cellular uptake of CHAP peptides

Most CPPs enter the cells through either endocytosis-based or membrane-based pathways [13, 27]. However, CPPs can also adopt multiple pathways to penetrate

cell membrane. The mechanism of uptake for CPPs is dependent on various physico-chemical factors of temperature, energy-availability, chemical stimulation, etc. [26, 28]. Cellular uptake at low temperatures and energy-depleted conditions are usually attributed to the uptake through direct translocation pathways, due to the inhibition of endocytosis in these conditions. Nevertheless, blocking one pathway can also result to increased cellular uptake through the other modes [13]. To study the pathway of uptake for CHAP peptides, cervical (HeLa) and breast (MDA-MB-231) cancer cells were treated with 10 μM CHAP-CF conjugates at 4°C and in energy-depleted conditions using fluorescence spectroscopy (Figure 7.4C-7.4D). Cellular uptake of CHAP peptides in these conditions was compared to the uptake of 10 μM CHAP peptides at 37 °C (control). The uptake of CHAP-CF conjugates reduced by about 30 % in the two differing conditions of temperature and energy-availability. This suggests that the uptake of the designed CHAP series of peptides follow both endocytic and membrane-based pathways.

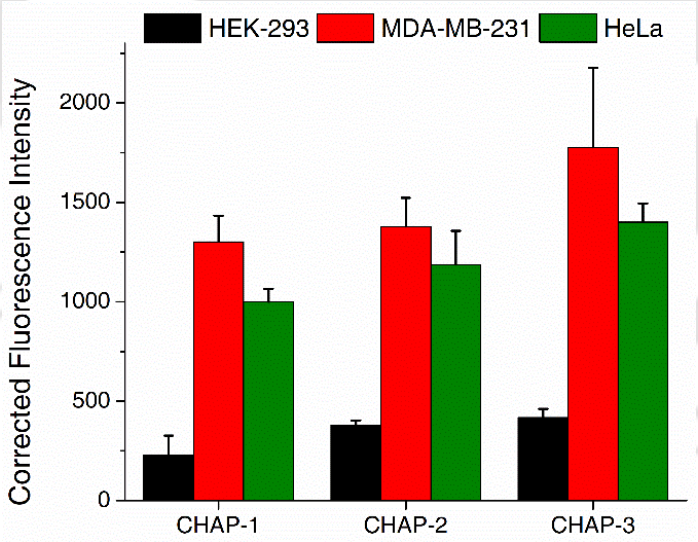

Figure 7.5. ***Cell-type specific uptake of CHAP peptides.*** *HEK-293, MDA-MB-231 and HeLa cells were treated with 10 μM of CHAP-CF peptide conjugates for four hours at 37 °C. The uptake of CHAP-CF conjugates in three different cell lines was quantified using fluorescence spectroscopy.*

7.2.4. Cell-type specific uptake of CHAP peptides

To investigate the specificity of the designed peptides towards cervical and breast cancer cells, the uptake of the designed peptides in HeLa, MDA-MB-231

and HEK-293 cells was compared (Figure 7.5). CHAP peptides had lower uptake in HEK-293 cells in comparison to cervical and breast cancer cells. The failure of the flip-flop mechanism of lipid exchange among the membrane bilayer leads to the exposure of negatively charged Phosphoserine residues on the outer membrane in a cancer cell [29-32]. This increases the negative charge on the surface of the cancer cell with simultaneous increase in net electrostatic potential on cellular surface [33, 34]. This may explain the basis behind the higher uptake rates of cationic peptides in cancer cells, in comparison to non-cancerous cells.

7.2.5. Biocompatible activity of CHAP peptides

Loss of activity in the presence of serum and proteolytic instability have long been a major bottleneck in the development of cell penetrating peptides [35]. To test the biocompatible activity of the CHAP peptides in bovine serum, CHAP-CF conjugates were treated with bovine serum for one hour at 37 °C. MDA-MB-231 cells were treated with same stock of CHAP-CF conjugates for four hours at 37 °C and analyzed for cell associated fluorescence using flow cytometry. The cellular uptake of the serum treated peptide-CF conjugates was compared with the uptake of peptide-CF conjugates not treated with serum under similar conditions (Figure 7.6). CHAP peptides retained their penetration capability in the presence of serum.

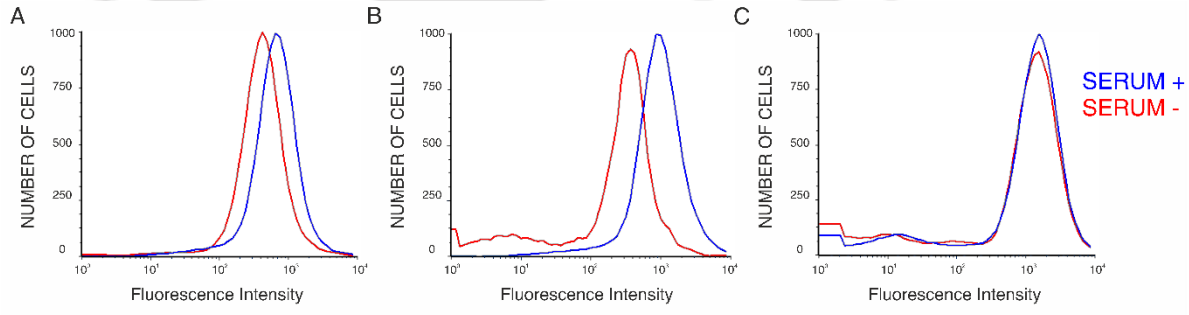

Figure 7.6. ***Biocompatibility of CHAP peptides.*** *Peptide-CF conjugates were treated with bovine serum for one hour prior at 37 °C. The cellular uptake of serum treated peptides in MDA-MB-231 cells was compared with the uptake of untreated peptide-CF conjugates under similar conditions.*

7.2.6. Drug Delivery Potential of CHAP peptides

The requirements of a typical drug delivery vehicle is to "deliver" the functionally intact drug, and therefore, Methotrexate (MTX) was conjugated to the N-terminus of the designed peptides. Peptide-MTX conjugates were tested for drug action by evaluating the cell viability in varying concentrations of peptide-drug conjugates against breast (MDA-MB-231) and cervical (HeLa) cancer cells. The cytotoxicity of MTX increased when delivered as CHAP-MTX conjugates, as illustrated by the reduced IC_{50} values (Table 7.1). The delivery of MTX as CHAP-MTX conjugates were able to overcome the drug resistance of MDA-MB-231 cells [26, 36]. The peptide-CF conjugates showed no significant toxicity to either of the cell types.

Table 7.1: ***IC_{50} values for peptide-MTX conjugates against cancer and non-cancerous cells.*** *The peptide-MTX conjugates had higher toxicity levels than methotrexate (MTX) against cancer cells.*

SAMPLE	IC_{50} ± Standard Deviation (μM)		
	HeLa	MDA-MB-231	HEK-293
Methotrexate (MTX)	4.54 ± 0.25	> 40	2.24 ± 0.11
CHAP-1-MTX	1.10 ± 0.25	0.91 ± 0.09	> 50
CHAP-2-MTX	1.95 ± 0.27	1.52 ± 0.19	5.20 ± 0.92
CHAP-3-MTX	0.45 ± 0.06	0.39 ± 0.07	8.65 ± 1.12

Further, HEK-293 cells were treated with MTX and CHAP-MTX conjugates under similar conditions. The reduced uptake of CHAP-MTX in HEK-293 cells led to increased IC_{50} values for CHAP-MTX conjugates towards HEK-293 cells than HeLa and MDA-MB-231 cells. In other words, the CHAP-MTX conjugates were less toxic to HEK-293 cells than cervical (HeLa) and breast (MDA-MB-231) cancer cells.

7.2.7. Hemotoxicity of CHAP-MTX conjugates

Most chemotherapy drugs are administered intravenously for the purpose of increased bioavailability at tumor location. Blood is the first tissue which comes in contact with chemotherapy drugs and thus, the blood related side effects including anemia, blood thinning, etc. will arise. Therefore, it is of utmost importance that the drug delivery vehicle should not be toxic to the RBCs. The toxicity of CHAP-MTX conjugates towards mammalian RBCs was evaluated using the Hemolytic assay. CHAP-MTX conjugates showed minimal toxicity towards mammalian RBCs over a treatment of four hours at 37 °C (Figure 7.7).

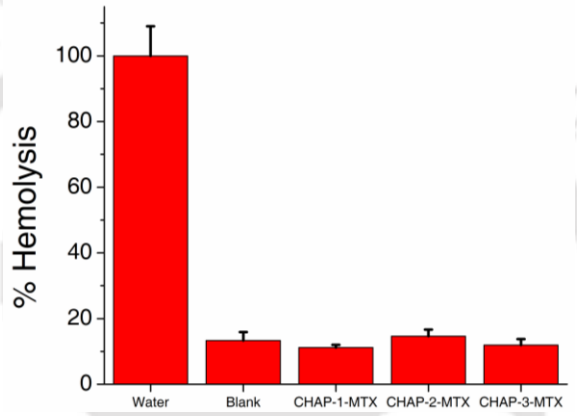

Figure 7.7. ***Hemotoxicity of STRAP-MTX conjugates.*** *The peptide-MTX conjugates had minimal toxicity towards mammalian RBC's at 50 μM treatment concentration for four hours incubation at 37 °C.*

7.3. CONCLUSION

Most of the peptide-based delivery systems, like TAT and Penetratin are based on sequences from naturally occurring proteins of different origins. A class of cationic, helical and amphipathic peptides (CHAPs) with cell penetrating ability is presented. The peptides were designed with a constrained conformation by positioning an unnatural amino acid (α-amino isobutyric acid, Aib), and were tested for their cell penetration and drug delivery potential. The peptides have a higher cellular uptake than the TAT peptide in breast and cervical cancer cells. The cellular uptake of the designed peptides is independent of temperature and energy availability. The peptides have higher cellular uptake in MDA-MB-231 and HeLa cells than HEK-293 cells. Further, the peptides have biocompatible activity and are efficient in delivering functionally active MTX as peptide-MTX conjugates

to the cells. Therefore, these peptides present themselves as strong contenders for further development as potential drug delivery agents.

7.4. REFERENCES

[1] Skalko-Basnet N. Biologics: the role of delivery systems in improved therapy. Biologics : targets & therapy 2014;8:107-14.
[2] de Vries JW, Zhang F, Herrmann A. Drug delivery systems based on nucleic acid nanostructures. Journal of Controlled Release 2013;172:467-83.
[3] Horner S, Knauer S, Uth C, Jost M, Schmidts V, Frauendorf H, Thiele CM, Avrutina O, Kolmar H. Nanoscale Biodegradable Organic-Inorganic Hybrids for Efficient Cell Penetration and Drug Delivery. Angewandte Chemie (International ed in English) 2016;55:14842-6.
[4] Liechty WB, Kryscio DR, Slaughter BV, Peppas NA. Polymers for Drug Delivery Systems. Annual review of chemical and biomolecular engineering 2010;1:149-73.
[5] Perni S, Prokopovich P. Poly-beta-amino-esters nano-vehicles based drug delivery system for cartilage. Nanomedicine: Nanotechnology, Biology and Medicine 2017;13:539-48.
[6] Zununi Vahed S, Salehi R, Davaran S, Sharifi S. Liposome-based drug co-delivery systems in cancer cells. Materials science & engineering C, Materials for biological applications 2017;71:1327-41.
[7] Douat C, Aisenbrey C, Antunes S, Decossas M, Lambert O, Bechinger B, Kichler A, Guichard G. A cell-penetrating foldamer with a bioreducible linkage for intracellular delivery of DNA. Angewandte Chemie (International ed in English) 2015;54:11133-7.
[8] Frankel AD, Pabo CO. Cellular uptake of the tat protein from human immunodeficiency virus. Cell 1988;55:1189-93.
[9] Jang S, Hyun S, Kim S, Lee S, Lee IS, Baba M, Lee Y, Yu J. Cell-penetrating, dimeric alpha-helical peptides: nanomolar inhibitors of HIV-1 transcription. Angewandte Chemie (International ed in English) 2014;53:10086-9.
[10] Bechara C, Sagan S. Cell-penetrating peptides: 20years later, where do we stand? FEBS Letters 2013;587:1693-702.
[11] Derossi D, Joliot AH, Chassaing G, Prochiantz A. The third helix of the Antennapedia homeodomain translocates through biological membranes. The Journal of biological chemistry 1994;269:10444-50.
[12] Agrawal P, Bhalla S, Usmani SS, Singh S, Chaudhary K, Raghava Gajendra P S, Gautam A. CPPsite 2.0: a repository of experimentally validated cell-penetrating peptides. Nucleic Acids Research 2016;44:D1098-D103.
[13] Copolovici DM, Langel K, Eriste E, Langel Ü. Cell-Penetrating Peptides: Design, Synthesis, and Applications. ACS Nano 2014;8:1972-94.

[14] Medina SH, Miller SE, Keim AI, Gorka AP, Schnermann MJ, Schneider JP. An Intrinsically Disordered Peptide Facilitates Non-Endosomal Cell Entry. Angewandte Chemie International Edition 2016;55:3369-72.

[15] Lindberg M, Biverstahl H, Graslund A, Maler L. Structure and positioning comparison of two variants of penetratin in two different membrane mimicking systems by NMR. European journal of biochemistry 2003;270:3055-63.

[16] Ye J, Fox SA, Cudic M, Rezler EM, Lauer JL, Fields GB, Terentis AC. Determination of Penetratin Secondary Structure in Live Cells with Raman Microscopy. Journal of the American Chemical Society 2010;132:980-8.

[17] Bruckner H, Graf H. Paracelsin, a peptide antibiotic containing alpha-aminoisobutyric acid, isolated from Trichoderma reesei Simmons. Part A. Experientia 1983;39:528-30.

[18] Conlon JM, Al-Kharrge R, Ahmed E, Raza H, Galadari S, Condamine E. Effect of aminoisobutyric acid (Aib) substitutions on the antimicrobial and cytolytic activities of the frog skin peptide, temporin-1DRa. Peptides 2007;28:2075-80.

[19] Zelezetsky I, Tossi A. Alpha-helical antimicrobial peptides—Using a sequence template to guide structure–activity relationship studies. Biochimica et Biophysica Acta (BBA) - Biomembranes 2006;1758:1436-49.

[20] Bahnsen JS, Franzyk H, Sandberg-Schaal A, Nielsen HM. Antimicrobial and cell-penetrating properties of penetratin analogs: Effect of sequence and secondary structure. Biochimica et Biophysica Acta (BBA) - Biomembranes 2013;1828:223-32.

[21] Toniolo C, Bonora GM, Bavoso A, Benedetti E, di Blasio B, Pavone V, Pedone C. Preferred conformations of peptides containing α,α-disubstituted α-amino acids. Biopolymers 1983;22:205-15.

[22] Marshall GR, Hodgkin EE, Langs DA, Smith GD, Zabrocki J, Leplawy MT. Factors governing helical preference of peptides containing multiple alpha,alpha-dialkyl amino acids. Proceedings of the National Academy of Sciences 1990;87:487-91.

[23] Basu G, Kuki A. Conformational preferences of oligopeptides rich in α-aminoisobutyric acid. II. A model for the 310/α-helix transition with composition and sequence sensitivity. Biopolymers 1992;32:61-71.

[24] Wang D, Chen K, Kulp Iii JL, Arora PS. Evaluation of biologically relevant short alpha-helices stabilized by a main-chain hydrogen-bond surrogate. Journal of the American Chemical Society 2006;128:9248-56.

[25] Banerjee R, Basu G. Direct evidence for alteration of unfolding profile of a helical peptide by far-ultraviolet circular dichroism aromatic side-chain contribution. FEBS Letters 2002;523:152-6.

[26] Louis-Jeune C, Andrade-Navarro MA, Perez-Iratxeta C. Prediction of protein secondary structure from circular dichroism using theoretically derived spectra. Proteins: Structure, Function, and Bioinformatics 2012;80:374-81.

[27] Heitz F, Morris MC, Divita G. Twenty years of cell-penetrating peptides: from molecular mechanisms to therapeutics. British Journal of Pharmacology 2009;157:195-206.

[28] Cascales L, Henriques ST, Kerr MC, Huang Y-H, Sweet MJ, Daly NL, Craik DJ. Identification and Characterization of a New Family of Cell-penetrating Peptides: CYCLIC CELL-PENETRATING PEPTIDES. Journal of Biological Chemistry 2011;286:36932-43.

[29] Klahn M, Zacharias M. Transformations in plasma membranes of cancerous cells and resulting consequences for cation insertion studied with molecular dynamics. Physical Chemistry Chemical Physics 2013;15:14427-41.

[30] WOEHLECKE H, POHL A, ALDER-BAERENS N, LAGE H, HERRMANN A. Enhanced exposure of phosphatidylserine in human gastric carcinoma cells overexpressing the half-size ABC transporter BCRP (ABCG2). Biochemical Journal 2003;376:489-95.

[31] Ran S, Downes A, Thorpe PE. Increased Exposure of Anionic Phospholipids on the Surface of Tumor Blood Vessels. Cancer Research 2002;62:6132-40.

[32] Zachowski A. Phospholipids in animal eukaryotic membranes: transverse asymmetry and movement. Biochemical Journal 1993;294:1-14.

[33] Yang M, Brackenbury WJ. Membrane potential and cancer progression. Frontiers in Physiology 2013;4:185.

[34] Chen B, Le W, Wang Y, Li Z, Wang D, Ren L, Lin L, Cui S, Hu JJ, Hu Y, Yang P, Ewing RC, Shi D, Cui Z. Targeting Negative Surface Charges of Cancer Cells by Multifunctional Nanoprobes. Theranostics 2016;6:1887-98.

[35] Kim H, Jang JH, Kim SC, Cho JH. De novo generation of short antimicrobial peptides with enhanced stability and cell specificity. The Journal of antimicrobial chemotherapy 2014;69:121-32.

[36] Worm J, Kirkin AF, Dzhandzhugazyan KN, Guldberg P. Methylation-dependent Silencing of the Reduced Folate Carrier Gene in Inherently Methotrexate-resistant Human Breast Cancer Cells. Journal of Biological Chemistry 2001;276:39990-40000.

8

Emergence of a Backbone and Sequence Optimization Platform

The peptides reported in the previous chapters provide immense insights for the development of a computational platform for designing peptides with tailored features and functions. The design platform encompasses multiple information in regards to a stable backbone architecture, amino acid side-chain dihedral preferences and amino acid substitution matrices. The functional outcome of this multi-dimensional design platform in theory would be novel peptide sequences with unique spatial electrostatic fingerprints, responsible for specific functions, which in this case is cell penetration.

Articles based on this chapter; *Jerath et al.* Mapping the Geometric Evolution of Protein Folding Motor. *Plos ONE*. (2016) **11(10)**: e0163993.

Jerath et al. bPE toolkit: toolkit for computational protein engineering. *Systems and Synthetic Biology*. (2014) **8**:337–341.

8.1. INTRODUCTION

The previous chapters have described the design philosophies explored for designing novel cell penetrating peptides with various chemical as well as conformational features related to their potency. Therefore, it is important to analyze the key fingerprints from these peptides in order to model and design peptides with tailored functional elements. Electrostatic interactions are the primary interactions for a majority of biological reactions, which are involved in the identification and binding of a pair of ligand and receptor [1]. The designed peptides discussed in this thesis have unique associated electrostatic signatures due to the changes in stereochemistry and sequence inversion. The differences in the activity of various stereochemical analogues discussed in the previous chapters provide a vital platform for understanding the underlying effects of sequence alteration on its penetrative capability. In principle, stereochemistry decides the positioning of side-chains in the geometrical plane and sequence alteration provides the optimization of electrostatic features owing to differential chemistry of amino acid side-chains. Another factor playing an important role towards the fixation of electrostatic potential variables is the differences in amino acid side-chains to adopt a specific rotamer, due to the preferential distribution of dihedral angles [2]. For example, a proline side-chain is mostly confined to a very limited space in the rotational plane, whereas the side-chain of lysine, though similar in size has more theoretically allowed regions in the rotational plane [2].

Therefore, a design framework built on the three above-mentioned characteristics can be highly useful for the development of next-generation drug delivery vectors. To commence the development of such a design platform, a thorough analysis of spatial electrostatic signatures of the penetrating peptides would help in identifying regions of peptide sequences with the highest probability of instigating penetrative properties in a designed peptide. Moreover, the point mutations may be helpful in providing additional structural stability to a peptide, which is integral to maintaining its spatial electrostatic signature. Even though there are substitution matrices available for sequence alignment based

on the probability of different amino acids replacing each other in protein sequences, they do not differ between mutations capable of inducing loss of function in proteins [3]. For example, a substitution of alanine to proline can lead to loss of protein structure and function of a protein due to constriction of topological planes for protein folding, whereas, a change to phenylalanine or tryptophan may not have such adverse effects on protein structure and function. However, the present substitution matrices do not take into account of such predicaments arising from the geometrical preferences of side-chain and main chain dihedral angles. Thus, a study on the geometrical preferences of different backbone and side-chain dihedral angles for different amino acids is required for the evolution of the discussed peptide design framework.

In this chapter, it is attempted to construct and develop a platform, which will provide a multi-dimensional basis of designing peptides with tailored features for specific applications. The chapter has been segregated into three sections discussing the spatial electrostatic signatures of the previously described peptides, the rotational preferences of different amino acid side-chains and development of specific tools to evaluate various features of the designed peptides.

8.2. BACKBONE ARCHITECTURE and ELECTROSTATIC SIGNATURES

In the previous chapters 5-7, the backbone architecture involved in the design of SARTHI, STRAP and CHAP series of peptides with cell penetrative potential was discussed. The stability of peptide backbone plays a crucial role in maintaining a peptide's electrostatic potential distribution. Electrostatic potential at any given point is highly affected by the nature of charged particles in its proximity. Therefore, a stable backbone architecture would ideally provide the necessary template for the incorporation of specific design features in a peptide side-chain sequence. The most vital feature remains the distribution of electrostatic potential across the peptide surface. Electrostatic interactions are among the strongest non-covalent associations in biological chemistry [1]. The spatial distribution of electrostatic potential is significant in all receptor-ligand binding

interactions, a property mimicked by multiple drugs in comparison to the natural ligand for the target receptor.

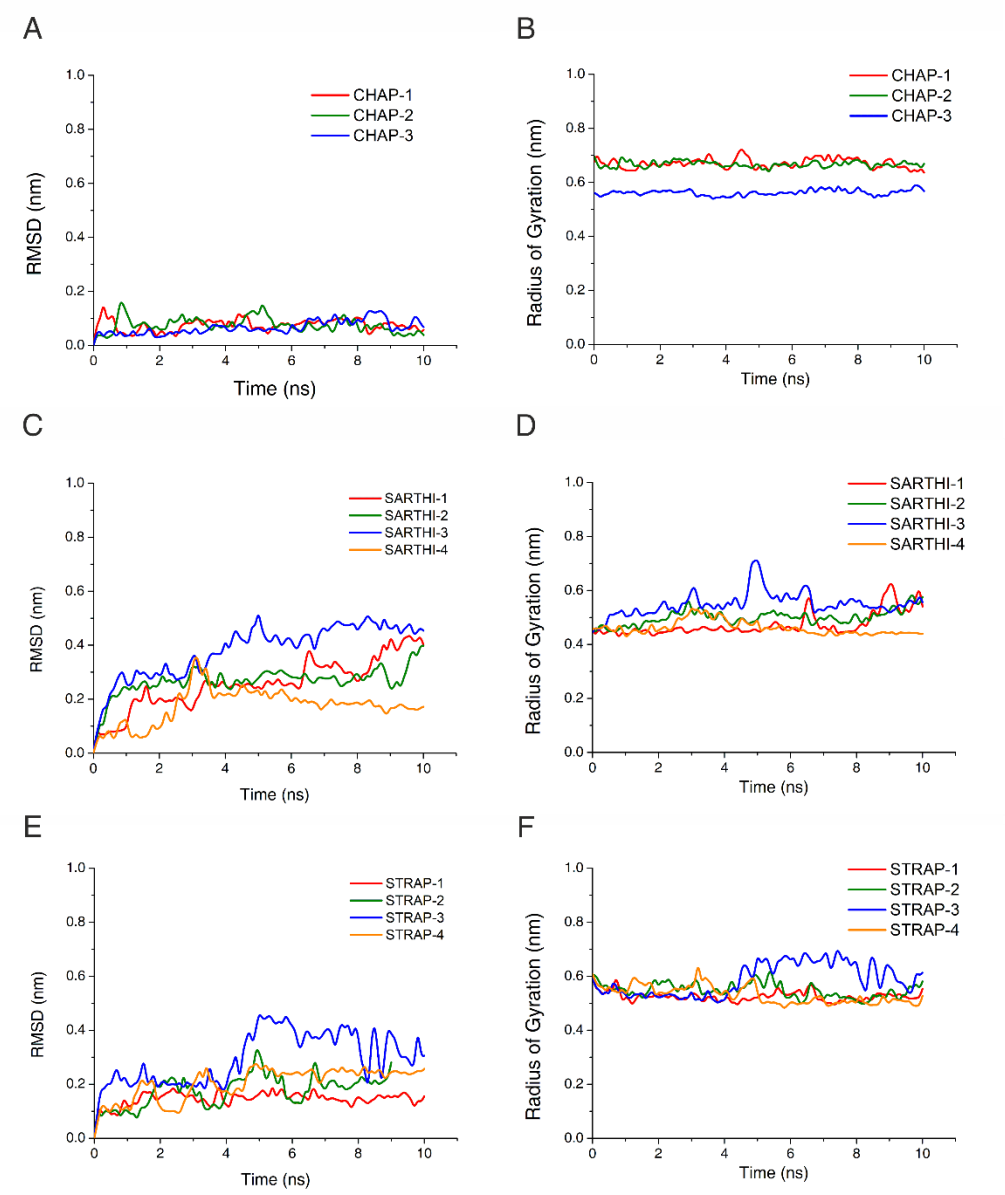

Figure 8.1. ***RMSD and R_g distributions.*** *The RMSD and R_g plotted as a function of time for the simulated structures of the three designed peptide series, CHAPs (A,B), SARTHI(C,D) and STRAPs(E,F) for 10 ns MD production run.*

A combination of topologically constrained backbone and tailored electrostatic potential distributions, in theory, would provide a useful platform for protein design. Therefore, the stability of topological constrictions of the designed peptides discussed in this thesis was evaluated through Molecular Dynamics

simulations using a water solvent system. The stability of backbone for CHAP, SARTHI and STRAP peptides was verified by comparing the Root Mean Square Deviations (RMSD) of the peptide backbone and the Radius of Gyration (R_g) distributions as a function of time over a 10 nano-seconds MD production run. The system consisting of a single peptide molecule was energy minimized in vacuum and water using the steepest descent algorithm. The system was further simulated for 10 ns and the resultant trajectories were analyzed using the g_rms and g_gyrate programs of the GROMACS [4, 5] molecular dynamics suite. All designed peptide structures were stable in water with the RMSD and Rg distributions within the acceptable range (Figure 8.1).

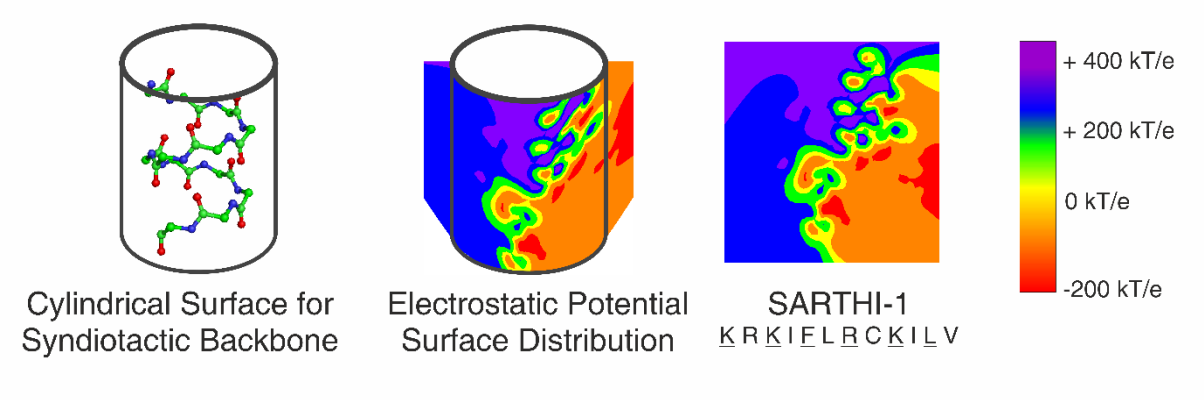

Figure 8.2. ***Construction of Electrostatic fingerprints.*** *The electrostatic fingerprints were developed by calculating the electrostatic potential at different atom positions in the peptide structure by solving finite distance Poisson-Boltzmann equation. The electrostatic potential was projected on the curved surface of a cylinder for each amino acid side-chain atom (B). Further, electrostatic potential was represented as per the provided color bar in a two dimensional fingerprint (C).*

The stability of the peptide backbone relates to the stability of the designed electrostatic signatures for each peptide. The results of the circular dichroism spectroscopy experiment for SARTHI and STRAP peptides in water suggests the stable conformations of the peptides (see sections 5.2.2 and 6.2.2). The results from both the *in silico* and experimental studies indicate that these two series of peptides have stable topological elements and therefore, do possess stable

electrostatic signatures. These electrostatic signatures were deduced by solving the finite distance Poisson-Boltzmann equation for peptide structures. Therefore, DelPhi [6] was used to calculate the electrostatic potential at each atom position for the designed peptides. The electrostatic potential at every atom was summed for each amino acid side-chain. This represents the sum total electrostatic potential at each amino acid position. Further, this electrostatic potential was mapped using the peptide backbone architecture, which gives rise to unique electrostatic fingerprints of the designed peptides. The designed backbone structures conform to either α or Π helical conformations for each series of the designed peptides. All helices essentially have a cylindrical geometry. Therefore, the three-dimensional electrostatic fingerprints for each peptide can be represented as the curved surface of a cylinder. The process for calculating the electrostatic fingerprint using SARTHI-1 as an example is shown in Figure 8.2.

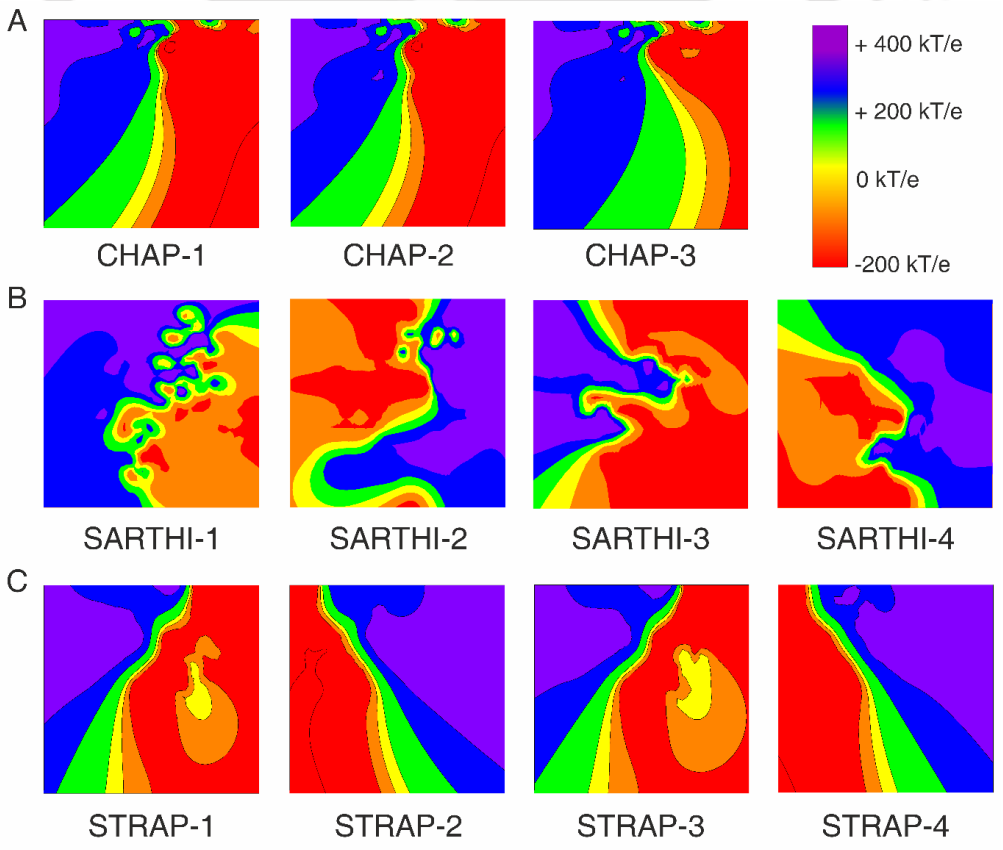

Figure 8.3. ***Electrostatic Fingerprints.*** *Electrostatic fingerprints for the designed peptides as per the color bar. Electrostatic potential is expressed in kT/e units.*

The electrostatic fingerprints of all the designed peptides were calculated similarly by normalizing the size of the electrostatic signature as a function of the diameter and length of the cylindrical peptide surface (Figure 8.3). The sequence alterations in CHAP series of peptides adds to the changes in their electrostatic signatures and thus contributes to their different cell penetrative efficiencies. On the other hand, the differential electrostatic signatures for SARTHI and STRAP peptides are due to sequence inversion and steroechemical variations.

8.3. GEOMETRICAL DIRECTIVES for SEQUENCE DESIGN

The electrostatic signatures exhibited by a peptide in addition to backbone architecture, is also dependent on the amino acid side chain sequence. For, it is the amino acid side-chains that contribute the most towards the electrostatic potential distribution across the peptide sequence. Thus, it is vital to understand the relative effects of substituting different amino acids with others and their effect on the electrostatic distributions of the designed peptides. The dependency of the backbone dihedral angles on side-chain dihedrals further adds to the complexity of choosing a substitute amino acid for protein design. Therefore, a substitution based scoring system is required for designing novel peptide sequences with tailored features.

Dihedral angle rotations play a crucial role in the formation of protein secondary structures [7-9]. However, the folding of a polypeptide chain and their guiding principles is an important scientific problem, yet to be completely solved. A solution to the protein folding problem would provide the ability to predict protein structures from sequence. Presently, structure prediction is attempted through the alignment of amino acid sequences. Only about 1500 distinct protein folds are present in over one-lakh protein structures available in the PDB [7, 10] . This implies that multiple amino acid sequences can form a specific fold. Therefore, protein design is a more manageable problem than folding. Rotamer libraries by Dunbrack [11], Richardson [12] and studies by Pal *et al.* [13] have provided significant advancements in quantifying side-chain geometries. However, studies on protein folding are more concentrated towards the

thermodynamics of folding rather on the role of side-chain geometry and its effect on protein folding.

A protein structure is characterized geometrically by mapping its backbone dihedral angles, ϕ and ψ. Side-chain dihedral angles χ_1 and χ_2 and their effects on backbone dihedral angles are a major concern for protein designers and crystallographers, in order to optimize the side-chain packing in a given fold. Allowed regions of ϕ and ψ combinations for majority of the amino acids in a Ramachandran plot is very limited. Therefore, structural diversity of protein secondary structures is limited to α-helices, β-sheets and their inter-connecting segments.

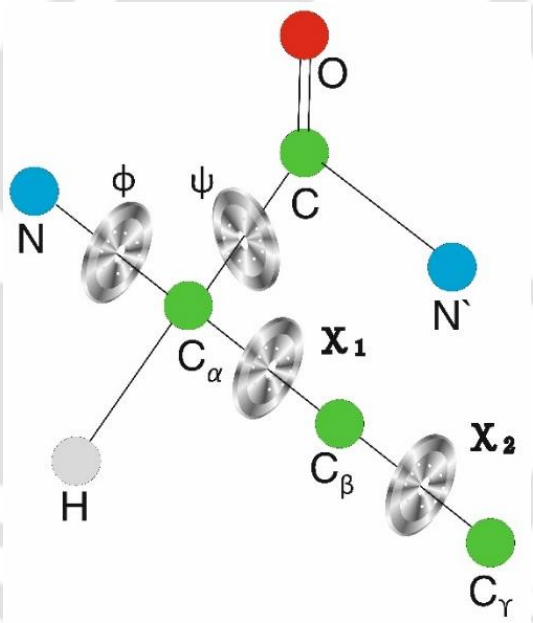

Figure 8.4. ***Dihedral Rotors.*** *The dihedral angles ϕ, ψ, χ_1 and χ_2 represented as mechanical rotors.*

A self-folding polypeptide chain may be assumed as a mechanical motor with four rotors (mechanical gears capable of rotation) ϕ, ψ, χ_1, χ_2, (Figure 8.4) and all other elements being stators. The driving force for either folding or unfolding may come from the mutual dispensation of enthalpic and entropic forces within the chain, subject to reaction conditions. The torque required for folding a polypeptide chain, may come from within, and thermodynamics of folding has

been extensively studied. It is safe to assume that the torque manifests through dihedral angle movements. Therefore, to map the sequential geometric events of folding, the movements of four dihedral angles in the rotational plane were studied during secondary structure formation and breaking.

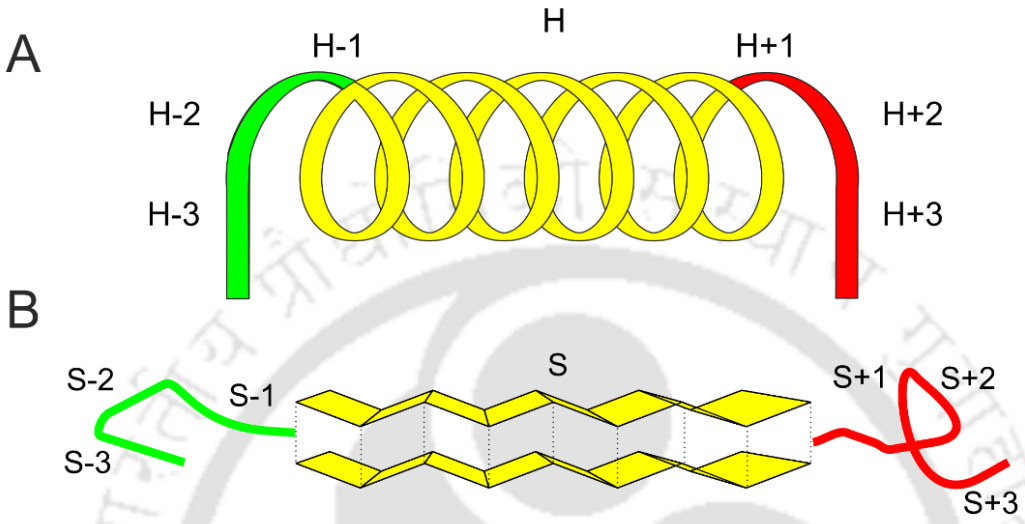

Figure 8.5. ***Nomenclature for Secondary structure and flanking regions.*** *The nomenclature followed for the flanking regions of helix (A) and sheet (B) used for studying secondary structure formation and breakdown.*

8.3.1. **Dataset**

The list of non-redundant protein structures available in the PDB, consisting of over 23,000 structures was taken from Dunbrack's library [14]. The amino acids preceding and succeeding alpha helices and beta sheets were also taken into account. The positions used in the analysis were, H-3, H-2, H-1, H, H+1, H+2 and H+3 for helices; and S-3, S-2, S-1, S, S+1, S+2 and S+3 for sheets (Figure 8.5). The objective behind such classification was to map the early events of folding and to understand the driving force responsible.

8.3.2. **Relative motions of secondary structure forming dihedral angle rotors**

The dihedral angle rotors of individual amino acids in a polypeptide chain can be viewed analogous to the rotors of an Enigma machine. The cumulative code

arising from an Enigma machine represents here the specific fold arising due to different dihedral angle rotations of individual amino acids. It was observed that a helix is formed due to the differential rotational motion of its flanking regions (Figure 8.6). The χ_1 counter-rotates with ϕ while helix formation and breaking. The successive rotors, χ_1 and χ_2 dihedral angles also counter-rotate. Therefore, the folding-unfolding machine has three rotors counter-rotating, for a helical structure. Further, the ψ dihedral angle rotor has a left-handed rotation throughout the formation and breaking of helix. During the formation of a sheet or a beta strand, χ_1 rotor rotates (clock-wise) to the right. The ϕ dihedral angle rotor rotates in a counter direction to χ_1 (Figure 8.6). χ_2 dihedral angle also counter-rotates with respect to the χ_1 rotor. Both ϕ and ψ rotate in counter direction while breaking.

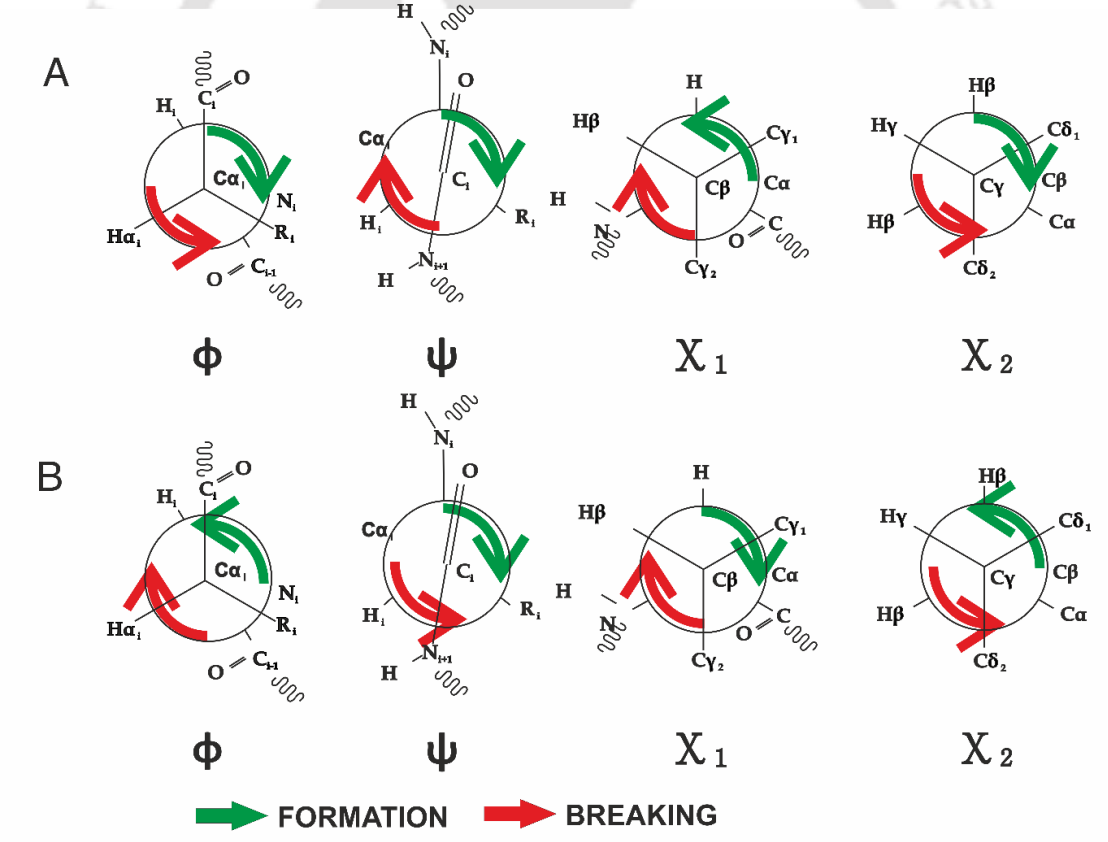

Figure 8.6. ***Rotation of Dihedral Angles in Protein Secondary Structures.*** *The dihedral angle rotations during the formation and breakdown of a helix (A) and sheet (B) in protein structures.*

Therefore, tracing dihedral angle rotations in the geometrical plane has led to some interesting revelations summarized as follows:

i) Geometric evolution of helices and sheets are distinctly different and in most cases opposite.

ii) Rotor motions, through which these differential evolution patterns orchestrate, are unique for a given secondary structure.

iii) Secondary structure formation is a result of cumulative rotor motions, though the reason of differential driving forces for these secondary structures are still unclear.

8.3.3. Dihedral angle rotor patterns and amino-acid choices

Next, the dihedral preferences of individual amino acids in protein structures were evaluated using the available data. It was vital to explore in order to understand the basis of sequence-structure relationship in protein folding. The polypeptide backbone of any protein sequence is essentially a constant. The differences in side-chains, however, influences its evolution to a functional fold. As evident from the previous section, the rotation configurations of side-chain rotors influences the backbone rotor motions, which eventually leads to a distinct secondary structure. Gln, Ile, Pro, Trp, Tyr and Val were taken as representative amino acids. The dihedral angle rotational preferences were plotted for helix and sheet. The amino acid-wise rotor patterns were similar to the cumulative dataset as presented in the previous sections. However, there were many new findings related to differential preferences of dihedral rotors in the geometrical plane ~. These observations were:

i) The non-branched side chains, both light (Gln) and bulky (Trp & Tyr) showed similar dihedral angle rotations.

ii) The χ_1 for Pro, like ϕ had constricted number of conformations in comparison to others, and was present in two continuous basins viz. (-150)-(-180) and (130)-(180).

iii) The left-handed helix conformation was observed at flanking positions in most of the residues with more prominence in Gln and Lys, while completely missing in Ile, Val and Pro. It may arise due to the β-branching of amino acid side-chains as observed by Kleywegt *et al.* [31].

8.3.4. Translation of rotor preferences to substitution matrices: The MIDMAT Series

The above-mentioned study was based on seven amino acids that represent the set of 20 naturally occurring amino acids in protein sequences. Though this data provides immense insights into the dihedral angle preferences for the different classes of amino acids, it is only a prelude to the extensive amino acid based preference pattern for dihedral angles. Therefore, the study was expanded to all amino acids. A methodology to convert the amino acid-wise dihedral angle distribution data in protein structures to relevant substitution matrices. Majority of substitution matrices are derived from the evolution of a protein sequence. However, they discount the dependency of structure on sequence and therefore, function on sequence. To construct the matrices, the geometrical rotational plane was divided into four basins, from +150 to -150 (via ±180), -150 to -50, -50 to +50 and +50 to +150 degrees in the rotational plane. The statistical free energy for each dihedral angle in the four basins was calculated as per the following equation:

$$\Delta G = -RTln\frac{N_x}{B} \quad \text{(eq 8.1.)}$$

Where, ΔG is the energy of the basin, R is the Universal Gas Constant, T is temperature (kept constant at 25^0C), N_x is the number of basin entries, and B is the variable which was computed using three different equations leading to the formation of three different matrices:

i) The sum of entries in remaining basins.

$$\text{MIDMAT-1: } B_i = \left(\sum_{i=1}^{n} b_i\right) - b_i \quad \text{(eq 8.2.)}$$

ii) Average of remaining basins.

$$\text{(eq 8.3.)} \qquad \text{MIDMAT-2: } B_i = \frac{\left(\left(\sum_{i=1}^{n} b_i\right) - b_i\right)}{n-1}$$

iii) Average over all the four basins.

$$\text{(eq 8.4.)} \qquad \text{MIDMAT-3: } B_i = \frac{\left(\sum_{i=1}^{n} b_i\right)}{n}$$

where, B_i is the value of B for i^{th} basin and b_i is the total number of entries in i^{th} basin

The statistical free energy for each basin per dihedral angle was calculated for the four rotors (ϕ, ψ, χ_1 and χ_2). These basin energies were compared for every amino acid pair to measure the Euclidean distance between each amino acid pair as per the following equation.

$$\text{(eq 8.5.)} \quad D_{xy} = \sum_{i=1}^{n} \sqrt{\left(\Phi_{ix} - \Phi_{iy}\right)^2 + \left(\Psi_{ix} - \Psi_{iy}\right)^2 + \left(\chi_{1\text{ix}} - \chi_{1\text{iy}}\right)^2 + \left(\chi_{2\text{ix}} - \chi_{2\text{iy}}\right)^2}$$

where, D_{xy} is the distance, which inversely represents the likeliness of amino acid x and amino acid y. ϕ_i, ψ_i , χ_{1i}, χ_{2i} represent the basin energies for the i^{th} basin for ϕ, ψ, χ_1 and χ_2 dihedral distributions for the amino acids x and y.

The distance values calculated for all amino acid pairs is synonymous in the nature and physical meaning to a typical amino acid substitution matrix. The distance matrix, thus created was further normalized by dividing the values by a common denominator, 1000.

The normalized distance matrix was further processed. Substitution values for each amino acid pair (SV_{xy}) were calculated as follows:

$$\text{(eq 8.6.)} \qquad SV_{xy} = 0.5 \times \left(Median\left(\left(D_{x1y1}\right)\left(D_{x1y2}\right)..\left(D_{\text{xn yn}}\right)\right) - D_{xy}\right)$$

To calculate the substitution value of an amino acid with itself (e.g. ala with ala), the maximum substitution value (SV) in the entire substitution matrix was added to the existing maximum substitution value of the same amino acid.

(eq 8.7.) $SV_{xx} = Max\ (SV_{x1y1} \quad SV_{x1y2} \ \ldots \ SV_{\text{xn yn}}) + Max\ (SV_{x1y1} \quad SV_{x1y2} \ \ldots \ SV_{\text{x1 yn}})$

The values were then rounded off to the nearest decimal point to give the final substitution score required for the construction of three substitution matrices, MIDMAT-1 MIDMAT-2 and MIDMAT-3 (Annexure 1) as per the equations 8.2-8.4 respectively.

The three substitution matrices constructed as per the mentioned methodology represent a novel set of amino acid substitution matrices, which are derived from experimental data generated for over 23,000 protein structures. Further, these matrices are representative of the structural and geometrical preferences of amino acids. Moreover, these matrices do provide a basis for amino acid substitution or point mutation in future protein design applications.

8.4. TOOLKIT FOR PROTEIN DESIGN: *bPE TOOLKIT*

In addition to the above-discussed methodologies and substitution matrices, a set of tools for supporting the design paradigm were developed [15]. These tools were constructed with the mindset of using them as modules in a future automated protein design platform. Moreover, these tools do provide a number of analysis routines that can be employed for evaluating different properties of peptides and proteins. A detailed account of each tool is discussed in the following sub-sections.

8.4.1. ProChiral: Chirality Check Program

All biomolecules from carbohydrates, proteins to nucleic acids are chiral in nature. This means that these molecules do not have a super-imposable mirror image. In amino acids, all except for glycine are chiral molecules. The alpha carbon (C_A) in amino acids is the chiral center and the orientation of the side chain with respect to the peptide backbone determines the form of a

stereoisomer. It is determined by calculating the improper dihedral angle formed by the planes involving N-C_A-C and C-C_A-C_B atoms. A positive value for the angle represents the Levorotatory or L-isoform and a negative value signifies the Dextrorotatory form.

ProChiral was developed to identify the chirality of amino acids in a peptide sequence from its structure. The Gramicidin peptide is among the few proteins composed of both L- and D- amino acids; therefore, its structure (1GRM.pdb) was used to evaluate ProChiral. Further, multiple hetero-chiral PDB structures were generated to evaluate the efficiency of the designed tool. The program successfully identified the chiral orientation of amino acids with 100% accuracy . These findings were verified with the HandleCheck program from the WHAT IF web-server [16].

8.4.2. CoMa: Contact Map Program

Contact Maps describe the spatial arrangement of the amino acids with respect to each other in a given protein structure. It is usually constructed by calculating the distance for either the C_A-C_A or the C_B-C_B (C_A in case of glycine) atom pairs. The cutoff for a contact varies from 6-12 Å. The contact map is majorly used for identifying parallel, anti-parallel beta sheets and alpha helix. It is also used for identifying and/or predicting protein folds [17, 18]. The contact map program reports a contact by calculating the distance between two CA atoms in a protein structure. The cutoff for a contact is eight angstroms. For obvious reasons, two immediate sequential neighbors (i, i±2) are exempted from the contact list. The program was tested for 10 PDB structures and the results are compared with an existing CMView [19] program. Each structure had sequence length in the range of 150-200 residues.

8.4.3. DaRe: Data Redundancy and Homology Program

The utility of this program is to avoid duplication of protein structures. This is vital for deducing analytical conclusions using various computational or statistical methods. The global alignment algorithm for sequence identity was

used for the design of DaRe [20]. Therefore, it is also a useful tool for determining the percentage sequence identity among a given set of structures [21]. The program removes redundant PDB files to a truncated PDB file folder. The redundancy of data is evaluated through the percent identity among the sequences of PDB structures. The sequence from the PDB file is read through the SEQRES entries else through the list of coordinates. Percent sequence identity is calculated among all structures in the working directory. The redundancy cutoff of sequence identity is user defined. Structures with maximum sequence length are taken as the representatives of their respective redundant entries.

DaRe was evaluated using the structures of Dihydrofolate reductase enzyme deposited in PDB. All human variants of the structure were more than 90 % similar to each other. For the mentioned dataset, DaRe consumed 0.3 seconds to complete the redundancy check.

8.4.4. HyPE: Hydrogen-Bond Potential Energy Program

Hydrogen Bonding is among the most important non-bonding interactions for bio-molecules. HyPE was designed to calculate the potential energy of hydrogen bonds between the N-H and C=O backbone atoms of a protein structure. The hydrogen bond potential energy was calculated in accordance with the 12-10 model [22]. The program requires a protein structure with all hydrogen atom positions provided explicitly as an input. The program uses a cutoff distance of 0.35nm and angle cutoff of 30° for the acceptor-donor-hydrogen angle to report a hydrogen bond. The following equation, described by Gordon et al. [22] was used for calculating the hydrogen bond potential energy:

$$E_{HB} = D_0 \left[5. \left(\frac{R_0}{R}\right)^{12} - 6. \left(\frac{R_0}{R}\right)^{10} \right] cos^2\theta \; cos^2\Phi$$

where R_0 is the equilibrium distance, D_0 is the well depth and R is the interatomic distance between the donor and acceptor heavy atoms. The angles θ and Φ refer to the hydrogen–acceptor–base angle (where the base is the atom covalently

attached to the acceptor) and the angle between the normals of the planes defined by the six atoms attached to the two centers, respectively.

HyPE was validated using eight trajectory structures extracted from the energy minimization procedure of six protein structures [15]. The g_hbond command of GROMACS was used to validate the the number of hydrogen bonds reported by the HyPE program. The numbers of hydrogen bonds predicted by HyPE were consistently equal to the ones predicted by the g_hbond of the GROMACS package.

8.4.5. EslnE: Electrostatic Interaction Energy:

Electrostatic interactions play a vital role to assess functional properties of proteins. These interactions are more significant to determine the specificity of protein functional interactions, rather than stability. The electrostatic interaction energy between two point charges was calculated as a derivative of Coulomb's law [22]:

$$E_{EI} = 322.0637 \times \frac{(q_i \cdot q_j)}{\varepsilon \cdot R_{ij}}$$

where, q_i and q_j are point charges separated by a distance R_{ij} in a medium with dielectric constant ε.

The program calculates the electrostatic interactions prevalent in a protein structure in a solvent system described by user-defined dielectric constant. The output is the total interaction energy for electrostatic interactions in a protein structure. EsInE was evaluated by calculating the correlation of the interaction energy calculated, and the total Coulomb's energy calculated using the g_energy program of GROMACS. The test set used for EsInE was the same as HyPE.

All programs described in the toolkit in section 8.4., had substitutes in public repositories. These tools were coded with a long-term objective to design a comprehensive design program suite, with an automated workflow.

8.5. REFERENCES

[1] Jobin M-L, Alves ID. On the importance of electrostatic interactions between cell penetrating peptides and membranes: A pathway toward tumor cell selectivity? Biochimie 2014;107:154-9.

[2] Schrauber H, Eisenhaber F, Argos P. Rotamers: To be or not to be?: An Analysis of Amino Acid Side-chain Conformations in Globular Proteins. Journal of Molecular Biology 1993;230:592-612.

[3] Yamada K, Tomii K. Revisiting amino acid substitution matrices for identifying distantly related proteins. Bioinformatics (Oxford, England) 2014;30:317-25.

[4] Abraham MJ, Murtola T, Schulz R, Páll S, Smith JC, Hess B, Lindahl E. GROMACS: High performance molecular simulations through multi-level parallelism from laptops to supercomputers. SoftwareX 2015;1-2:19-25.

[5] David VDS, Erik L, Berk H, Gerrit G, E. MA, C. BHJ. GROMACS: Fast, flexible, and free. Journal of Computational Chemistry 2005;26:1701-18.

[6] Li L, Li C, Sarkar S, Zhang J, Witham S, Zhang Z, Wang L, Smith N, Petukh M, Alexov E. DelPhi: a comprehensive suite for DelPhi software and associated resources. BMC Biophysics 2012;5:9.

[7] Kuhlman B, Dantas G, Ireton GC, Varani G, Stoddard BL, Baker D. Design of a novel globular protein fold with atomic-level accuracy. Science (New York, NY) 2003;302:1364-8.

[8] Dahiyat BI, Mayo SL. Protein design automation. Protein science : a publication of the Protein Society 1996;5:895-903.

[9] Looger LL, Dwyer MA, Smith JJ, Hellinga HW. Computational design of receptor and sensor proteins with novel functions. Nature 2003;423:185-90.

[10] Schaeffer RD, Daggett V. Protein folds and protein folding. Protein engineering, design & selection : PEDS 2011;24:11-9.

[11] Shapovalov MV, Dunbrack RL, Jr. A smoothed backbone-dependent rotamer library for proteins derived from adaptive kernel density estimates and regressions. Structure (London, England : 1993) 2011;19:844-58.

[12] Lovell SC, Word JM, Richardson JS, Richardson DC. The penultimate rotamer library. Proteins: Structure, Function, and Bioinformatics 2000;40:389-408.

[13] Chakrabarti P, Pal D. The interrelationships of side-chain and main-chain conformations in proteins. Progress in Biophysics and Molecular Biology 2001;76:1-102.

[14] Wang G, Dunbrack RL, Jr. PISCES: a protein sequence culling server. Bioinformatics 2003;19:1589-91.

[15] Jerath G, Hazam PK, Ramakrishnan V. bPE toolkit: toolkit for computational protein engineering. Systems and synthetic biology 2014;8:337-41.

[16] Rodriguez R, Chinea G, Lopez N, Pons T, Vriend G. Homology modeling, model and software evaluation: three related resources. Bioinformatics 1998;14:523-8.

[17] Barah P, Sinha S. Analysis of protein folds using protein contact networks. Pramana - J Phys Pramana: Springer-Verlag; 2008. p. 369-78.

[18] Vendruscolo M, Najmanovich R, Domany E. Protein Folding in Contact Map Space. Physical Review Letters 1999;82:656-9.

[19] Vehlow C, Stehr H, Winkelmann M, Duarte JM, Petzold L, Dinse J, Lappe M. CMView: Interactive contact map visualization and analysis. Bioinformatics 2011;27:1573-4.

[20] Needleman SB, Wunsch CD. A general method applicable to the search for similarities in the amino acid sequence of two proteins. Journal of Molecular Biology 1970;48:443-53.

[21] Berman HM, Westbrook J, Feng Z, Gilliland G, Bhat TN, Weissig H, Shindyalov IN, Bourne PE. The Protein Data Bank. Nucleic Acids Research 2000;28:235-42.

[22] Gordon DB, Marshall SA, Mayot SL. Energy functions for protein design. Current Opinion in Structural Biology 1999;9:509-13.

9

Conclusions And Future Directions

9.1. CONCLUSIONS

The drug delivery applications of cell-penetrating peptides is a lucrative prospect as it facilitates the use of existing drug molecules for the development of new therapies. The biosafety issues pertaining to the use of other forms of polymeric delivery vehicles are minimized due to the biological nature of peptides. In the present thesis, the development of three different series of peptides with cell-penetrative ability and drug delivery potential have been described and discussed. These series of peptides have been developed through Sequence engineering of about 50 different amino acid sequences, diverse in their chemical and stereochemical sequence.

The first series of peptides (Chapter 5) are syndiotactic peptides with alternating L- and D-amino acids, which forms a $\Pi_{(L,D)}$ helix in water. This helix is energetically more favorable than other isotactic helices. The designed peptides (SARTHI) have 10-100 fold higher cellular uptake than the TAT (48-60) peptide in cancer cells under similar treatment conditions. The uptake of peptides in cancer cells is independent of the concentration, temperature, energy and clathrin mediated endocytosis. The interaction of peptides with a POPG bilayer indicates a pore formation model for their cell permeation. The peptides are biocompatible in both serum and plasma. Two of the designed peptides selectively delivered MTX to cancer cells.

STRAP series of peptides (Chapter 6) describes a series of short syndiotactic peptides for cell penetration and drug delivery applications. The cellular uptake of the designed peptides was largely unaffected by the reduced peptide length. This suggests that for a syndiotactic peptide maintaining its geometrical conformation, chain length does not affect its inherent ability to traverse live cell membranes. Further, these peptides have similar cellular uptake profiles as SARTHI series of peptides in terms of cellular uptake, mechanism of uptake, biocompatibility and drug delivery potential.

In the third series of peptides (Chapter 7), it was attempted to fix the topology of the peptide in an α-helical conformation through the use of a non-

proteogenic amino acid (AiB). These cationic amphipathic peptides (CHAP-1-CHAP-3) were sequential mutants of each other. The amino acid composition of the sequence on mutation provided different measures of helicity in their structure in water as observed from the CD Spectroscopy. The peptides exhibit different levels of cell-penetrative ability and penetrate the cells through a mixture of endocytic and membrane transducing modes of cellular uptake. This is further stressed by their non-specific intracellular localization. The cell-penetrative property of the designed peptides is stable in serum, which can be due to the presence of Aib. Further, the peptides have a cell-dependent cellular uptake with higher uptake in cancer cells. The peptides were conjugated with Methotrexate to test their drug delivery potential. CHAP-MTX conjugates were more toxic to cancer cells than MTX alone, which affirms their use as delivery vehicles for transport of small molecules under in vitro conditions.

Together, these three series of peptides present themselves as strong contenders for applications as targeted drug delivery vectors.

Further, these peptides also present a dataset for understanding the basis of their cell penetrative ability. The spatial orientation of amino acid side chains is responsible for protein function, which is also applicable to CPPs. The interaction of CPPs with cell surface is dependent on electrostatic, hydrophobic and hydrogen bonding interactions. Electrostatic forces are prima facie the foremost interactions between two biological moieties. Therefore, mapping the three-dimensional distribution of electrostatic potential for the designed peptides would in principle help as a learning set for development of an automated design platform. The stable conformations of the designed peptides as seen from both MD simulations and wet-lab experiments, further aide in determining their electrostatic fingerprints/ signatures. The inclusion of dihedral preferences for different amino acids provide a unique blend of side chain assisted design of novel peptides with both tailored structural features and consequent functions. The tools developed during the course of the study were envisaged to be a part of a future automated peptide design protocol. The combination of stable backbone template with amino acid side-chain

preferences and three-dimensional electrostatic fingerprinting provide the required tools for the design of future peptide-based drug delivery vehicles.

9.2. FUTURE DIRECTIONS

The end of the present study presents the foundation stone for the initiation of multiple future studies pertaining to the development of peptide-based therapies against different disease models. These include but are not limited to:

1. *in vivo* studies on the distribution of the designed peptides to localize to tumor sites.
2. *in vivo* testing of designed peptides to treat malignant tumors.
3. Design of novel sequences with tailored properties and functions.
4. Development of future peptide-based drug delivery vectors.
5. Overcoming the multi-drug resistance of malignant tumors.
6. Emergence of a completely automated design platform for designing therapeutic novel peptides.

APPENDIX #1

MIDMAT SUBSTITUTION MATRICES

The substitution matrices constructed from the preferential dihedral angle distribution of different amino acids in over 23, 000 protein structures as explained in section 8.3.

Appendix 1
MIDMAT Substitution Matrices

Table A1.1. MIDMAT-1 Substitution Matrix

		Ala	Arg	Asn	Asp	Cys	Gln	Glu	Gly	His	Ile	Leu	Lys	Met	Phe	Pro	Ser	Thr	Trp	Tyr	Val
		A	R	N	D	C	Q	E	G	H	I	L	K	M	F	P	S	T	W	Y	V
Ala	A	9	-2	-1	0	1	-2	-2	-1	-1	-3	-4	-3	-2	-1	-4	2	1	0	-1	0
Arg	R	-2	15	-1	-1	-1	6	6	-6	2	3	2	7	6	0	-9	-1	-1	0	0	-2
Asn	N	-1	-1	13	6	3	0	-1	-2	3	-3	-2	-1	0	3	-9	2	1	3	3	-1
Asp	D	0	-1	6	13	3	0	-1	-3	3	-3	-2	-1	0	3	-8	3	2	4	2	0
Cys	C	1	-1	3	3	13	0	-1	-2	3	-1	-2	-1	0	3	-7	5	5	3	2	3
Gln	Q	-2	6	0	0	0	14	7	-5	3	3	2	7	6	1	-8	0	-1	1	1	-1
Glu	E	-2	6	-1	-1	-1	7	14	-6	2	3	2	6	6	0	-8	-1	-1	0	0	-1
Gly	G	-1	-6	-2	-3	-2	-5	-6	6	-4	-8	-8	-6	-6	-5	-10	-2	-4	-5	-5	-6
His	H	-1	2	3	3	3	3	2	-4	12	0	-1	2	3	5	-9	2	1	4	5	0
Ile	I	-3	3	-3	-3	-1	3	3	-8	0	11	2	3	4	0	-9	-2	-1	-1	0	-2
Leu	L	-4	2	-2	-2	-2	2	2	-8	-1	2	10	3	3	-1	-9	-3	-2	-2	-2	-2
Lys	K	-3	7	-1	-1	-1	7	6	-6	2	3	3	14	6	0	-9	-1	-2	0	0	-2
Met	M	-2	6	0	0	0	6	6	-6	3	4	3	6	14	2	-8	0	0	1	2	-1
Phe	F	-1	0	3	3	3	1	0	-5	5	0	-1	0	2	15	-8	2	1	6	7	2
Pro	P	-4	-9	-9	-8	-7	-8	-8	-10	-9	-9	-9	-9	-8	-8	3	-7	-7	-7	-8	-6
Ser	S	2	-1	2	3	5	0	-1	-2	2	-2	-3	-1	0	2	-7	13	5	2	1	2
Thr	T	1	-1	1	2	5	-1	-1	-4	1	-1	-2	-2	0	1	-7	5	12	2	1	2
Trp	W	0	0	3	4	3	1	0	-5	4	-1	-2	0	1	6	-7	2	2	13	6	2
Tyr	Y	-1	0	3	2	2	1	0	-5	5	0	-2	0	2	7	-8	1	1	6	15	1
Val	V	0	-2	-1	0	3	-1	-1	-6	0	-2	-2	-2	-1	2	-6	2	2	2	1	10

Appendix 1
MIDMAT Substitution Matrices

Table A1.2. MIDMAT-2 Substitution Matrix

		Ala	Arg	Asn	Asp	Cys	Gln	Glu	Gly	His	Ile	Leu	Lys	Met	Phe	Pro	Ser	Thr	Trp	Tyr	Val
		A	R	N	D	C	Q	E	G	H	I	L	K	M	F	P	S	T	W	Y	V
Ala	A	10	-1	1	1	2	0	0	-2	1	-2	-2	-1	0	0	-4	3	2	1	0	1
Arg	R	-1	14	-1	-1	0	6	6	-4	2	2	2	7	5	0	-9	0	-1	-1	0	-1
Asn	N	1	-1	13	5	4	0	-1	-1	3	-3	-2	-1	0	3	-9	3	2	3	2	0
Asp	D	1	-1	5	12	4	-1	-1	-2	2	-3	-2	-1	-1	2	-8	3	2	3	2	0
Cys	C	2	0	4	4	12	1	1	-2	4	-1	-1	1	1	4	-8	5	4	4	3	2
Gln	Q	0	6	0	-1	1	13	6	-4	3	2	2	6	6	1	-9	1	0	0	1	0
Glu	E	0	6	-1	-1	1	6	13	-5	2	3	2	6	6	0	-8	0	0	0	0	-1
Gly	G	-2	-4	-1	-2	-2	-4	-5	6	-3	-8	-7	-4	-5	-4	-10	-1	-3	-4	-4	-6
His	H	1	2	3	2	4	3	2	-3	12	0	-1	2	3	5	-9	3	2	4	5	1
Ile	I	-2	2	-3	-3	-1	2	3	-8	0	10	1	2	3	-1	-9	-1	0	-1	-1	-1
Leu	L	-2	2	-2	-2	-1	2	2	-7	-1	1	9	2	2	-2	-9	-2	-2	-2	-2	-1
Lys	K	-1	7	-1	-1	1	6	6	-4	2	2	2	14	6	0	-9	0	-1	-1	0	-1
Met	M	0	5	0	-1	1	6	6	-5	3	3	2	6	13	1	-9	1	0	1	1	0
Phe	F	0	0	3	2	4	1	0	-4	5	-1	-2	0	1	14	-8	2	2	6	7	2
Pro	P	-4	-9	-9	-8	-8	-9	-8	-10	-9	-9	-9	-9	-9	-8	2	-7	-7	-7	-8	-6
Ser	S	3	0	3	3	5	1	0	-1	3	-1	-2	0	1	2	-7	12	4	3	2	1
Thr	T	2	-1	2	2	4	0	0	-3	2	0	-2	-1	0	2	-7	4	12	3	2	1
Trp	W	1	-1	3	3	4	0	0	-4	4	-1	-2	-1	1	6	-7	3	3	13	6	2
Tyr	Y	0	0	2	2	3	1	0	-4	5	-1	-2	0	1	7	-8	2	2	6	14	2
Val	V	1	-1	0	0	2	0	-1	-6	1	-1	-1	-1	0	2	-6	1	1	2	2	9

Table A1.3. MIDMAT-3 Substitution Matrix

		Ala	Arg	Asn	Asp	Cys	Gln	Glu	Gly	His	Ile	Leu	Lys	Met	Phe	Pro	Ser	Thr	Trp	Tyr	Val
		A	R	N	D	C	Q	E	G	H	I	L	K	M	F	P	S	T	W	Y	V
Ala	A	9	-1	1	1	2	0	0	-2	1	-1	-1	-1	0	1	-3	3	2	1	1	1
Arg	R	-1	12	-1	-1	1	5	5	-4	2	2	1	6	5	0	-7	0	0	0	1	-1
Asn	N	1	-1	11	5	3	0	-1	-1	3	-3	-1	0	0	2	-7	3	1	2	2	0
Asp	D	1	-1	5	11	4	0	-1	-2	3	-3	-1	-1	0	3	-6	3	2	3	2	0
Cys	C	2	1	3	4	11	1	1	-2	4	-1	0	1	1	3	-5	5	4	4	3	2
Gln	Q	0	5	0	0	1	12	6	-4	3	2	2	6	5	1	-6	1	0	0	1	0
Glu	E	0	5	-1	-1	1	6	12	-4	2	2	1	5	5	1	-6	0	0	0	1	0
Gly	G	-2	-4	-1	-2	-2	-4	-4	5	-3	-7	-6	-4	-4	-4	-8	-1	-3	-4	-4	-5
His	H	1	2	3	3	4	3	2	-3	10	0	0	2	3	4	-6	3	2	3	4	1
Ile	I	-1	2	-3	-3	-1	2	2	-7	0	9	1	2	3	0	-6	-1	0	-1	0	0
Leu	L	-1	1	-1	-1	0	2	1	-6	0	1	8	2	2	0	-6	-1	-1	0	0	0
Lys	K	-1	6	0	-1	1	6	5	-4	2	2	2	12	5	1	-7	0	0	0	1	0
Met	M	0	5	0	0	1	5	5	-4	3	3	2	5	12	2	-6	1	1	1	2	1
Phe	F	1	0	2	3	3	1	1	-4	4	0	0	1	2	12	-6	2	2	5	6	2
Pro	P	-3	-7	-7	-6	-5	-6	-6	-8	-6	-6	-6	-7	-6	-6	3	-5	-4	-4	-6	-3
Ser	S	3	0	3	3	5	1	0	-1	3	-1	-1	0	1	2	-5	11	4	3	2	1
Thr	T	2	0	1	2	4	0	0	-3	2	0	-1	0	1	2	-4	4	10	3	2	2
Trp	W	1	0	2	3	4	0	0	-4	3	-1	0	0	1	5	-4	3	3	11	5	2
Tyr	Y	1	1	2	2	3	1	1	-4	4	0	0	1	2	6	-6	2	2	5	12	2
Val	V	1	-1	0	0	2	0	0	-5	1	0	0	0	1	2	-3	1	2	2	2	9

Appendix 1
MIDMAT Substitution Matrices

APPENDIX #2

MALDI-TOF SPECTRA

The MALDI-TOF spectra for the molecular masses reported in Table 5.1 and Table 6.1.

Appendix 2
MALDI-TOF SPECTRA

Peptide: SARTHI-1-CF

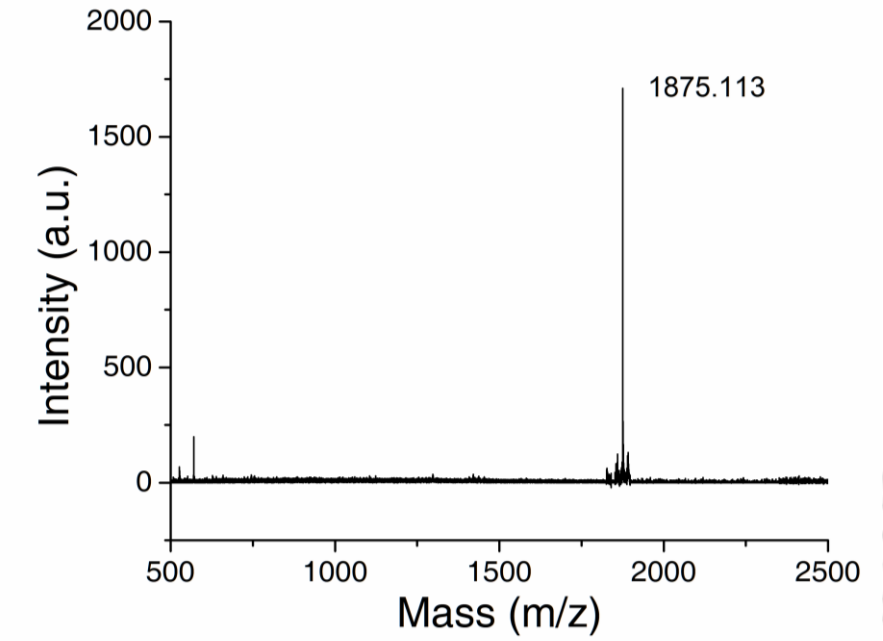

Peptide: SARTHI-2-CF

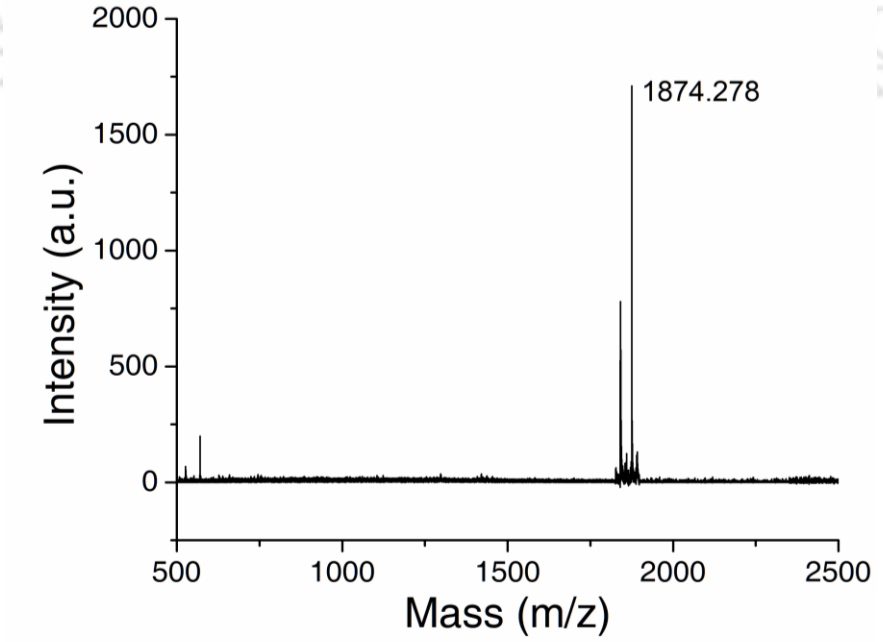

Peptide: SARTHI-3-CF

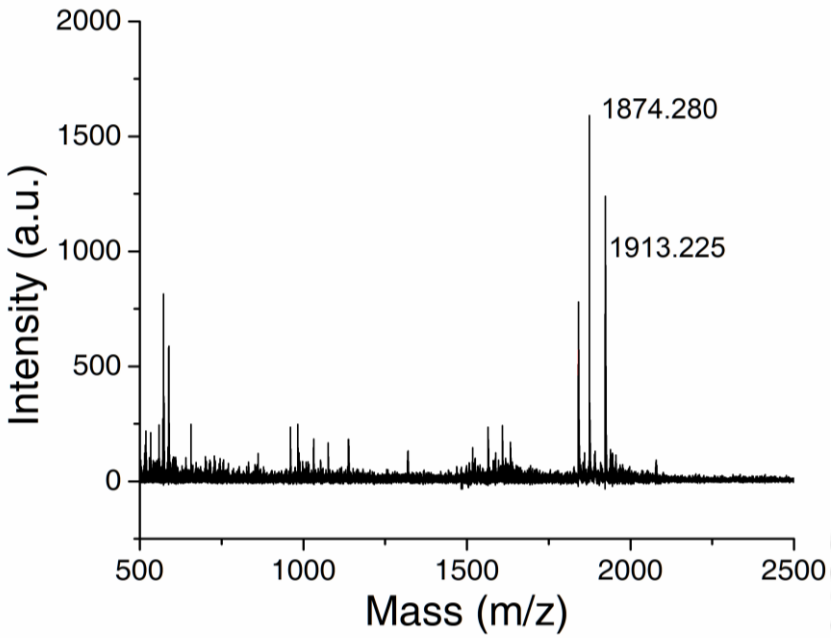

Peptide: SARTHI-4-CF

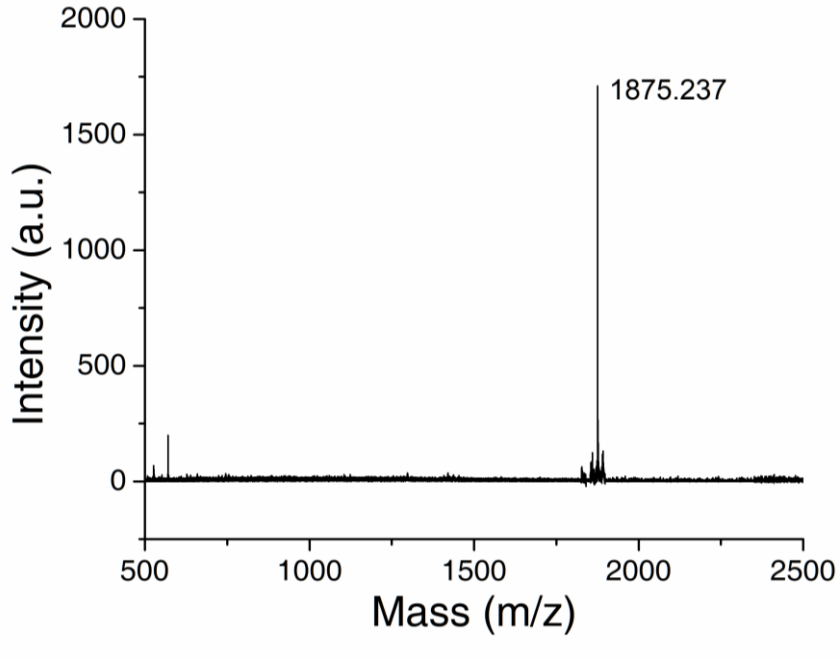

\

Peptide: SARTHI-1-MTX

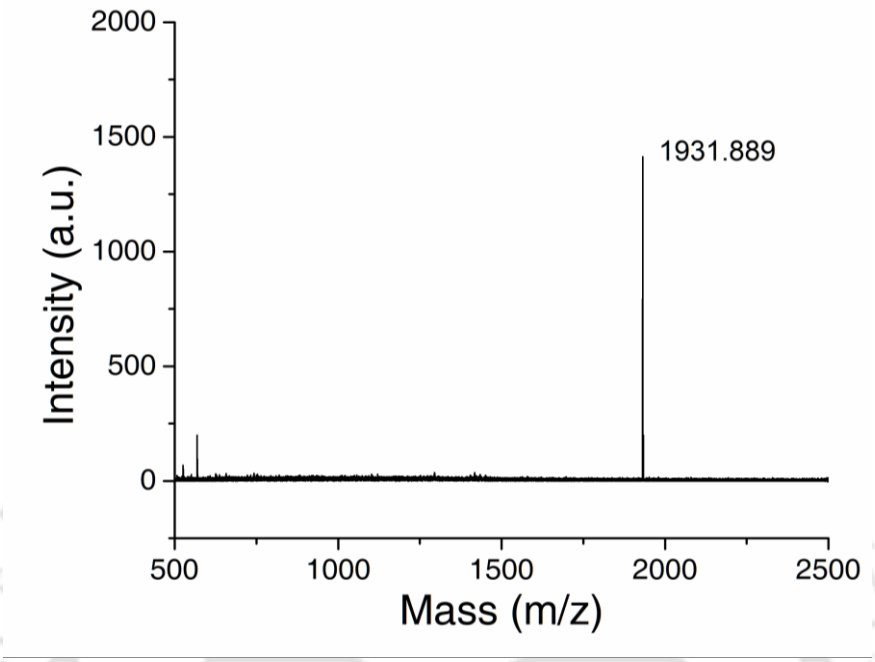

Peptide: SARTHI-2-MTX

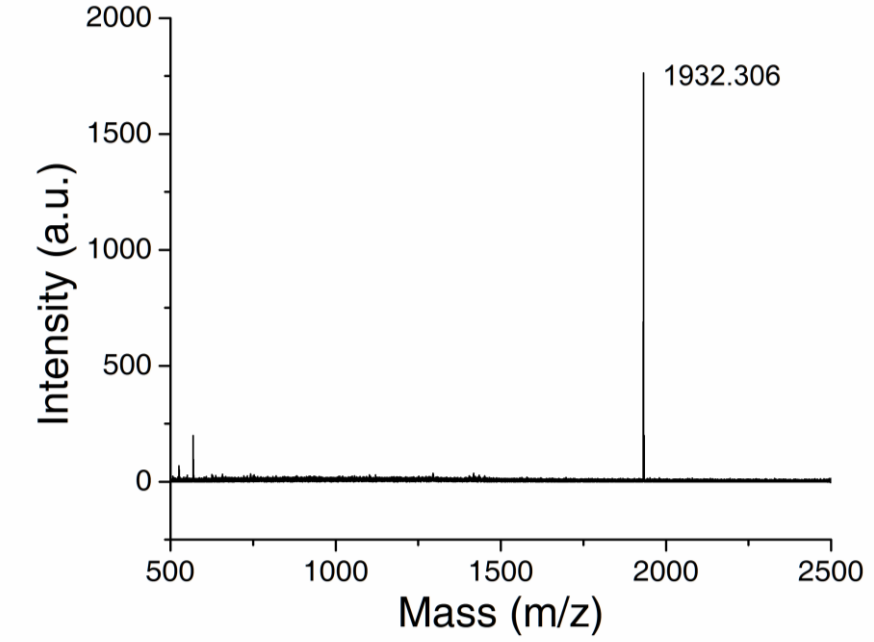

Peptide: SARTHI-3-MTX

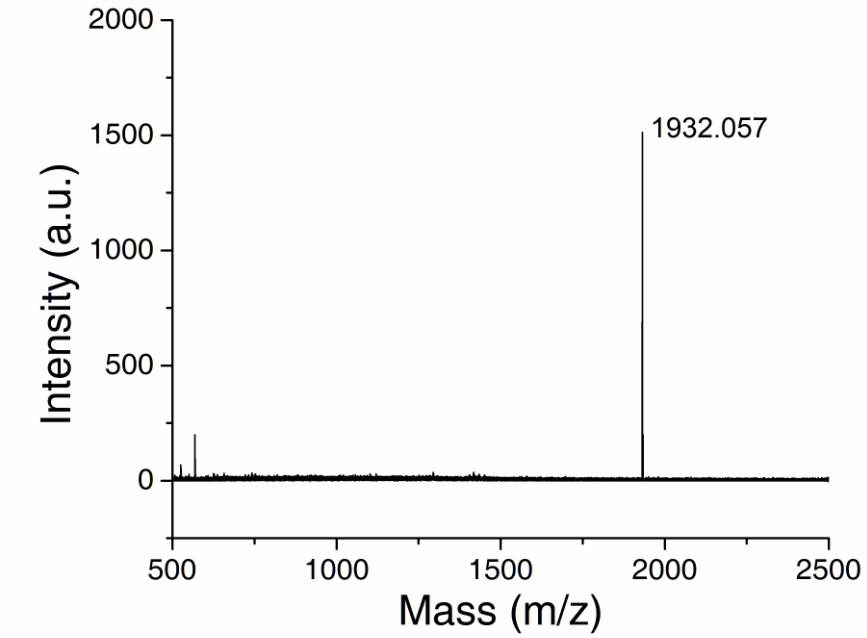

Peptide: SARTHI-4-MTX

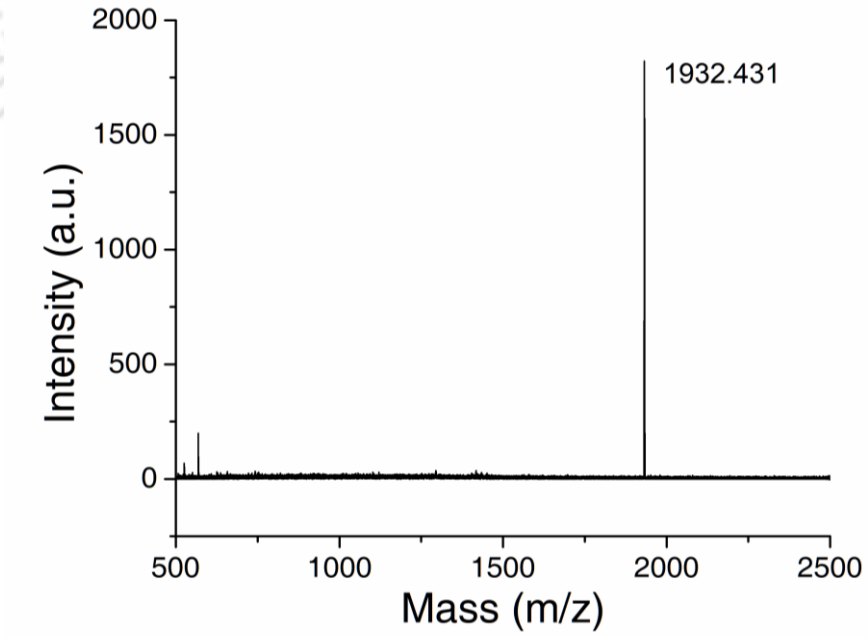

Peptide: STRAP-1-CF

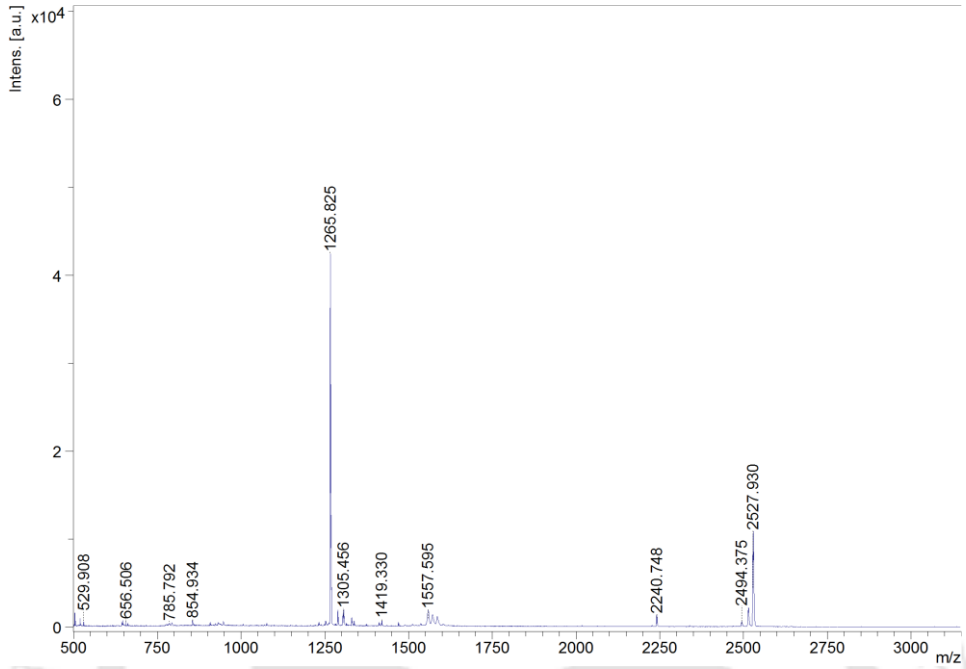

Peptide: STRAP-2-CF

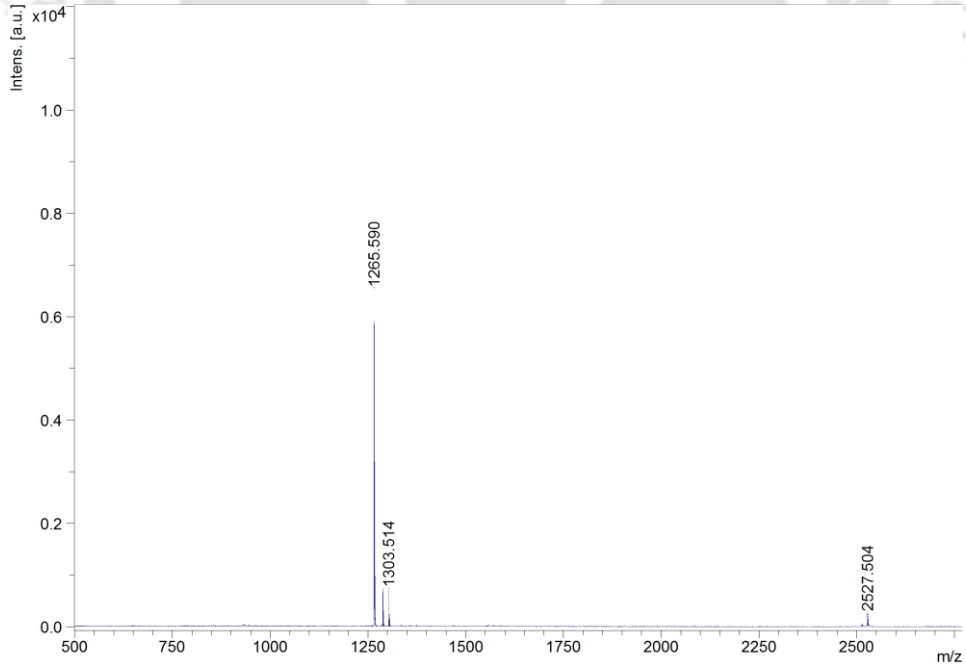

Peptide: STRAP-3-CF

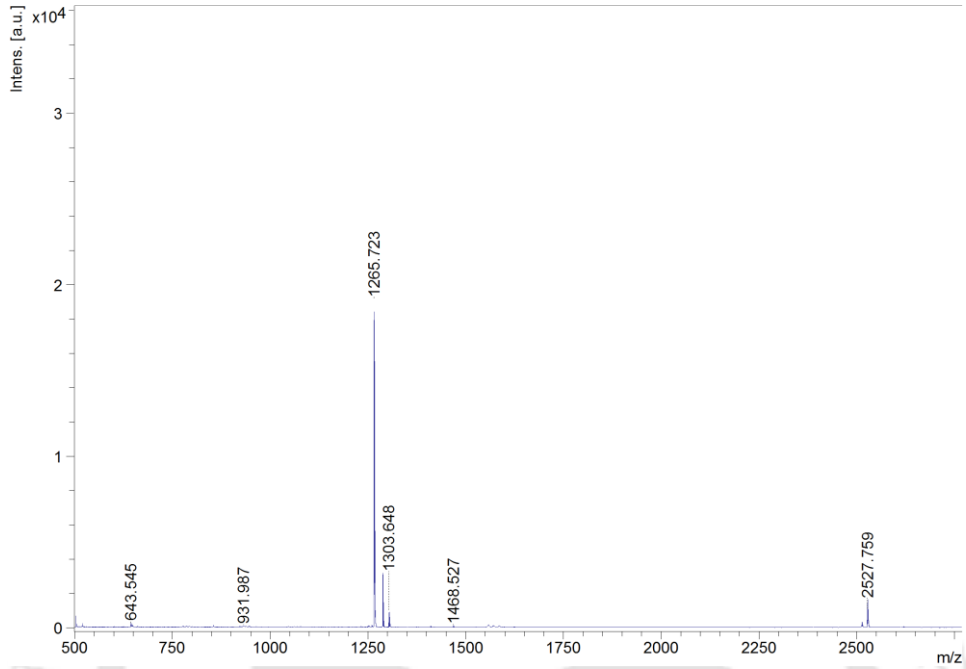

Peptide: STRAP-4-CF

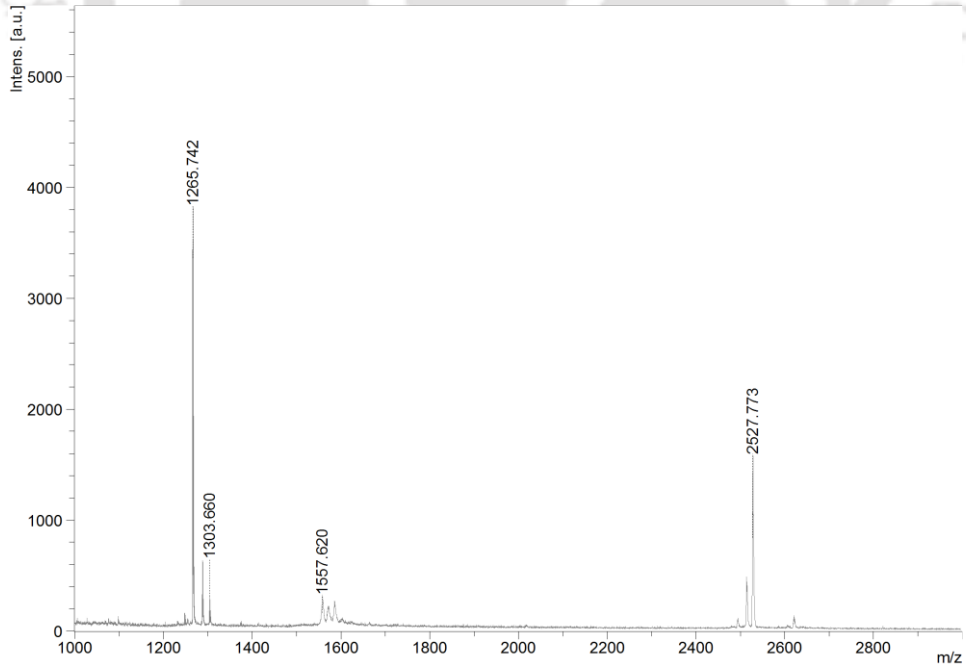

Peptide: STRAP-1-MTX

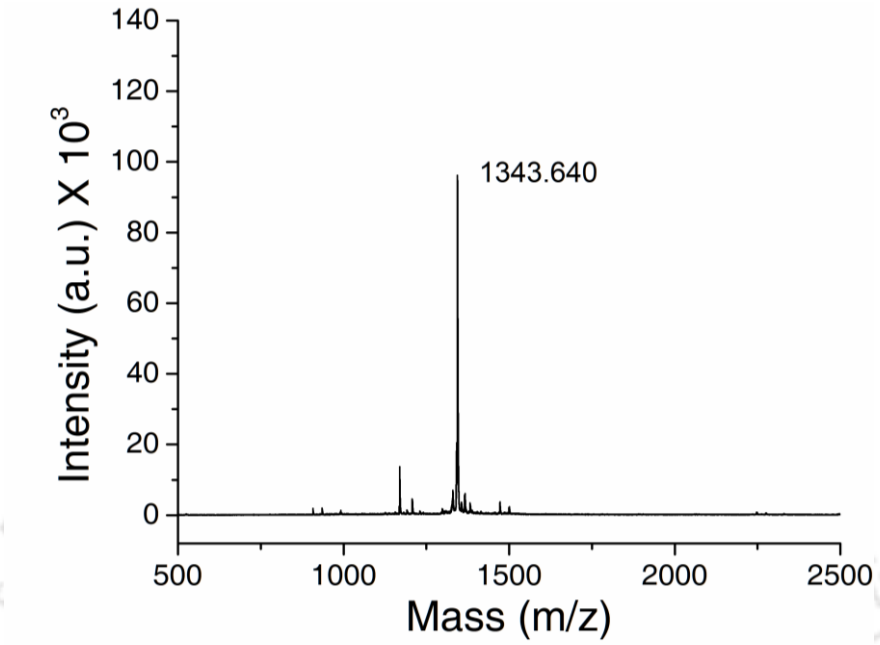

Peptide: STRAP-2-MTX

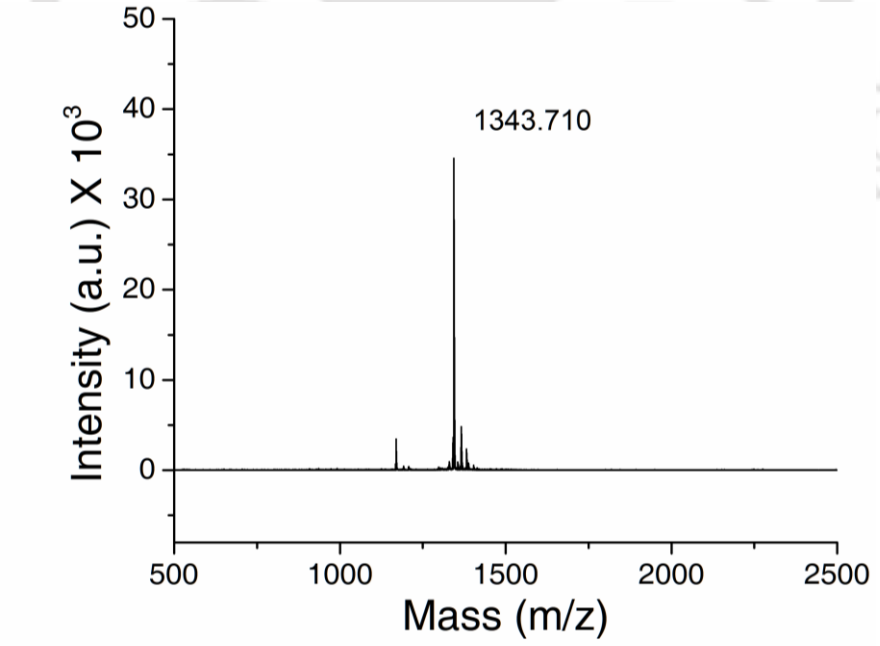

Peptide: STRAP-3-MTX

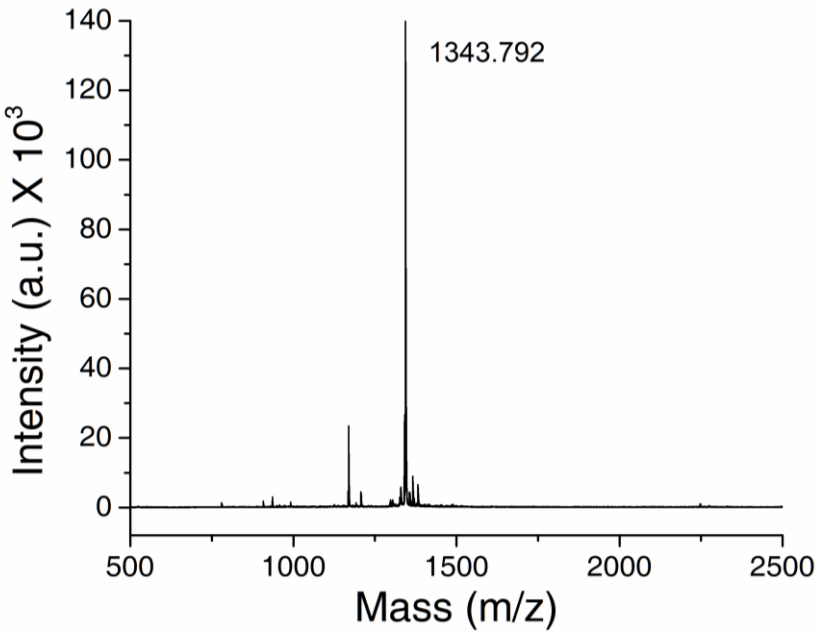

Peptide: STRAP-4-MTX

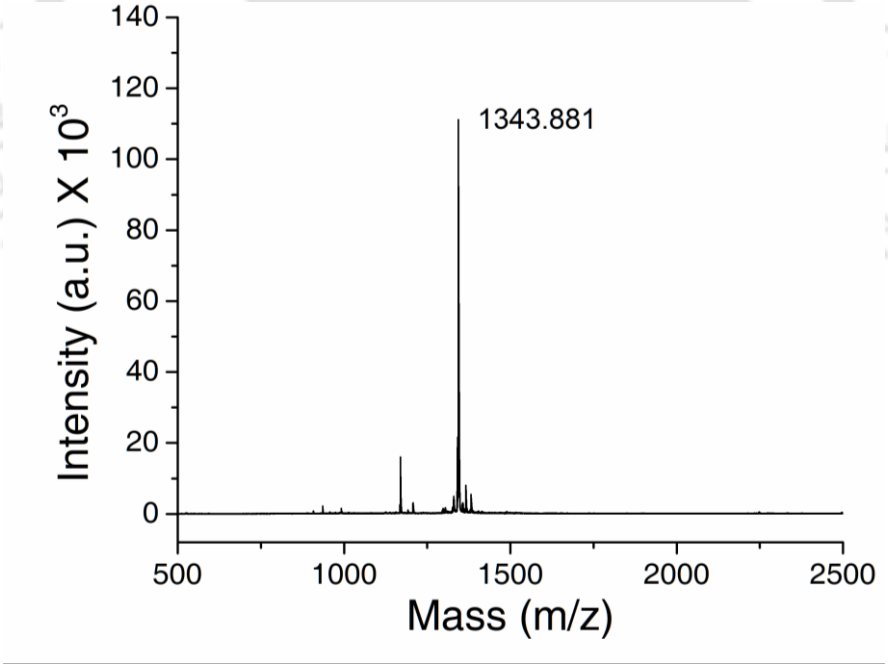

LIST of PUBLICATIONS:

Patent:

I. Field of Invention: Syndiotactic Peptides
Patent No: 333/KOL/2015
dated 26/03/2015, published on 30/09/2016

Journal Articles:

I. **Gaurav Jerath**, Ruchika Goyal, Vishal Trivedi, T. R. Santhoshkumar and Vibin Ramakrishnan. Syndiotactic Peptides for Targeted Delivery. ***Acta Biomaterialia***. (2019) 87:130-139.

II. Prakash Kishore Hazam, Akhil R, **Gaurav Jerath**, Jahnu Saikia, Vibin Ramakrishnan. Topological effects on the designability and bactericidal potency of antimicrobial peptides. ***Biophysical Chemistry*** (2019), doi.org/10.1016/j.bpc.2019.02.005.

III. Prakash Kishore Hazam, **Gaurav Jerath**, Nitin Chaudhary and Vibin Ramakrishnan. Peptido-mimetic approach in the design of syndiotactic antimicrobial peptides. ***International Journal of Peptide Research and Therapeutics*** (2018) 24 (2), 299-307.

IV. Prakash Kishore Hazam, **Gaurav Jerath**, Anil Kumar, Nitin Chaudhary and Vibin Ramakrishnan. Effect of tacticity-derived topological constraints in bactericidal peptides. ***Biochimica et Biophysica Acta (BBA)-Biomembranes*** (2017) 1859 (8), 1388-1395

V. **Gaurav Jerath**, Prakash Kishore Hazam, Shashi Shekhar and Vibin Ramakrishnan. Mapping the Geometric Evolution of Protein Folding Motor. ***Plos ONE.*** (2016) 11(10): e0163993. doi:10.1371/journal.pone.0163993.

List of Publications

VI. A. Mehra, **Gaurav Jerath**, Vibin Ramakrishnan and Vishal Trivedi. Characterization of ICAM-1 biophore to design cytoadherence blocking peptides. ***Journal of Molecular Graphics & Modelling*****.** (2015) 57, 27–35.

VII. **Gaurav Jerath**, Prakash Kishore Hazam and Vibin Ramakrishnan. bPE toolkit: toolkit for computational protein engineering. ***Systems and Synthetic Biology*****.** (2014) 8:337–341.

VIII. Rahul Metri, **Gaurav Jerath**, Govind Kailas, Adityabarna Pal and Vibin Ramakrishnan. Structure Based Barcoding of Proteins. *Protein Science* (2014) 23, 117-120.

IX. **Gaurav Jerath** and Vibin Ramakrishnan. Web-resources in Post Genomic Era. *Health* Sciences (2014) 1(3), JS002A.